VOLUME 84 NO. SM3
AUGUST 1958
PART 1

JOURNAL of the

Soil Mechanics and Foundations Division

PROCEEDINGS OF THE

AMERICAN SOCIETY OF CIVIL ENGINEERS

BASIC REQUIREMENTS FOR MANUSCRIPTS

This Journal represents an effort by the Society to deliver information to the reader with the greatest possible speed. To this end the material herein has none of the usual editing required in more formal publications.

Original papers and discussions of current papers should be submitted to the Manager of Technical Publications, ASCE. Authors should indicate the technical division to which the paper should be referred. The final date on which a discussion should reach the Society is given as a footnote with each paper. Those who are planning to submit material will expedite the review and publication procedures by complying with the following basic requirements:

1. Titles should have a length not exceeding 50 characters and spaces.

2. A 50-word summary should accompany the paper.

3. The manuscript (a ribbon copy and two copies) should be double-spaced on one side of 8½-in. by 11-in. paper. Papers that were originally prepared for oral presentation must be rewritten into the third person before being submitted.

4. The author's full name, Society membership grade, and footnote reference stating present employment should appear on the first page of the paper.

5. Mathematics are reproduced directly from the copy that is submitted. Because of this, it is necessary that capital letters be drawn, in black ink, ⅛-in. high (with all other symbols and characters in the proportions dictated by standard drafting practice) and that no line of mathematics be longer than 6½-in. Ribbon copies of typed equations may be used but they will be proportionately smaller in the printed version.

6. Tables should be typed (ribbon copies) on one side of 8½-in. by 11-in. paper within a 6½-in. by 10½-in. invisible frame. Small tables should be grouped within this frame. Specific reference and explanation should be made in the text for each table.

7. Illustrations should be drawn in black ink on one side of 8½-in. by 11-in. paper within an invisible frame that measures 6½-in. by 10½-in.; the caption should also be included within the frame. Because illustrations will be reduced to 69% of the original size, the capital letters should be ⅛-in. high. Photographs should be submitted as glossy prints in a size that is less than 6½-in. by 10½-in. Explanations and descriptions should be made within the text for each illustration.

8. Papers should average about 12,000 words in length and should be no longer than 18,000 words. As an approximation, each full page of typed text, table, or illustration is the equivalent of 300 words.

Further information concerning the preparation of technical papers is contained in the "Technical Publications Handbook" which can be obtained from the Society.

This Journal is published bi-monthly by the American Society of Civil Engineers. Publication office is at 2500 South State Street, Ann Arbor, Michigan. Editorial and General Offices are at 33 West 39 Street, New York 18, New York. $4.00 of a member's dues are applied as a subscription to this Journal. Second-class mail privileges are authorized at Ann Arbor, Michigan.

SM.HY,PO,SA,ST.

Journal of the

SOIL MECHANICS AND FOUNDATIONS DIVISION

Proceedings of the American Society of Civil Engineers

CONTENTS

August, 1958

Papers

Paper 1727 August, 1958 SM 3

Journal of the
SOIL MECHANICS AND FOUNDATIONS DIVISION
Proceedings of the American Society of Civil Engineers

PREDICTING SEEPAGE UNDER DAMS ON MULTI-LAYERED FOUNDATIONS[a]

Paul H. Shea[1] and Harry E. Whitsett[2]
(Proc. Paper 1727)

SYNOPSIS

During the design of the Central and Southern Florida Project it became necessary to develop methods for predicting rates of seepage under dams and levees on multi-layered foundations since there were no published mathematical or graphical methods which were applicable. The methods developed are presented in this paper. A description of the pumping test procedure used to implement those methods is included.

INTRODUCTION

Determination of the quantity and effect of seepage under dams and levees on pervious foundations may be accomplished quite simply when the foundation contains a single pervious layer which is open to the reservoir or river. Where the pervious foundation is blanketed by a relatively impervious layer, underseepage may be computed by the method described by Bennett[3] or may be derived from a flow net when differences in permeability are not too great. In cases where more than one pervious layer and more than one impervious layer is present, the construction of a flow net is so time-consuming that it becomes impractical. Even in cases where there is only one pervious and one impervious layer, a flow net is impractical if there is a very great difference in permeability between the layers because of the need for drawing either

Note: Discussion open until January 1, 1959. To extend the closing date one month, a written request must be filed with the Executive Secretary, ASCE. Paper 1727 is part of the copyrighted Journal of the Soil Mechanics and Foundations Division, Proceedings of the American Society of Civil Engineers, Vol. 84, No. SM 3, August, 1958.

a. Presented at meeting of ASCE, New York, N. Y., October, 1957.

1. Chf., Foundations and Materials Branch, U. S. Army, Engr. Dist., Jacksonville, Fla.
2. Mathematician, Foundations and Materials Branch, U. S. Army, Engr. Dist., Jacksonville, Fla.

3. ASCE Trans., III (1946), 215.

extremely large or minutely small "squares". Solution of such problems by mathematical processes was found to be possible, however, provided that the field conditions conform reasonably well to the following assumptions:

(1) Each blanket and each aquifer is a homogeneous medium of uniform thickness.
(2) Each blanket has a constant vertical permeability and each aquifer has a constant horizontal permeability.
(3) Flow is laminar and therefore conforms to Darcy's law.
(4) Flow is vertical in the blankets.
(5) Head loss accompanying vertical flow in the aquifers is negligible as compared to vertical head loss in the blankets.

If the results of borings indicate that the geologic conditions at a given site conform generally to assumption (1) above, conformity to the other assumptions may be checked by one or more field pumping tests. Such tests are the only practicable means for determining the transmissibilities of the various strata. Laboratory testing of so-called "undisturbed" samples would provide a very unreliable basis for the required analysis. Aside from the enormous number of samples which would be required to obtain representative permeabilities, there is the added difficulty that those materials which are most pervious are the most difficult to sample and also the most difficult to prepare for testing. In the case of rock foundations, where leakage occurs along open joints and bedding planes and through solution holes, laboratory testing of rock samples would be futile.

If foundation conditions are so non-uniform that the observed radial flow pattern to a pumped well cannot be analyzed, there is no method by which flow through such a foundation under prototype conditions can be determined. On the other hand, if the radial flow pattern can be analyzed, the flow under a dam or levee on the same or similar foundation can be predicted with reasonable accuracy.

From the foregoing discussion it can be seen that there are three prerequisites to the computation of seepage quantities under water-retaining structures on multi-layered foundations. They are (1) direct observation of radial flow in the foundation by means of a pumping test; (2) a method for analysis of radial flow in a multi-layered foundation; and (3) a method for analysis of flow under a dam or levee on the same foundation.

Development and Use of Procedure for Underseepage Estimates

The necessity for development of a method for predicting seepage quantities under levees on multi-layered foundations arose during the design of the Central and Southern Florida Project. That project (still incomplete) will eventually be an integrated system of water-control works for flood control, drainage, and water-conservation—covering all eastern Florida from the latitude of Orlando southward. Included in the project will be hundreds of miles of canals and levees, numerous small dams and spillways, and several very large pumping stations.

The project provides for the retention of excess rainfall in conservation areas to be ringed with levees. Water thus stored could be used, when needed, for irrigation. Obviously, it would be desirable to keep seepage losses at a minimum from those areas. Unfortunately, much of the reservoir area is

underlaid by very porous and permeable limestones extending from—or near—the ground surface to depths of 50 feet or more. The limestones are perforated with solution channels ranging from a fraction of an inch to 6 in. or 8 in. in diameter.

Throughout most of the area, the uppermost limestone is much less pervious than the remainder because of the sealing of pores and solution channels by peat, marl, or redeposited calcite. The thickness of the relatively tight layer varies from a few inches to 2 feet or 3 feet. A further complication is the presence of horizontal beds of relatively impervious fresh-water limestone dividing the more pervious marine limestone into two or three aquifers.

Prevention or reduction of underseepage by grouting the porous rock or providing cutoff walls is not economically feasible. The cost of such treatment would be many times the cost of the levees. Canals, pumping stations, and control structures in the areas that will be affected by the seepage must be designed with capacities that will include underseepage flow. A reasonably accurate estimate of the quantity of underseepage that will occur when water is stored in the conservation areas is required for the design of these structures.

Soon after work on the project began it became apparent that none of the published methods for the determination of underseepage was applicable to the multi-layered condition encountered. The development of the computation methods described in this paper was necessary to the design of the project.

Guidance in the early stages of the underseepage investigations was furnished by P. T. Bennett[4] and R. A. Barron.[5] The pumping test procedure originally set up was followed with only minor modifications throughout the investigation. The derivations and solutions of the differential equations for flow in systems having more than one aquiclude and aquifer were done by the junior author and are included as appendices. Those for flow in a single-blanketed aquifer were published or implied in Bennett's paper referenced above.

The estimates of underseepage used in design were based on pumping tests performed at rather widely spaced locations along the levee alinements. Interpolation between tests locations was based on geologic studies of core samples and the results of "recharge" tests made by pumping into core borings along the alinements.

Predicted underseepage quantities have been checked by metering the continuous borrow pits on the landside of several of the levees. The metering results have been erratic but they have indicated that seepage quantities estimated from pumping tests have good probable accuracy. Metered quantities have varied from 60 to 110 per cent of those estimated. Comparisons of computed and measured underseepage are shown on Figs. 1 and 2. "Measured underseepage" is the increase in flow between two points in the continuous landside borrow pit which parallels each levee. That flow does not necessarily represent all the underseepage since some of the seepage may by-pass the borrow pit and particularly at low stages, some flow may be contributed by depletion of ground water storage. Fig. 1 shows very good agreement between the computed and measured values. In Fig. 2 the metering results are very erratic. The apparent average of the measurements is about 70 per cent of the computed underseepage. After several years of metering, the seepage

4. Engineer, Missouri River Division, C. of E.
5. Engineer, Office, Chief of Engineers.

quantities computed from the pumping tests are still considered the most accurate data for use in hydrologic studies.

Details of Procedure

General

As stated above, the process of making an underseepage estimate consists of three steps: Performing a pumping test or tests; computing transmissibilities from the results of the test; and computing prototype underseepage from the transmissibilities. Uplift pressures at the base of the top blanket or aquiclude can also be computed.

The Pumping Test

The proper performance of the pumping test is of paramount importance. Adequate observational data are essential if a reasonably accurate prediction of underseepage is to be made. A procedure which has been used successfully by the U. S. Army Engineer District, Jacksonville, Florida, is described in some detail below.

Preliminary Exploration.—Small diameter borings are put down to determine the general geology of the area. The depth to which pervious materials extend and the elevations of impervious layers are determined. Sites for one or more pumping tests are selected at points where conditions are best suited for the tests. If possible, tests are performed at locations where the effects of streams, drainage from hillsides, and other features which might affect the results are unimportant.

The Pump Well.—The pump well is drilled to the full depth of the pervious formations. It is screened and gravel-packed through unconsolidated sediments and uncased through rock except that slotted casing is installed in zones where caving is anticipated. A clay or grout seal is placed at the surface to prevent entrance of surface water.

Placement of Piezometers.—Depths of observation wells or piezometers are based on a study of the samples recovered in the preliminary borings and on a vertical velocity-meter traverse made up and down the well during pumping to determine the distribution of inflow to the well. A set of piezometers is installed in each layer which contributes an appreciable portion of the inflow. Piezometers are located along straight lines passing through the pump well. Spacing of piezometers is selected to give equal increments of the log of the radial distance from the pump well. The length of the lines must be great enough to define both the straight and curved portions of the curve of drawdown versus the log of the radial distance. An estimate of that length is made for the initial installation and the lines are extended, if necessary, after the drawdown curves are plotted for the first pumping of the well. Standard well points are used for piezometers placed in sand or gravel beds. For piezometers in rock, open end pipes are used. The bottom of the pipe is placed one foot above the bottom of a drilled hole and is grouted into place. All piezometer pipes extend far enough above the ground to prevent debris and water from entering. Piezometers are flushed with clear water after installation to make certain that they are clean and open.

Methods of Measuring Drawdown.—In very pervious formations, drawdowns are small and very accurate methods of water-level determination are required. If the water level in the piezometers is high enough, a point gage

connected in series with a small battery and voltmeter gives excellent results. When the point of the gage makes contact with the water surface, completion of the circuit is indicated by the voltmeter. Readings accurate to .001 foot can be obtained by using the verneir on the point gage. When the water level is too low to permit use of the point gage, another electrical water-level indicator can be used. This instrument makes use of two insulated wires, with tape markings for measurement of depth, connected in parallel with a battery and neon lamp. When the gage comes in contact with the water, the circuit is shorted out, extinguishing the lamp. Readings accurate to .01 foot can be made with this instrument.

Test Procedure.—Before pumping the well, the distance from the top of the pipe to the water surface is measured in each piezometer. The static levels thus measured furnish the datum from which drawdowns observed during pumping are plotted. True elevations are not required. After static levels are established, the time lag for each piezometer is checked by filling the pipe with water and observing the time interval required for the water to return to the static level. The time lag is nearly always negligible. After static levels and time lags are known, the pump is started, and pumping is continued at a constant discharge rate. Piezometers are then read at regular intervals until little or no change in drawdown can be observed between successive readings. Drawdown curves are plotted as soon as the first pumping test is completed. An examination of the curves indicates where additional piezometers, if any, are needed, and whether the pumping rate is in the optimum range. If the pumping rate is too high, drawdowns in the piezometers nearest the well are excessive, indicating turbulent flow. If it is too low, drawdowns in the piezometers farthest from the well are too small to plot accurately. Any necessary changes in piezometer lay-out are made before the well is pumped again. Two or more pumping tests are conducted at each well with pumping rates which are as different as practicable. For each test, static levels are taken and the same procedure is followed in reading piezometers as is used in the first test.

Computation of Transmissibilities

The layers of the foundation are numbered for convenient reference. The numbers increase from the top downward, layer 1 being the top blanket, layer 2 the top aquifer, etc. The permeability and thickness of a layer are designated by k_i and z_i respectively, where the subscript indicates the layer. The permeabilities considered are those in the vertical direction in blankets and those in horizontal directions in aquifers. The vertical transmissibility of a blanket is defined to be $C_i = \frac{k_i}{z_i}$, where i must be an odd number. The horizontal transmissibility of an aquifer is $C_i = k_i z_i$, where i must be even.

Computation of transmissibilities from pumping test results are made by the formulas presented below. These formulas are based on the assumption that the water table is horizontal and is located above the top blanket. Field conditions in the Everglades, where pumping tests for the Central and Southern Florida project were made, always satisfied that condition. Some modification of the method is required if this condition is not satisfied. For example, laboratory tests would be required to obtain the permeability of the top blanket where the water level is well below the surface. The contributions of the various aquifers to the well discharge, Q_i where i is even, must

be known. Drawdown data should be expressed as drawdown curves—plots of drawdown vs. log r, where r is the radial distance from the pump well. In the vicinity of the pump well the drawdown curves are straight lines and the total radial flow in each aquifer is a constant. From Darcy's law, the equation for radial flow in an aquifer is

$$Q_i(r) = 2\pi C_i r \frac{dh_i}{dr}$$

where h_i is the drawdown in the aquifer.

$$\frac{dh_i}{dr} = \frac{dh_i}{d(\log r)} \cdot \frac{d \log r}{dr} = \frac{dh_i}{d(\log r)} \cdot \frac{1}{r} \log e .$$

Let

$$S_i(r) = \frac{dh_i}{d(\log r)}$$

the slope of the drawdown curve.

$$Q_i(r) = 2\pi C_i S_i(r) \log e = 2.73\, C_i S_i(r) .$$

In the vicinity of the pump well Q_i (r) and S_i (r) have constant values, Q_i and S_i.

$$Q_i = 2.73\, C_i S_i .$$

This is the formula used for computing the horizontal transmissibilities of aquifers.

In the case of one aquifer, the vertical transmissibility, C_1, of the blanket is determined from the "radius of influence", r_e. r_e is defined as the value of r at the point where the extended straight-line portion of the drawdown curve intersects the line $h_2 = 0$. The "radius of influence" satisfies the relation

$$ar_e = 1.123 .$$

Since $a = +\sqrt{\frac{C_1}{C_2}}$,

the vertical transmissibility, C_1, of the blanket can be computed when r_e and C_2 are known.

In the case of two aquifers, the transmissibilities of the blankets can not be computed by a method similar to that used in the case of one aquifer because the "radii of influence" are not independent of the constants of integration in the solution of the differential equations. The vertical transmissibilities of the blankets are obtained from the differential equations, the drawdown curves, and the horizontal transmissibilities of the aquifers. Two values of r (r_1 and r_2) at which the slopes of the drawdown curves are measurably different are selected.

Since $\Delta Q_i = Q_i(r_2) - Q_i(r_1)$, $(i = 2, 4)$.

$Q_i(r) = 2.73\, C_i S_i(r)$,

$$\Delta Q_i = 2.73\, C_i [S_i(r_2) - S_i(r_1)], \quad (i = 2, 4).$$

The C_i's are known and the S_i's can be measured on the drawdown curves. Water can enter the aquifers only by passing through the blankets, so

$$\Delta Q_1 = \Delta Q_2 + \Delta Q_4 ,$$

$$\Delta Q_3 = \Delta Q_4 .$$

From Darcy's law, the equations for flow in the blankets are

$$dQ_1 = 2\pi C_1 r h_2 dr ,$$

$$dQ_3 = 2\pi C_3 r (h_4 - h_2)\, dr .$$

Thus,

$$\Delta Q_1 = \int_{r=r_1}^{r_2} dQ_1 = 2\pi C_1 \int_{r_1}^{r_2} r h_2\, dr ,$$

$$\Delta Q_3 = \int_{r=r_1}^{r_2} dQ_3 = 2\pi C_3 \left[\int_{r_1}^{r_2} r h_4\, dr - \int_{r_1}^{r_2} r h_2\, dr \right] .$$

When values of the integrals are known, these equations can be solved for C_1 and C_3. The values of the integrals may be obtained by numerical integration, or by plotting the curves and planimetering the areas.

The method used for computing transmissibilities of the blankets in the two-aquifer case is used in the three-aquifer case also. The formulas required are:

$$\Delta Q_i = 2.73\, C_i [S_i(r_2) - S_i(r_1)], \quad (i = 2, 4, 6),$$

$$\Delta Q_1 = \Delta Q_2 + \Delta Q_4 + \Delta Q_6 ,$$

$$\Delta Q_3 = \Delta Q_4 + \Delta Q_6 ,$$

$$\Delta Q_5 = \Delta Q_6 ,$$

$$\Delta Q_1 = 2\pi C_1 \int_{r_1}^{r_2} r h_2\, dr ,$$

$$\Delta Q_3 = 2\pi C_3 \left[\int_{r_1}^{r_2} r h_4\, dr - \int_{r_1}^{r_2} r h_2\, dr \right] ,$$

$$\Delta Q_5 = 2\pi C_5 \left[\int_{r_1}^{r_2} r h_6 \, dr - \int_{r_1}^{r_2} r h_4 \, dr \right] .$$

Computation of Underseepage and Uplift Pressures

The region being considered is a strip of the foundation one unit wide and normal to the dam. Q_i, i being an even number, is the rate at which water seeps past the center line of the dam in aquifer i. The sign of Q_i indicates whether the direction of flow is the same as or opposite to the direction arbitrarily chosen as positive on the x axis. Q is the total seepage rate through a one unit wide strip of the foundation. Q is always taken to be positive. The symbol L is used for the base width of the dam. H is the head differential across the dam. The dam is assumed to be impervious, so no water seeps through the top blanket in the region beneath the dam. For derivations of all equations see Appendices A and B.

The One-Blanket-One-Aquifer Case.—The underseepage per unit length of a dam or levee is given by the formula

$$Q = \frac{C_2 H}{L + 2x_r} , \quad \text{where}$$

$$a = + \sqrt{\frac{C_1}{C_2}} \quad \text{and} \quad x_r = \frac{1}{a} .$$

If the soil properties are obtained from a pumping test, then the permeabilities need not be known since C_2 and r_e are determined directly and "a" can be obtained from the relationship

$$a r_e = 1.123$$

(r_e is defined as the radial distance at which the extended straight-line portion of a curve of drawdown versus log r intersects the line of zero drawdown).

In the portion of the aquifer located beneath the dam the hydraulic head referred to tail water is given by

$$h = \frac{H}{2} - \frac{Q}{C_2} x , \quad \left(-\frac{L}{2} \le x \le \frac{L}{2} \right) ,$$

where X = 0 at the centerline of the dam and X = L/2 at the toe of the dam.

The Two-Blanket-Two-Aquifer Case.—The following quantities are used in the formulas:

$$\alpha_{12} = \frac{C_1}{C_2} , \quad \alpha_{32} = \frac{C_3}{C_2} , \quad \alpha_{34} = \frac{C_3}{C_4} ,$$

$$a = \alpha_{12} + \alpha_{32} + \alpha_{34} , \quad b = \alpha_{12} \alpha_{34} ,$$

$$f^2 = \frac{a + \sqrt{a^2 - 4b}}{2} , \quad g^2 = \frac{a - \sqrt{a^2 - 4b}}{2} , \quad (f > g > 0) ,$$

$$j = \frac{\alpha_{12} + \alpha_{32} - f^2}{\alpha_{32}}, \quad m = \frac{\alpha_{12} + \alpha_{32} - g^2}{\alpha_{32}},$$

$$c^2 = \alpha_{32} + \alpha_{34}, \quad (c > 0), \quad s = -\frac{\alpha_{34}}{\alpha_{32}} = -\frac{C_2}{C_4}.$$

The underseepage per unit length of dam is given by the formula

$$Q = -[Q_2 + Q_4], \text{ where}$$

$$Q_2 = \frac{\overline{\Delta Q_2}}{\Delta}, \quad Q_4 = \frac{\overline{\Delta Q_4}}{\Delta},$$

$$\overline{\Delta Q_2} = C_2 H \begin{vmatrix} c\left[1 - e^{\frac{cL}{2}}\right]^2 & -f & -g \\ (s-1)\left[1 - e^{cL}\right] & 1-j & 1-m \\ c(s-1)\left[1 + e^{cL}\right] & f(1-j) & g(1-m) \end{vmatrix},$$

$$\overline{\Delta Q_4} = C_4 H \begin{vmatrix} sc\left[1 - e^{\frac{cL}{2}}\right]^2 & -jf & -mg \\ (s-1)\left[1 - e^{cL}\right] & 1-j & 1-m \\ c(s-1)\left[1 + e^{cL}\right] & f(1-j) & g(1-m) \end{vmatrix},$$

$$\Delta = - \begin{vmatrix} L(1-j) & (s-j)\left[1 - e^{cL}\right] & j-m \\ 2+fL & -c\left[1 + e^{cL}\right] + f\left[1 - e^{cL}\right] & g-f \\ 2(1-j) & c(j-s)\left[1 + e^{cL}\right] & g(m-j) \end{vmatrix}.$$

A substantial simplification of the formulas for underseepage without great loss of accuracy can be accomplished by making the assumption that no water passes through the portion of the lower blanket located beneath the dam. In this case

$$Q = -[Q_2 + Q_4], \text{ where}$$

$$Q_2 = \frac{C_2 H}{j-m}\left[\frac{f(m-1)}{2+fL} + \frac{g(1-j)}{2+gL}\right] \text{ and}$$

$$Q_4 = \frac{C_4 H}{j-m}\left[j\frac{f(m-1)}{2+fL} + m\frac{g(1-j)}{2+gL}\right].$$

Since transmissibilities rather than permeabilities are used in the formulas for underseepage, the permeabilities need not be known if the transmissibilities are obtained from a pumping test. The two-aquifer case differs from the one-aquifer case in that there are no convenient quantities like x_r and r_e to simplify the application of pumping test results to computation of underseepage.

In the portion of the upper aquifer located beneath the dam, the hydraulic head referred to tail water is given by

$$h_2 = \frac{H}{2} - \frac{Q}{C_2+C_4}X + \left(\frac{Q_2}{C_2} - \frac{Q_4}{C_4}\right)\frac{\sinh cX}{c(1-s)}, \quad \left(-\frac{L}{2} \le X \le \frac{L}{2}\right).$$

Here X = 0 at the centerline of the dam and X = L/2 at the toe of the dam.

An approximate formula can be obtained by assuming that no water passes through the portion of the lower blanket located beneath the dam.

$$h_2 = \frac{H}{2} + \frac{Q_2}{C_2}X, \quad \left(-\frac{L}{2} \le X \le \frac{L}{2}\right).$$

This formula can be written in another way for comparison with the precise formula:

$$h_2 = \frac{H}{2} - \frac{Q}{C_2+C_4}X + \left(\frac{Q_2}{C_2} - \frac{Q_4}{C_4}\right)\frac{cX}{c(1-s)}, \quad \left(-\frac{L}{2} \le X \le \frac{L}{2}\right).$$

The approximate formula is conservative in that it gives uplift pressures that are too high under the downstream half of the dam.

The Three-Blanket-Three-Aquifer Case.—Formulas for underseepage that take into account the flow through the two lower blankets in the region beneath the dam are too unwieldy for convenient computation since the determinants involved can not readily be reduced to lower order than the fifth. For this reason they are not presented here. It is assumed that no flow through the lower blankets occurs in the region beneath the dam. The following quantities are used in the formulas:

$$\alpha_{12} = \frac{C_1}{C_2}, \quad \alpha_{32} = \frac{C_3}{C_2}, \quad \alpha_{34} = \frac{C_3}{C_4}, \quad \alpha_{54} = \frac{C_5}{C_4}, \quad \alpha_{56} = \frac{C_5}{C_6},$$

$$a = \alpha_{12} + \alpha_{32} + \alpha_{34} + \alpha_{54} + \alpha_{56},$$

$$b = \alpha_{12}(\alpha_{34} + \alpha_{54} + \alpha_{56}) + \alpha_{32}(\alpha_{54} + \alpha_{56}) + \alpha_{34}\alpha_{56},$$

$$c = \alpha_{12}\alpha_{34}\alpha_{56},$$

p^2, q^2, r^2 are the roots of $z^3 - az^2 + bz - c = 0$,

p, q, r are the positive square roots of p^2, q^2, r^2,

$$f = \frac{\alpha_{12} + \alpha_{32} - p^2}{\alpha_{32}}, \quad g = \frac{\alpha_{12} + \alpha_{32} - q^2}{\alpha_{32}}, \quad j = \frac{\alpha_{12} + \alpha_{32} - r^2}{\alpha_{32}},$$

$$k = \frac{(\alpha_{34} + \alpha_{54} - p^2) f - \alpha_{34}}{\alpha_{54}}, \quad m = \frac{(\alpha_{34} + \alpha_{54} - q^2) g - \alpha_{34}}{\alpha_{54}},$$

$$n = \frac{(\alpha_{34} + \alpha_{54} - r^2) j - \alpha_{34}}{\alpha_{54}},$$

$$\Delta_1 = \begin{vmatrix} 1 & 1 & 1 \\ 1 & g & j \\ 1 & m & n \end{vmatrix}, \quad \Delta_2 = \begin{vmatrix} 1 & 1 & 1 \\ f & 1 & j \\ k & 1 & n \end{vmatrix},$$

$$\Delta_3 = \begin{vmatrix} 1 & 1 & 1 \\ f & g & 1 \\ k & m & 1 \end{vmatrix}, \quad \Delta = \begin{vmatrix} 1 & 1 & 1 \\ f & g & j \\ k & m & n \end{vmatrix}.$$

The underseepage per unit length of levee is given by the formula

$$Q = -[Q_2 + Q_4 + Q_6]$$

, where

$$Q_2 = -\frac{C_2 H}{\Delta}\left[\frac{p\Delta_1}{2+pL} + \frac{q\Delta_2}{2+qL} + \frac{r\Delta_3}{2+rL}\right],$$

$$Q_4 = -\frac{C_4 H}{\Delta}\left[f\frac{p\Delta_1}{2+pL} + g\frac{q\Delta_2}{2+qL} + j\frac{r\Delta_3}{2+rL}\right],$$

$$Q_6 = -\frac{C_6 H}{\Delta}\left[k\frac{p\Delta_1}{2+pL} + m\frac{q\Delta_2}{2+qL} + n\frac{r\Delta_3}{2+rL}\right].$$

As before, the transmissibilities, rather than the permeabilities, of the layers of the foundation are the soil properties required for computation.

The precise formula for pressure distribution in the top aquifer would be cumbersome. The formula presented here is approximate, based on the assumption that no water flows through the portions of the lower blankets located beneath the dam. In the portion of the top aquifer located beneath the dam, the hydraulic head referred to tail water is given approximately by the formula

$$h_2 = \frac{H}{2} + \frac{Q_2}{C_2}x, \quad \left(-\frac{L}{2} \le x \le \frac{L}{2}\right),$$

where X = 0 at the centerline of the dam and X = L/2 at the toe of the dam. This formula gives uplift pressures that are too high under the downstream half of the dam.

Uses of Computations

The computation methods described above were developed for estimating the seepage under levees in south Florida where the foundations are composed of relatively thick beds of very pervious marine limestone with thin interbeds of dense fresh-water limestone. The methods are also applicable to seepage under any other water-retaining structure on a foundation consisting of alternating impervious and pervious materials.

Underseepage computations are particularly valuable in cases where water conservation, either for water supply or for the generation of power, is a primary consideration. Such computations can indicate whether or not the cost of the provision of an upstream blanket or a cut-off can be justified by the benefits which will be realized. All too often such features are incorporated in designs without a complete analysis of their economic justification. Computations of uplift pressures are very useful in indicating whether or not pressure-relief devices such as toe drains, drainage blankets, and relief wells are required to prevent possible piping.

It is not meant to imply that exact, or even very accurate, predictions of underseepage quantities and uplift pressures can be made by the methods described above. The methods require an idealizing of the non-uniform conditions actually encountered in nature. Furthermore, it is unlikely that the basic data used in the computations can be obtained with a high degree of accuracy. It should be noted, however, that these qualifications are equally applicable to all soil mechanics design computations.

CONCLUSIONS

Methods for computing seepage and head distribution through foundations made up of alternating impervious and pervious layers have been developed. These methods can be used for determining seepage quantities and uplift pressures in systems which are too complex for the practical application of flow-net analyses.

APPENDIX A

Derivation and Solution of Differential Equations for Head Distribution in Flow Through Layered Systems

Derivations of the Differential Equations

The One-Aquifer Case

The differential equation for flow in a single blanketed aquifer can be derived by considering a region of the aquifer with length dx, width dy and height z_2.

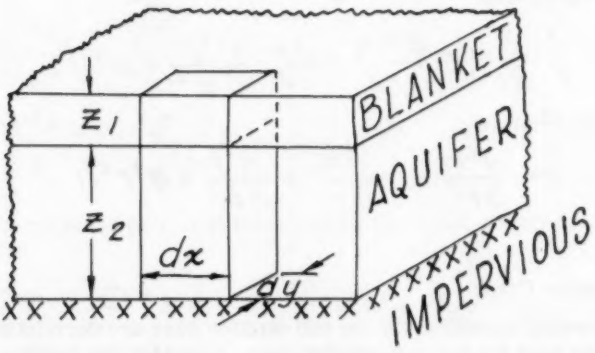

The total flow out through the sides of the region is equal to the total flow in through the top.

$$\frac{\partial V_x}{\partial x} dx\, z_2 dy + \frac{\partial V_y}{\partial y} dy\, z_2 dx = k_1 \frac{p_o - p}{z_1} dx\, dy,$$

where V_x and V_y are velocity components, p is the hydraulic head in the aquifer, and p_o is the constant hydraulic head at the top of the blanket. The last term in the above equation was obtained from Darcy's law, $V = -k\nabla p$. Dividing the equation by dx . dy gives

$$z_2 \frac{\partial}{\partial x} V_x + z_2 \frac{\partial}{\partial y} V_y = \frac{k_1}{z_1} (p_o - p).$$

Let $h = p_o - p$, $C_1 = \frac{k_1}{z_1}$, $C_2 = k_2 z_2$. Darcy's law gives $V_x = -k_2 \frac{\partial p}{\partial x} = k_2 \frac{\partial h}{\partial x}$, $V_y = -k_2 \frac{\partial p}{\partial y} = k_2 \frac{\partial h}{\partial y}$.

Substituting in the equation,

$$C_2 \frac{\partial^2 h}{\partial x^2} + C_2 \frac{\partial^2 h}{\partial y^2} = C_1 h.$$

Let

$$a = +\sqrt{\frac{C_1}{C_2}} \quad .$$

$$\frac{\partial^2 h}{\partial x^2} + \frac{\partial^2 h}{\partial y^2} = a^2 h \ .$$

This is the required differential equation. In cylindrical coordinates the differential equation is

$$\frac{1}{r}\frac{\partial}{\partial r}\left(r\frac{\partial h}{\partial r}\right) + \frac{1}{r^2}\frac{\partial^2 h}{\partial \theta^2} = a^2 h \ .$$

Multiplying by r^2 gives

$$r^2\frac{\partial^2 h}{\partial r^2} + r\frac{\partial h}{\partial r} + \frac{\partial^2 h}{\partial \theta^2} = a^2 r^2 h \ .$$

The Two-Aquifer Case

The differential equations for the two-aquifer case are derived by the same method as was used for the one-aquifer case. Consider the regions of the two aquifers inclosed by a prism with length dx and width dy. For each region the total flow out through the sides is equal to the total flow in through the top and bottom.

$$\frac{\partial (V_2)_x}{\partial x} dx \ z_2 dy + \frac{\partial (V_2)_y}{\partial y} dy \ z_2 dx = k_1 \frac{p_0 - p}{z_1} dx dy$$

$$- k_3 \frac{p_2 - p_4}{z_3} dx dy,$$

$$\frac{\partial (V_4)_x}{\partial x} dx \ z_4 dy + \frac{\partial (V_4)_y}{\partial y} dy \ z_4 dx = k_3 \frac{p_2 - p_4}{z_3} dx dy \ .$$

$$z_2 \frac{\partial}{\partial x}(V_2)_x + z_2 \frac{\partial}{\partial y}(V_2)_y = \frac{k_1}{z_1}(p_0 - p_2) - \frac{k_3}{z_3}(p_2 - p_4),$$

$$z_4 \frac{\partial}{\partial x}(V_4)_x + z_4 \frac{\partial}{\partial y}(V_4)_y = \frac{k_3}{z_3}(p_2 - p_4) \ .$$

Let

$$h_2 = p_0 - p_2, h_4 = p_0 - p_4, C_1 = \frac{k_1}{z_1}, C_3 = \frac{k_3}{z_3}, C_2 = k_2 z_2, C_4 = k_4 z_4 \ .$$

From Darcy's law,

$$(V_i)_x = -k_i \frac{\partial p_i}{\partial x} = k_i \frac{\partial h_i}{\partial x}, (V_i)_y = -k_i \frac{\partial p_i}{\partial y} = k_i \frac{\partial h_i}{\partial y}, (i = 2, 4) \ .$$

Substituting in the equations,

$$C_2 \frac{\partial^2 h_2}{\partial x^2} + C_2 \frac{\partial^2 h_2}{\partial y^2} = C_1 h_2 - C_3 (h_4 - h_2),$$

$$C_4 \frac{\partial^2 h_4}{\partial x^2} + C_4 \frac{\partial^2 h_4}{\partial y^2} = C_3 (h_4 - h_2).$$

Let

$$\alpha_{12} = \frac{C_1}{C_2}, \quad \alpha_{32} = \frac{C_3}{C_2}, \quad \alpha_{34} = \frac{C_3}{C_4}.$$

$$\frac{\partial^2 h_2}{\partial x^2} + \frac{\partial^2 h_2}{\partial y^2} = \alpha_{12} h_2 - \alpha_{32} (h_4 - h_2),$$

$$\frac{\partial^2 h_4}{\partial x^2} + \frac{\partial^2 h_4}{\partial y^2} = \alpha_{34} (h_4 - h_2).$$

This is the required pair of simultaneous differential equations. In cylindrical coordinates

$$\frac{1}{r} \frac{\partial}{\partial r} \left(r \frac{\partial h_2}{\partial r} \right) + \frac{1}{r^2} \frac{\partial^2 h_2}{\partial \theta^2} = \alpha_{12} h_2 - \alpha_{32} (h_4 - h_2),$$

$$\frac{1}{r} \frac{\partial}{\partial r} \left(r \frac{\partial h_4}{\partial r} \right) + \frac{1}{r^2} \frac{\partial^2 h_4}{\partial \theta^2} = \alpha_{34} (h_4 - h_2).$$

Multiplying by r^2 gives

$$r^2 \frac{\partial^2 h_2}{\partial r^2} + r \frac{\partial h_2}{\partial r} + \frac{\partial^2 h_2}{\partial \theta^2} = \alpha_{12} r^2 h_2 - \alpha_{32} r^2 (h_4 - h_2),$$

$$r^2 \frac{\partial^2 h_4}{\partial r^2} + r \frac{\partial h_4}{\partial r} + \frac{\partial^2 h_4}{\partial \theta^2} = \alpha_{34} r^2 (h_4 - h_2).$$

The Three-Aquifer Case

Derivation of the differential equations for the three aquifer case is so similar to that for the two-aquifer case that there is no need for including the details of the derivation. The simultaneous differential equations are

$$\frac{\partial^2 h_2}{\partial x^2} + \frac{\partial^2 h_2}{\partial y^2} = \alpha_{12} h_2 - \alpha_{32} (h_4 - h_2),$$

$$\frac{\partial^2 h_4}{\partial x^2} + \frac{\partial^2 h_4}{\partial y^2} = \alpha_{34} (h_4 - h_2) - \alpha_{54} (h_6 - h_4),$$

$$\frac{\partial^2 h_6}{\partial x^2} + \frac{\partial^2 h_6}{\partial y^2} = \alpha_{56}(h_6 - h_4).$$

Solutions of the Differential Equations

The One-Aquifer Case

Sheet Flow.—Consider the flow toward a dam in a strip of the foundation one unit wide. Let x equal zero at the heel of the dam and increase in the upstream direction. Only the region $x \geq 0$ is considered here. Since $h = h(x)$, $\frac{\partial^2 h}{\partial y^2} = 0$ and the differential equation becomes

$$\frac{d^2 h}{dx^2} = a^2 h .$$

$$(D^2 - a^2)\, h = 0 .$$

$$(D-a)(D+a)\, h = 0 .$$

The general solution of the differential equation is

$$h = M_1 e^{ax} + M_2 e^{-ax} ,$$

Where M_1 and M_2 are arbitrary constants. From the physical conditions of the problem,

$$\lim_{x \to \infty} h = 0 .$$

Since

$$e^{ax} \to \infty \text{ as } x \to \infty, \quad M_1 = 0 .$$

$$h = M_2 e^{-ax} .$$

Consider the tangent to the curve h versus x at $x = 0$. The x-coordinate, x_r, of the point where the tangent intersects the line $h = 0$, is called the "resistance" of the blanketed aquifer.

$$\frac{d}{dx} h(x) = -a M_2 e^{-ax} .$$

$$\frac{d}{dx} h(0) = -a M_2 = -a h(0) .$$

$$\frac{d}{dx} h(0) = -\frac{h(0)}{x_r} .$$

$$x_r = \frac{1}{a} .$$

Radial Flow.—Consider the flow toward a well with its centerline at r = 0. Since h = h (r), $\frac{\partial^2 h}{\partial \theta^2} = 0$ and the differential equation becomes

$$r^2 \frac{d^2h}{dr^2} + r\frac{dh}{dr} = a^2 r^2 h.$$

$$(r^2 D^2 + rD - a^2 r^2)\, h = 0.$$

Let

$$\delta = rD.$$

$$r^2 D^2 + rD = r\delta D + \delta = (\delta - 1)\delta + \delta = \delta^2.$$

$$(\delta^2 - a^2 r^2)\, h = 0.$$

I_0 (ar) and K_0 (ar)—the zero-order modified Bessel functions of the first kind and second kind respectively—are linearly independent particular solutions of this differential equation. The infinite series expressions for these functions can be found in Tables of Integrals and Other Mathematical Data, by Dwight (formulas 813.1 and 815.1). They are:

$$I_0(x) = \sum_{n=0}^{\infty} \frac{x^{2n}}{2^{2n}(n!)^2} \quad \text{and}$$

$$K_0(x) = -\left(\gamma + \ln \frac{x}{2}\right) I_0(x) + \sum_{n=1}^{\infty} \left[\frac{x^{2n}}{2^{2n}(n!)^2} \sum_{s=1}^{n} \frac{1}{s}\right],$$

where γ is Euler's constant, 0.5772... . Values of the function

$$i H_0^{(1)}(ix) = \frac{2}{\pi} K_0(x)$$

are tabulated on pages 236-242 of Tables of Functions, by Jahnke and Emde. The general solution of the differential equation

$$(\delta^2 - a^2 r^2)\, h = 0$$

is $h = N_1 I_0$ (ar) + $N_2 K_0$ (ar), where N_1 and N_2 are arbitrary constants. From the physical conditions of the problem,

$$\lim_{r \to \infty} h = 0.$$

Since

$$I_0(ar) \to \infty \text{ as } r \to \infty \text{ and } \lim_{r \to \infty} K_0(ar) = 0,$$

$$N_1 = 0. \qquad h = N_2 K_0(ar).$$

When r is small, then, approximately,

$$h = -N_2 \left(\gamma + \ln \frac{ar}{2}\right).$$

The approximation gets better as r becomes smaller. The drawdown curves (plots of h vs. log r) obtained from observations made during pumping tests exhibit straight-line portions for small values of r.

r_e, the value of r at the point where the extended straight-line portion of a drawdown curve intersects the line h = 0, is called the "radius of influence" of the blanketed aquifer.

$$-N_2\left(\gamma+\ln\frac{ar_e}{2}\right)=0.$$

$$ar_e = 2e^{-\gamma} = 1.123 \ .$$

The Two-Aquifer Case

Sheet Flow.—Consider the flow toward a dam in a strip of the foundation one unit wide. Let x equal zero at the heel of the dam and increase in the upstream direction. Only the region $x \geq 0$ is considered here. Since h_2 and h_4 are independent of y, $\frac{\partial h_2}{\partial y^2} = \frac{\partial^2 h_4}{\partial y^2} = 0$ and the differential equations become

$$\frac{d^2h_2}{dx^2} - \alpha_{12}h_2 + \alpha_{32}(h_4-h_2)=0,$$

$$\frac{d^2h_4}{dx^2} - \alpha_{34}(h_4-h_2)=0.$$

$$\begin{cases}\left[D^2-(\alpha_{12}+\alpha_{32})\right]h_2+\alpha_{32}h_4=0,\\ \alpha_{34}h_2+\left[D^2-\alpha_{34}\right]h_4=0.\end{cases}$$

This pair of simultaneous equations will be solved in the following manner. The variable h_4 will be eliminated between these equations. The resulting equation will be solved for h_2. When h_2 is known, h_4 will be obtained from the first equation of the pair. Operate on the first equation with $\left[D^2-\alpha_{34}\right]$ and then subtract the product of α_{32} and the second equation.

$$\left[D^2-\alpha_{34}\right]\left[D^2-(\alpha_{12}+\alpha_{32})\right]h_2-\alpha_{32}\alpha_{34}h_2=0.$$

$$\left[D^4-(\alpha_{12}+\alpha_{32}+\alpha_{34})D^2+\alpha_{12}\alpha_{34}\right]h_2=0.$$

Let

$$a=\alpha_{12}+\alpha_{32}+\alpha_{34}, \quad b=\alpha_{12}\alpha_{34}.$$

$$\left[D^4-aD^2+b\right]h_2=0.$$

$$D^4-aD^2+b=\left[D^2-\frac{a+\sqrt{a^2-4b}}{2}\right]\left[D^2-\frac{a-\sqrt{a^2-4b}}{2}\right].$$

Let

$$f^2 = \frac{a+\sqrt{a^2-4b}}{2},\quad g^2 = \frac{a-\sqrt{a^2-4b}}{2},\quad (f>g>0)\ .$$

$$[D^2-f^2][D^2-g^2]h_2 = 0\ .$$

$$[D-f][D+f][D-g][D+g]h_2 = 0\ .$$

The general solution of this differential equation is

$$h_2 = M_1 e^{fx} + M_2 e^{-fx} + M_3 e^{gx} + M_4 e^{-gx}\ ,$$

where the M's are arbitrary constants. Now that h_2 is known h_4 can be obtained from the equation

$$h_4 = \frac{1}{\alpha_{32}}[\alpha_{12}+\alpha_{32}-D^2]h_2\ .$$

Let

$$j = \frac{\alpha_{12}+\alpha_{32}-f^2}{\alpha_{32}},\quad m = \frac{\alpha_{12}+\alpha_{32}-g^2}{\alpha_{32}}\ .$$

$$h_4 = jM_1 e^{fx} + jM_2 e^{-fx} + mM_3 e^{gx} + mM_4 e^{-gx}\ .$$

The general solution of the pair of differential equations is

$$\begin{cases} h_2 = M_1 e^{fx} + M_2 e^{-fx} + M_3 e^{gx} + M_4 e^{-gx}\ , \\ h_4 = jM_1 e^{fx} + jM_2 e^{-fx} + mM_3 e^{gx} + mM_4 e^{-gx}\ , \end{cases}$$

where the M's are arbitrary constants.

From the physical conditions of the problem,

$$\lim_{x\to-\infty} h_2 = \lim_{x\to-\infty} h_4 = 0\ .$$

Since

$$e^{fx}\to 0 \text{ and } e^{gx}\to 0 \text{ as } x\to-\infty,\ M_1 = M_3 = 0\ .$$

$$\begin{cases} h_2 = M_2 e^{-fx} + M_4 e^{-gx}\ , \\ h_4 = jM_2 e^{-fx} + mM_4 e^{-gx}\ . \end{cases}$$

The quantities corresponding to the "resistance of the blanketed aquifer in the one-aquifer case will now be obtained.

$$\frac{d}{dx} h_2(0) = -(f M_2 + g M_4) .$$

$$\frac{d}{dx} h_2(0) = -\frac{h_2(0)}{x_r} = -\frac{M_2 + M_4}{x_r} .$$

$$-(f M_2 + g M_4) = -\frac{M_2 + M_4}{x_r} .$$

For the upper aquifer,

$$x_r = \frac{M_2 + M_4}{f M_2 + g M_4} .$$

Similarly, for the lower aquifer,

$$x_r = \frac{j M_2 + m M_4}{f j M_2 + g m M_4} .$$

In the region beneath an impermeable dam no water can pass through the top blanket. The derivation of differential equations already presented applies to this case when the term associated with flow through the top blanket is omitted. The required differential equations are

$$\frac{d^2 h_2}{dx^2} + \alpha_{32}(h_4 - h_2) = 0 ,$$

$$\frac{d^2 h_4}{dx^2} - \alpha_{34}(h_4 - h_2) = 0 ,$$

Since

$$\frac{\partial^2 h_2}{\partial y^2} = \frac{\partial^2 h_4}{\partial y^2} = 0 .$$

$$\begin{cases} [D^2 - \alpha_{32}] h_2 + \alpha_{32} h_4 = 0 , \\ \alpha_{34} h_2 + [D^2 - \alpha_{34}] h_4 = 0 . \end{cases}$$

Solution for h_2 can be effected by eliminating h_4 between these equations. The first equation of the pair then gives h_4. Operate on the first equation with $[D^2 - \alpha_{34}]$ and then subtract the product of α_{32} and the second equation.

$$[D^2 - \alpha_{34}][D^2 - \alpha_{32}] h_2 - \alpha_{32} \alpha_{34} h_2 = 0 .$$

$$[D^4 - (\alpha_{32} + \alpha_{34}) D^2] h_2 = 0.$$

Let

$$c^2 = \alpha_{32} + \alpha_{34}, \quad c > 0.$$

$$D^2 [D-c][D+c] h_2 = 0.$$

$$h_2 = R_1 + R_2 x + R_3 e^{cx} + R_4 e^{-cx},$$

where the R's are arbitrary constants.

$$h_4 = \frac{1}{\alpha_{32}} [\alpha_{32} - D^2] h_2.$$

$$h_4 = \frac{1}{\alpha_{32}} [\alpha_{32} R_1 + \alpha_{32} R_2 x + (\alpha_{32} - c^2) R_3 e^{cx} + (\alpha_{32} - c^2) R_4 e^{-cx}.$$

Let

$$s = \frac{\alpha_{32} - c^2}{\alpha_{32}}. \quad s = -\frac{\alpha_{34}}{\alpha_{32}} = -\frac{C_2}{C_4}.$$

The general solution of the pair of differential equations is

$$\begin{cases} h_2 = R_1 + R_2 x + R_3 e^{cx} + R_4 e^{-cx}, \\ h_4 = R_1 + R_2 x + s R_3 e^{cx} + s R_4 e^{-cx}, \end{cases}$$

where the R's are arbitrary constants.

Radial Flow.—Consider the flow toward a well with its centerline at r = 0. $\frac{\partial^2 h_2}{\partial \theta^2} = \frac{\partial^2 h_4}{\partial \theta^2} = 0$, and the differential equations become

$$r^2 \frac{d^2 h_2}{dr^2} + r \frac{dh_2}{dr} = \alpha_{12} r^2 h_2 - \alpha_{32} r^2 (h_4 - h_2),$$

$$r^2 \frac{d^2 h_4}{dr^2} + r \frac{dh_4}{dr} = \alpha_{34} r^2 (h_4 - h_2).$$

$$[r^2 D^2 + rD - (\alpha_{12} + \alpha_{32}) r^2] h_2 + \alpha_{32} r^2 h_4 = 0,$$

$$\alpha_{34} r^2 h_2 + [r^2 D^2 + rD - \alpha_{34} r^2] h_4 = 0.$$

Let

$$\delta = r D .$$

$$r^2 D^2 + rD = r\delta D + \delta = (\delta - 1)\delta + \delta = \delta^2 .$$

$$\begin{cases} [\delta^2 - (\alpha_{12} + \alpha_{32}) r^2] h_2 + \alpha_{32} r^2 h_4 = 0 , \\ \alpha_{34} r^2 h_2 + [\delta^2 - \alpha_{34} r^2] h_4 = 0 . \end{cases}$$

Analogy with the one-aquifer case indicates that the general solution of this pair of equations should be

$$\begin{cases} h_2 = N_1 I_0(fr) + N_2 K_0(fr) + N_3 I_0(gr) + N_4 K_0(gr) , \\ h_4 = j N_1 I_0(fr) + j N_2 K_0(fr) + m N_3 I_0(gr) + m N_4 K_0(gr) , \end{cases}$$

where the N's are arbitrary constants. This solution can be verified by substitution in the differential equations. The required formulas for derivatives of Bessel functions, which may be found in Tables of Integrals and Other Mathematical Data by Dwight, are

$$x I_n' = -n I_n + x I_{n-1} , \quad I_0' = I_1 ,$$

$$x K_n' = -n K_n - x K_{n-1} , \text{ and } K_0' = -K_1 .$$

From the physical conditions of the problem

$$\lim_{r \to \infty} h_2 = \lim_{r \to \infty} h_4 = 0 .$$

Since

$$I_0(x) \to \infty \text{ as } x \to \infty \text{ and } \lim_{x \to \infty} K_0(x) = 0 ,$$

$$N_1 = N_3 = 0 .$$

$$\begin{cases} h_2 = N_2 K_0(fr) + N_4 K_0(gr) , \\ h_4 = j N_2 K_0(fr) + m N_4 K_0(gr) . \end{cases}$$

The drawdown curves obtained from observations made during pumping tests have stright-line portions near the pump well. When r is small, then, approximately

$$K_0(fr) = -\left(\gamma + \ln \frac{fr}{2}\right) .$$

The equations of the straight-line portions of the drawdown curves are

$$h_2 = -(N_2+N_4)(\ln r - \ln 2 + \gamma) - N_2 \ln f - N_4 \ln g ,$$

$$h_4 = -(jN_2+mN_4)(\ln r - \ln 2 + \gamma) - jN_2 \ln f - mN_4 \ln g .$$

The quantities corresponding to the "radius of influence" in the one-aquifer case are the values of r at the points of intersection of those lines with the lines $h_2 = 0$ and $h_4 = 0$, respectively.

The Three-Aquifer Case

Sheet Flow.—Consider the flow toward a dam in a strip of the foundation one unit wide. Let x represent distance from the heel of the dam. Since h_2, h_4 and h_6 are independent of y, $\frac{\partial^2 h_2}{\partial y^2} = \frac{\partial^2 h_4}{\partial y^2} = \frac{\partial^2 h_6}{\partial y^2} = 0$ and the differential equations are

$$\frac{d^2h_2}{dx^2} - \alpha_{12} h_2 + \alpha_{32}(h_4 - h_2) = 0 ,$$

$$\frac{d^2h_4}{dx^2} - \alpha_{34}(h_4 - h_2) + \alpha_{54}(h_6 - h_4) = 0 ,$$

$$\frac{d^2h_6}{dx^2} - \alpha_{56}(h_6 - h_4) = 0 .$$

$$\begin{cases} \left[D^2 - (\alpha_{12}+\alpha_{32})\right] h_2 + \alpha_{32} h_4 = 0 , \\ \alpha_{34} h_2 + \left[D^2 - (\alpha_{34}+\alpha_{54})\right] h_4 + \alpha_{54} h_6 = 0 , \\ \alpha_{56} h_4 + \left[D^2 - \alpha_{56}\right] h_6 = 0 . \end{cases}$$

This system of simultaneous equations will be solved in the following manner. h_6 and h_4 will be eliminated to give a differential equation that can be solved for h_2. Then h_4 will be obtained from the first of the three equations, and h_6 from the second. Operate on the second equation with $\left[D^2 - \alpha_{56}\right]$ and subtract the product of α_{54} and the third equation.

$$\alpha_{34}\left[D^2 - \alpha_{56}\right] h_2 + \left\{\left[D^2 - \alpha_{56}\right]\left[D^2 - (\alpha_{34}+\alpha_{54})\right] - \alpha_{54}\alpha_{56}\right\} h_4 = 0 .$$

$$\alpha_{34}\left[D^2 - \alpha_{56}\right] h_2 + \left[D^4 - (\alpha_{34}+\alpha_{54}+\alpha_{56}) D^2 + \alpha_{34}\alpha_{56}\right] h_4 = 0 .$$

Multiply this equation by $-\alpha_{32}$, then operate on the first of the differential equations with $\left[D^4 - (\alpha_{34} + \alpha_{54} + \alpha_{56})\, D^2 + \alpha_{34}\, \alpha_{56}\right]$ and add results.

$$\left[D^4 - (\alpha_{34}+\alpha_{54}+\alpha_{56}) D^2 + \alpha_{34}\alpha_{56}\right]\left[D^2 - (\alpha_{12}+\alpha_{32})\right] h_2$$

$$-\alpha_{32}\,\alpha_{34}\left[D^2-\alpha_{56}\right]h_2=0.$$

$$\left\{D^6-\left[\alpha_{12}+\alpha_{32}+\alpha_{34}+\alpha_{54}+\alpha_{56}\right]D^4+\left[\alpha_{12}\left(\alpha_{34}+\alpha_{54}+\alpha_{56}\right)\right.\right.$$

$$\left.\left.+\alpha_{32}\left(\alpha_{54}+\alpha_{56}\right)+\alpha_{34}\,\alpha_{56}\right]D^2-\alpha_{12}\,\alpha_{34}\,\alpha_{56}\right\}h_2=0.$$

Let

$$a=\alpha_{12}+\alpha_{32}+\alpha_{34}+\alpha_{54}+\alpha_{56},$$

$$b=\alpha_{12}\left(\alpha_{34}+\alpha_{54}+\alpha_{56}\right)+\alpha_{32}\left(\alpha_{54}+\alpha_{56}\right)+\alpha_{34}\alpha_{56},$$

$$c=\alpha_{12}\,\alpha_{34}\,\alpha_{56}.$$

$$\left[D^6-aD^4+bD^2-c\right]h_2=0.$$

Since the physical conditions of the problem and the solutions in the cases of one and two aquifers indicate that there is nothing periodic about h_2, the above operator should factor as follows:

$$\left[D^6-aD^4+bD^2-c\right]=\left[D^2-p^2\right]\left[D^2-q^2\right]\left[D^2-r^2\right],$$

where p^2, q^2 and r^2, the roots of $z^3 - az^2 + bz - c = 0$, are real and positive. p, q, and r are taken to be positive.

$$\left[D-p\right]\left[D+p\right]\left[D-q\right]\left[D+q\right]\left[D-r\right]\left[D+r\right]h_2=0.$$

The general solution of this differential equation is

$$h_2=M_1e^{px}+M_2e^{-px}+M_3e^{qx}+M_4e^{-qx}+M_5e^{rx}+M_6e^{-rx},$$

where the M's are arbitrary constants. Now that h_2 is known, h_4 and h_6 can be obtained from the first two of the simultaneous equations.

$$h_4=\frac{1}{\alpha_{32}}\left[\left(\alpha_{12}+\alpha_{32}\right)-D^2\right]h_2.$$

Let

$$f=\frac{\alpha_{12}+\alpha_{32}-p^2}{\alpha_{32}},\quad g=\frac{\alpha_{12}+\alpha_{32}-q^2}{\alpha_{32}},\quad j=\frac{\alpha_{12}+\alpha_{32}-r^2}{\alpha_{32}}.$$

$$h_4=fM_1e^{px}+fM_2e^{-px}+gM_3e^{qx}+gM_4e^{-qx}+jM_5e^{rx}+jM_6e^{-rx}.$$

$$h_6=\frac{\left[\left(\alpha_{34}+\alpha_{54}\right)-D^2\right]h_4-\alpha_{34}h_2}{\alpha_{54}}.$$

Let

$$k = \frac{(\alpha_{34} + \alpha_{54} - p^2) f - \alpha_{34}}{\alpha_{54}}, \quad m = \frac{(\alpha_{34} + \alpha_{54} - q^2) g - \alpha_{34}}{\alpha_{54}},$$

$$n = \frac{(\alpha_{34} + \alpha_{54} - r^2) j - \alpha_{34}}{\alpha_{54}}.$$

$$h_6 = kM_1 e^{px} + kM_2 e^{-px} + mM_3 e^{qx} + mM_4 e^{-qx} + nM_5 e^{rx} + nM_6 e^{-rx}.$$

The general solution of the system of simultaneous differential equations is

$$\begin{cases} h_2 = M_1 e^{px} + M_2 e^{-px} + M_3 e^{qx} + M_4 e^{-qx} + M_5 e^{rx} + M_6 e^{-rx}, \\ h_4 = fM_1 e^{px} + fM_2 e^{-px} + gM_3 e^{qx} + gM_4 e^{-qx} + jM_5 e^{rx} + jM_6 e^{-rx}, \\ h_6 = kM_1 e^{px} + kM_2 e^{-px} + mM_3 e^{qx} + mM_4 e^{-qx} + nM_5 e^{rx} + nM_6 e^{-rx}, \end{cases}$$

where the M's are arbitrary constants. From the physical conditions of the problem,

$$\lim_{x \to \infty} h_2 = \lim_{x \to \infty} h_4 = \lim_{x \to \infty} h_6 = 0.$$

Since

$$e^{px} \to \infty, \ e^{qx} \to \infty, \text{ and } e^{rx} \to \infty \text{ as } x \to \infty, \ M_1 = M_3 = M_5 = 0.$$

$$\begin{cases} h_2 = M_2 e^{-px} + M_4 e^{-qx} + M_6 e^{-rx}, \\ h_4 = fM_2 e^{-px} + gM_4 e^{-qx} + jM_6 e^{-rx}, \\ h_6 = kM_2 e^{-px} + mM_4 e^{-qx} + nM_6 e^{-rx}. \end{cases}$$

APPENDIX B

Derivations of Formulas for Computation of Seepage and Uplift Pressures in Layered Systems

One-Aquifer Case

Seepage Under a Dam

The significance of the "resistance", x_r, of a blanketed aquifer is that, as far as h (0) and Q (0) are concerned, the infinite-blanketed aquifer in the region $x \geq 0$ is equivalent to an aquifer with the same permeability and thickness extending from x = 0 to $x = x_r$ and so arranged that the upper and lower boundaries are completely impervious and $h(x_r) = 0$. If there is no break in the blanket, then, for the purposes of computation, the infinite-blanketed aquifer on the pool side of the dam may be replaced by an aquifer of length x_r as indicated above. By symmetry, the same thing may be done on the other side of the dam. Let L be the base width of the dam and H be the head differential. The underseepage, Q, per unit length of dam is given by the formula

$$Q = k_2 \frac{H}{L + 2x_r}(z_2 \cdot 1) = \frac{C_2 H}{L + 2x_r},$$

where

$$x_r = \frac{1}{a} = \frac{r_e}{1.123}$$

Uplift Pressures

In the portion of the aquifer beneath a dam the hydraulic gradient is a constant equal to Q/C_2, so the hydraulic head varies linearly with x. Let x equal zero at the center line of the dam and increase in the upstream direction. The curve h vs. x should be symmetrical with respect to the point (O,H/2).

$$h = \frac{H}{2} - \frac{Q}{C_2}x, \quad \left(-\frac{L}{2} \leq x \leq \frac{L}{2}\right),$$

where h is the absolute value of the hydraulic head referred to head water. By symmetry, the same equation applies when the direction of x is reversed and h represents hydraulic head referred to tail water.

Two-Aquifer Case

Seepage Under a Dam

In the two-aquifer case, the quantities corresponding to the "resistance" of a blanketed aquifer have values that depend on boundary conditions as well as the constants of the formation. For this reason it is not convenient to use them in the derivation of formulas for underseepage. Let H be the head differential, and let x = 0 at the heel of the dam, x = -L/2 at the centerline of

the dam. Each of the curves (h_2 vs. x and h_4 vs. x) should be symmetrical with respect to the point (-L/2, H/2). The underseepage, Q, is the flow under the dam.

$$Q = -\left[Q_2\left(-L/2\right) + Q_4\left(-L/2\right)\right] = -\left[Q_2 + Q_4\right] .$$

Expressions have already been obtained for $h_2(x)$ and $h_4(x)$ in the regions

$$-L/2 \le x \le 0 \quad \text{and} \quad 0 \le x .$$

When

$$-L/2 \le x \le 0 ,$$

$$h_2 = R_1 + R_2 x + R_3 e^{cx} + R_4 e^{-cx} ,$$

$$h_4 = R_1 + R_2 x + s R_3 e^{cx} + s R_4 e^{-cx} .$$

When

$$0 \le x ,$$

$$h_2 = M_2 e^{-fx} + M_4 e^{-gx} ,$$

$$h_4 = j M_2 e^{-fx} + m M_4 e^{-gx} .$$

Considerations of symmetry and of continuity of head and gradient give a set of simultaneous equations that can be solved for Q_2 and Q_4:

$$h_2\left(-L/2\right) = h_4\left(-L/2\right) = H/2 ; \tag{a}$$

$$Dh_i\left(-L/2\right) = Q_i/C_i , \quad (i = 2, 4) ; \tag{b}$$

$$\lim_{x \to 0^-} h_i(x) = \lim_{x \to 0^+} h_i(x) , \quad (i = 2, 4) ; \tag{c}$$

$$\lim_{x \to 0^-} Dh_i(x) = \lim_{x \to 0^+} Dh_i(x) , \quad (i = 2, 4) . \tag{d}$$

From equation (a),

$$R_3 e^{-\frac{cL}{2}} + R_4 e^{\frac{cL}{2}} = 0 ,$$

$$R_1 - R_2 \frac{L}{2} = \frac{H}{2} .$$

From equation (b),

$$R_2 + cR_3 e^{-\frac{cL}{2}} - cR_4 e^{\frac{cL}{2}} = Q_2/C_2 ,$$

$$R_2 + scR_3 e^{-\frac{cL}{2}} - scR_4 e^{\frac{cL}{2}} = Q_4/C_4 .$$

From equation (c),

$$R_1 + R_3 + R_4 = M_2 + M_4 ,$$

$$R_1 + sR_3 + sR_4 = jM_2 + mM_4 .$$

From equation (d),

$$R_2 + cR_3 - cR_4 = -fM_2 - gM_4 ,$$

$$R_2 + scR_3 - scR_4 = -jfM_2 - mgM_4 .$$

Rewriting the above equations,

$$e^{-\frac{cL}{2}} R_3 + e^{\frac{cL}{2}} R_4 = 0,$$

$$R_1 - \frac{L}{2} R_2 = \frac{H}{2},$$

$$R_2 + ce^{-\frac{cL}{2}} R_3 - ce^{\frac{cL}{2}} R_4 - \frac{Q_2}{C_2} = 0,$$

$$R_2 + sce^{-\frac{cL}{2}} R_3 - sce^{\frac{cL}{2}} R_4 - \frac{Q_4}{C_4} = 0,$$

$$R_1 + R_3 + R_4 - M_2 - M_4 = 0,$$

$$R_1 + sR_3 + sR_4 - jM_2 - mM_4 = 0,$$

$$R_2 + cR_3 - cR_4 + fM_2 + gM_4 = 0,$$

$$R_2 + scR_3 - scR_4 + jfM_2 + mgM_4 = 0 .$$

Cramer's rule will be used to solve these equations for Q_2 and Q_4.

$$\Delta = \begin{vmatrix} 0 & 0 & e^{-\frac{cL}{2}} & e^{\frac{cL}{2}} & 0 & 0 & 0 & 0 \\ 1 & -\frac{L}{2} & 0 & 0 & 0 & 0 & 0 & 0 \\ 0 & 1 & ce^{-\frac{cL}{2}} & -ce^{\frac{cL}{2}} & 0 & 0 & -1/C_2 & 0 \\ 0 & 1 & sce^{-\frac{cL}{2}} & -sce^{\frac{cL}{2}} & 0 & 0 & 0 & -1/C_4 \\ 1 & 0 & 1 & 1 & -1 & -1 & 0 & 0 \end{vmatrix} ,$$

$$\Delta = \begin{vmatrix} 1 & 0 & s & s & -j & -m & 0 & 0 \\ 0 & 1 & c & -c & f & g & 0 & 0 \\ 0 & 1 & sc & -sc & jf & mg & 0 & 0 \end{vmatrix}$$

which reduces to

$$\Delta = -\frac{e^{-\frac{cL}{2}}}{C_2 C_4} \begin{vmatrix} \frac{L}{2}(1-j) & (s-j)(1-e^{cL}) & j-m \\ 1+f\frac{L}{2} & -c(1+e^{cL})+f(1-e^{cL}) & g-f \\ 1-j & c(j-s)(1+e^{cL}) & g(m-j) \end{vmatrix}.$$

$$\overline{\Delta Q_2} = \begin{vmatrix} 0 & 0 & e^{-\frac{cL}{2}} & e^{\frac{cL}{2}} & 0 & 0 & 0 & 0 \\ 1 & -\frac{L}{2} & 0 & 0 & 0 & 0 & \frac{H}{2} & 0 \\ 0 & 1 & ce^{-\frac{cL}{2}} & -ce^{\frac{cL}{2}} & 0 & 0 & 0 & 0 \\ 0 & 1 & sce^{-\frac{cL}{2}} & -sce^{\frac{cL}{2}} & 0 & 0 & 0 & -\frac{1}{C_4} \\ 1 & 0 & 1 & 1 & -1 & -1 & 0 & 0 \\ 1 & 0 & s & s & -j & -m & 0 & 0 \\ 0 & 1 & c & -c & f & g & 0 & 0 \\ 0 & 1 & sc & -sc & jf & mg & 0 & 0 \end{vmatrix},$$

which reduces to

$$\overline{\Delta Q_2} = \frac{He^{-\frac{cL}{2}}}{2C_4} \begin{vmatrix} c(e^{\frac{cL}{2}}-1)^2 & -f & -g \\ (s-1)(1-e^{cL}) & 1-j & 1-m \\ c(s-1)(1+e^{cL}) & f(1-j) & g(1-m) \end{vmatrix}.$$

$$\overline{\Delta Q_4} = \begin{vmatrix} 0 & 0 & e^{-\frac{cL}{2}} & e^{\frac{cL}{2}} & 0 & 0 & 0 & 0 \\ 1 & -\frac{L}{2} & 0 & 0 & 0 & 0 & 0 & \frac{H}{2} \\ 0 & 1 & ce^{-\frac{cL}{2}} & -ce^{\frac{cL}{2}} & 0 & 0 & -\frac{1}{C_2} & 0 \\ 0 & 1 & sce^{-\frac{cL}{2}} & -sce^{\frac{cL}{2}} & 0 & 0 & 0 & 0 \\ 1 & 0 & 1 & 1 & -1 & -1 & 0 & 0 \end{vmatrix},$$

$$\overline{\Delta Q_4} = \begin{vmatrix} 1 & 0 & s & s & -j & -m & 0 & 0 \\ 0 & 1 & c & -c & f & g & 0 & 0 \\ 0 & 1 & sc & -sc & jf & mg & 0 & 0 \end{vmatrix}$$

which reduces to

$$\overline{\Delta Q_4} = \frac{He^{-\frac{cL}{2}}}{2C_2} \begin{vmatrix} sc\left(e^{\frac{cL}{2}}-1\right)^2 & -jf & -mg \\ (s-1)(1-e^{cL}) & 1-j & 1-m \\ c(s-1)(1+e^{cL}) & f(1-j) & g(1-m) \end{vmatrix} .$$

The underseepage, Q, per unit length of dam is given by the formula

$$Q = -\left[Q_2 + Q_4\right], \quad \text{where}$$

$$Q_2 = \frac{\overline{\Delta Q_2}}{\Delta} , \quad Q_4 = \frac{\overline{\Delta Q_4}}{\Delta} ,$$

$$\overline{\Delta Q_2} = C_2 H \begin{vmatrix} c\left(e^{\frac{cL}{2}}-1\right)^2 & -f & -g \\ (s-1)(1-e^{cL}) & 1-j & 1-m \\ c(s-1)(1+e^{cL}) & f(1-j) & g(1-m) \end{vmatrix} ,$$

$$\overline{\Delta Q_4} = C_4 H \begin{vmatrix} sc\left(e^{\frac{cL}{2}}-1\right)^2 & -jf & -mg \\ (s-1)(1-e^{cL}) & 1-j & 1-m \\ c(s-1)(1+e^{cL}) & f(1-j) & g(1-m) \end{vmatrix} ,$$

$$\Delta = -2 \begin{vmatrix} \frac{L}{2}(1-j) & (s-j)(1-e^{cL}) & j-m \\ 1+f\frac{L}{2} & -c(1+e^{cL})+f(1-e^{cL}) & g-f \\ 1-j & c(j-s)(1+e^{cL}) & g(m-j) \end{vmatrix} .$$

The above expressions for $\overline{\Delta Q_2}$, $\overline{\Delta Q_4}$, and Δ were multiplied by $2\,C_2C_4\,e^{\frac{cL}{2}}$. Since only the ratios of those quantities are used, the results are not affected.

Approximate formulas for computing underseepage in the two-aquifer case can be obtained by assuming that there is no vertical flow through either blanket in the region beneath the dam.

When

$$0 \le x ,$$

$$h_2 = M_2 e^{-fx} + M_4 e^{-gx} ,$$

$$h_4 = j M_2 e^{-fx} + m M_4 e^{-gx} .$$

When

$$-\frac{L}{2} \le x \le 0 ,$$

$$h_i = \frac{Q_i}{C_i}\left(x + \frac{L}{2}\right) + \frac{H}{2} , \quad (i = 2,4) ,$$

since $Q_i = C_i \frac{dh_i}{dx}$ = a constant, and $h_i\,(-L/2) = H/2$. Continuity of head and gradient in each aquifer requires that

$$\lim_{x \to 0^-} h_i(x) = \lim_{x \to 0^+} h_i(x) , \quad (i = 2, 4) , \tag{e}$$

$$\lim_{x \to 0^-} Dh_i(x) = \lim_{x \to 0^+} Dh_i(x) , \quad (i=2,4). \tag{f}$$

From equation (e),

$$\frac{H}{2} + \frac{L Q_2}{2 C_2} = M_2 + M_4 ,$$

$$\frac{H}{2} + \frac{L Q_4}{2 C_4} = j M_2 + m M_4 .$$

From equation (f),

$$\left.\begin{aligned} \frac{Q_2}{C_2} &= -fM_2 - gM_4 \,, \\ \frac{Q_4}{C_4} &= -fjM_2 - gmM_4 \,. \end{aligned}\right\} \qquad (g)$$

Multiplying the last pair of equations by L/2 and subtracting from the preceding pair of equations gives

$$\frac{H}{2} = \left(1+f\frac{L}{2}\right)M_2 + \left(1+g\frac{L}{2}\right)M_4 \,,$$

$$\frac{H}{2} = j\left(1+f\frac{L}{2}\right)M_2 + m\left(1+g\frac{L}{2}\right)M_4 \,.$$

Let

$$\Delta = \begin{vmatrix} 1 & 1 \\ j & m \end{vmatrix}, \quad \Delta_1 = \begin{vmatrix} 1 & 1 \\ 1 & m \end{vmatrix}, \quad \Delta_2 = \begin{vmatrix} 1 & 1 \\ j & 1 \end{vmatrix} \,.$$

By Cramer's rule,

$$\left(1+f\frac{L}{2}\right)M_2 = \frac{H\Delta_1}{2\Delta} \,, \quad \left(1+g\frac{L}{2}\right)M_4 = \frac{H\Delta_2}{2\Delta} \,.$$

$$M_2 = \frac{H\Delta_1}{(2+fL)\Delta} = \frac{H(m-1)}{(2+fL)(m-j)} \,,$$

$$M_4 = \frac{H\Delta_2}{(2+gL)\Delta} = \frac{H(1-j)}{(2+gL)(m-j)} \,.$$

Substituting these values of M_2 and M_4 in equations (g) gives

$$Q_2 = \frac{C_2 H}{j-m}\left[\frac{f(m-1)}{2+fL} + \frac{g(1-j)}{2+gL}\right] \,,$$

$$Q_4 = \frac{C_4 H}{j-m}\left[j\frac{f(m-1)}{2+fL} + m\frac{g(1-j)}{2+gL}\right] \,.$$

The underseepage, Q, per unit length dam is given by the formula

$$Q = -\left[Q_2 + Q_4\right] \,,$$

where Q_2 and Q_4 are obtained from the preceding pair of equations.

Uplift Pressures

In the portion of the upper aquifer beneath a dam the absolute value of the hydraulic head referred to head water is given by

$$h_2 = R_1 + R_2 x + R_3 e^{cx} + R_4 e^{-cx}, \left(-\frac{L}{2} \le x \le 0\right),$$

where x = 0 at the heel of the dam. The first four of the eight simultaneous equations that were used in determining underseepage can be solved for the coefficients in this equation.

$$e^{-\frac{cL}{2}} R_3 + e^{\frac{cL}{2}} R_4 = 0,$$

$$R_1 - \frac{L}{2} R_2 = \frac{H}{2},$$

$$R_2 + ce^{-\frac{cL}{2}} R_3 - ce^{\frac{cL}{2}} R_4 = \frac{Q_2}{C_2},$$

$$R_2 + sce^{-\frac{cL}{2}} R_3 - sce^{\frac{cL}{2}} R_4 = \frac{Q_4}{C_4}.$$

$$\Delta = \begin{vmatrix} 0 & 0 & e^{-\frac{cL}{2}} & e^{\frac{cL}{2}} \\ 1 & -\frac{L}{2} & 0 & 0 \\ 0 & 1 & ce^{-\frac{cL}{2}} & -ce^{\frac{cL}{2}} \\ 0 & 1 & sce^{-\frac{cL}{2}} & -sce^{\frac{cL}{2}} \end{vmatrix},$$

which reduces to

$$\Delta = 2c(1-s) \cdot$$

$$\overline{\Delta R_1} = \begin{vmatrix} 0 & 0 & e^{-\frac{cL}{2}} & e^{\frac{cL}{2}} \\ \frac{H}{2} & -\frac{L}{2} & 0 & 0 \\ \frac{Q_2}{C_2} & 1 & ce^{-\frac{cL}{2}} & -ce^{\frac{cL}{2}} \\ \frac{Q_4}{C_4} & 1 & sce^{-\frac{cL}{2}} & -sce^{\frac{cL}{2}} \end{vmatrix}$$

$$= cH(1-s) + cL\left[\frac{Q_4}{C_4} - s\frac{Q_2}{C_2}\right].$$

Since

$$s = -\frac{C_2}{C_4} \quad \text{and} \quad Q = -Q_2 - Q_4,$$

$$\overline{\Delta R_1} = cH(1-s) - \frac{cLQ}{C_4} .$$

$$\overline{\Delta R_2} = \begin{vmatrix} 0 & 0 & e^{-\frac{cL}{2}} & e^{\frac{cL}{2}} \\ 1 & \frac{H}{2} & 0 & 0 \\ 0 & \frac{Q_2}{C_2} & ce^{-\frac{cL}{2}} & -ce^{\frac{cL}{2}} \\ 0 & \frac{Q_4}{C_4} & sce^{-\frac{cL}{2}} & -sce^{\frac{cL}{2}} \end{vmatrix}$$

$$= 2c\left(\frac{Q_4}{C_4} - s\frac{Q_2}{C_2}\right) = -\frac{2cQ}{C_4} .$$

$$\overline{\Delta R_3} = \begin{vmatrix} 0 & 0 & 0 & e^{\frac{cL}{2}} \\ 1 & -\frac{L}{2} & \frac{H}{2} & 0 \\ 0 & 1 & \frac{Q_2}{C_2} & -ce^{\frac{cL}{2}} \\ 0 & 1 & \frac{Q_4}{C_4} & -sce^{\frac{cL}{2}} \end{vmatrix}$$

$$= e^{\frac{cL}{2}}\left(\frac{Q_2}{C_2} - \frac{Q_4}{C_4}\right) .$$

$$\overline{\Delta R_4} = \begin{vmatrix} 0 & 0 & e^{-\frac{cL}{2}} & 0 \\ 1 & -\frac{L}{2} & 0 & \frac{H}{2} \\ 0 & 1 & ce^{-\frac{cL}{2}} & \frac{Q_2}{C_2} \\ 0 & 1 & sce^{-\frac{cL}{2}} & \frac{Q_4}{C_4} \end{vmatrix}$$

$$= -e^{-\frac{cL}{2}}\left(\frac{Q_2}{C_2} - \frac{Q_4}{C_4}\right) .$$

Using Cramer's rule,

$$R_1 = \frac{\overline{\Delta R_1}}{\Delta} = \frac{1}{2c(1-s)}\left[cH(1-s) - \frac{cLQ}{C_4}\right]$$

$$= \frac{H}{2} - \frac{LQ}{2(1-s)C_4} = \frac{H}{2} - \frac{LQ}{2(C_2+C_4)},$$

$$R_2 = \frac{\overline{\Delta R_2}}{\Delta} = \frac{1}{2c(1-s)}\left[-\frac{2cQ}{C_4}\right] = -\frac{Q}{(1-s)C_4} = -\frac{Q}{C_2+C_4},$$

$$R_3 = \frac{\overline{\Delta R_3}}{\Delta} = \frac{e^{\frac{cL}{2}}}{2c(1-s)}\left[\frac{Q_2}{C_2} - \frac{Q_4}{C_4}\right],$$

$$R_4 = \frac{\overline{\Delta R_4}}{\Delta} = \frac{-e^{-\frac{cL}{2}}}{2c(1-s)}\left[\frac{Q_2}{C_2} - \frac{Q_4}{C_4}\right].$$

$$h_2 = \frac{H}{2} - \frac{LQ}{2(C_2+C_4)} - \frac{Qx}{C_2+C_4} + \frac{e^{c\left(\frac{L}{2}+x\right)}}{2c(1-s)}\left[\frac{Q_2}{C_2} - \frac{Q_4}{C_4}\right] - \frac{e^{-c\left(\frac{L}{2}+x\right)}}{2c(1-s)}\left[\frac{Q_2}{C_2} - \frac{Q_4}{C_4}\right]$$

$$= \frac{H}{2} - \frac{Q}{C_2+C_4}\left(\frac{L}{2}+x\right) + \left[\frac{Q_2}{C_2} - \frac{Q_4}{C_4}\right]\frac{\sinh c\left(\frac{L}{2}+x\right)}{c(1-s)}, \left(-\frac{L}{2} \le x \le 0\right).$$

Let

$$X = \frac{L}{2} + x.$$

$$h_2 = \frac{H}{2} - \frac{Q}{C_2+C_4}X + \left[\frac{Q_2}{C_2} - \frac{Q_4}{C_4}\right]\frac{\sinh cX}{c(1-s)}, \quad \left(0 \le X \le \frac{L}{2}\right).$$

Since the curve h_2 versus X should be symmetrical with respect to the point (O, H/2), this equation also applies in the interval $\left(-\frac{L}{2} \le X \le O\right)$. Thus,

$$h_2 = \frac{H}{2} - \frac{Q}{C_2+C_4}X + \left[\frac{Q_2}{C_2} - \frac{Q_4}{C_4}\right]\frac{\sinh cX}{c(1-s)}, \quad \left(-\frac{L}{2} \le X \le \frac{L}{2}\right).$$

Because of symmetry this equation is also correct when X increases in the downstream direction and h_2 is the hydraulic head referred to tail water.

An approximate formula for the head in the portion of the upper aquifer that is beneath the dam can be obtained by assuming that the part of the lower

blanket that is beneath the dam is impervious. In this case the formula derived for a single aquifer will apply when h and Q are replaced by h_2 and $-Q_2$, respectively.

$$h_2 = \frac{H}{2} + \frac{Q_2}{C_2} X \ , \quad \left(-\frac{L}{2} \le x \le \frac{L}{2}\right) .$$

This formula can be written in another form for comparison with the precise formula.

$$h_2 = \frac{H}{2} + \frac{Q_2 + Q_4}{C_2 + C_4} X + \left[\frac{Q_2}{C_2} - \frac{Q_2 + Q_4}{C_2 + C_4}\right] X .$$

$$\left[\frac{Q_2}{C_2} - \frac{Q_2 + Q_4}{C_2 + C_4}\right] = \frac{C_4 Q_2 - C_2 Q_4}{C_2 (C_2 + C_4)} \cdot \frac{C_2 C_4}{C_2 C_4}$$

$$= \left[\frac{Q_2}{C_2} - \frac{Q_4}{C_4}\right] \frac{C_4}{C_2 + C_4} .$$

$$\left[\frac{Q_2}{C_2} - \frac{Q_2 + Q_4}{C_2 + C_4}\right] = \left[\frac{Q_2}{C_2} - \frac{Q_4}{C_4}\right] \frac{C_4}{-C_4 s + C_4} .$$

$$= \left[\frac{Q_2}{C_2} - \frac{Q_4}{C_4}\right] \frac{1}{1 - s} \cdot \frac{c}{c} .$$

$$Q_2 + Q_4 = -Q .$$

$$h_2 = \frac{H}{2} - \frac{Q}{C_2 + C_4} X + \left[\frac{Q_2}{C_2} - \frac{Q_4}{C_4}\right] \frac{cX}{c(1-s)} , \left(-\frac{L}{2} \le X \le \frac{L}{2}\right) .$$

Three-Aquifer Case

Seepage Under a Dam

The first method presented for computation of underseepage in the case of two aquifers is too cumbersome to be practicable in the three-aquifer case. Approximate formulas for computing underseepage in this case can be obtained by assuming that there is no vertical flow through any blanket in the region beneath the dam. Let x = 0 at the heel of the dam, x = -L/2 at the center line of the dam. Each of the curves h_i versus x (i = 2, 4, 6) should be symmetrical with respect to the point (-L/2, H/2), where H is the head differential across the dam.

When

$$0 \leq x ,$$

$$h_2 = M_2 e^{-px} + M_4 e^{-qx} + M_6 e^{-rx} ,$$

$$h_4 = f M_2 e^{-px} + g M_4 e^{-qx} + j M_6 e^{-rx} ,$$

$$h_6 = k M_2 e^{-px} + m M_4 e^{-qx} + n M_6 e^{-rx} .$$

When

$$-\frac{L}{2} \leq x \leq 0 ,$$

$$h_i = \frac{Q_i}{C_i}\left(x + \frac{L}{2}\right) + \frac{H}{2} , \quad (i = 2,4,6) ,$$

since $Q_i = C_i \frac{dh_i}{dx}$ = a constant, and $h_i\left(-\frac{L}{2}\right) = \frac{H}{2}$. Continuity of head and gradient in each aquifer requires that

$$\lim_{x \to 0^-} h_i(x) = \lim_{x \to 0^+} h_i(x), \quad (i=2,4,6), \tag{h}$$

$$\lim_{x \to 0^-} Dh_i(x) = \lim_{x \to 0^+} Dh_i(x), \quad (i=2,4,6). \tag{i}$$

From equation (h),

$$\frac{H}{2} + \frac{L Q_2}{2 C_2} = M_2 + M_4 + M_6 ,$$

$$\frac{H}{2} + \frac{L Q_4}{2 C_4} = f M_2 + g M_4 + j M_6 ,$$

$$\frac{H}{2} + \frac{L Q_6}{2 C_6} = k M_2 + m M_4 + n M_6 .$$

From equation (i),

$$\left.\begin{aligned} \frac{Q_2}{C_2} &= -p M_2 - q M_4 - r M_6 , \\ \frac{Q_4}{C_4} &= -fp M_2 - gq M_4 - jr M_6 , \\ \frac{Q_6}{C_6} &= -kp M_2 - mq M_4 - nr M_6 . \end{aligned}\right\} \tag{j}$$

Multiplying the last three equations by L/2 and subtracting from the preceding three equations gives

$$\frac{H}{2} = \left(1+p\frac{L}{2}\right)M_2 + \left(1+q\frac{L}{2}\right)M_4 + \left(1+r\frac{L}{2}\right)M_6 ,$$

$$\frac{H}{2} = f\left(1+p\frac{L}{2}\right)M_2 + g\left(1+q\frac{L}{2}\right)M_4 + j\left(1+r\frac{L}{2}\right)M_6 ,$$

$$\frac{H}{2} = k\left(1+p\frac{L}{2}\right)M_2 + m\left(1+q\frac{L}{2}\right)M_4 + n\left(1+r\frac{L}{2}\right)M_6 .$$

Let

$$\Delta = \begin{vmatrix} 1 & 1 & 1 \\ f & g & j \\ k & m & n \end{vmatrix}, \quad \Delta_1 = \begin{vmatrix} 1 & 1 & 1 \\ 1 & g & j \\ 1 & m & n \end{vmatrix}, \quad \Delta_2 = \begin{vmatrix} 1 & 1 & 1 \\ f & 1 & j \\ k & 1 & n \end{vmatrix}, \quad \Delta_3 = \begin{vmatrix} 1 & 1 & 1 \\ f & g & 1 \\ k & m & 1 \end{vmatrix} .$$

By Cramer's rule,

$$\left(1+p\frac{L}{2}\right)M_2 = \frac{H\Delta_1}{2\Delta}, \left(1+q\frac{L}{2}\right)M_4 = \frac{H\Delta_2}{2\Delta}, \left(1+r\frac{L}{2}\right)M_6 = \frac{H\Delta_3}{2\Delta} .$$

$$M_2 = \frac{H\Delta_1}{(2+pL)\Delta}, \quad M_4 = \frac{H\Delta_2}{(2+qL)\Delta}, \quad M_6 = \frac{H\Delta_3}{(2+rL)\Delta} .$$

Substituting these values of M_2, M_4, and M_6 in equations (j) gives

$$Q_2 = -\frac{C_2 H}{\Delta}\left[\frac{p\Delta_1}{2+pL} + \frac{q\Delta_2}{2+qL} + \frac{r\Delta_3}{2+rL}\right] ,$$

$$Q_4 = -\frac{C_4 H}{\Delta}\left[f\frac{p\Delta_1}{2+pL} + g\frac{q\Delta_2}{2+qL} + j\frac{r\Delta_3}{2+rL}\right] ,$$

$$Q_6 = -\frac{C_6 H}{\Delta}\left[k\frac{p\Delta_1}{2+pL} + m\frac{q\Delta_2}{2+qL} + n\frac{r\Delta_3}{2+rL}\right] .$$

The underseepage, Q, per unit length of dam is given by the formula

$$Q = -\left[Q_2 + Q_4 + Q_6\right] ,$$

where Q_2, Q_4, and Q_6 are obtained from the preceding three equations.

Uplift Pressures

The first method presented for computation of uplift pressures under a dam in the case of two aquifers would be very cumbersome in the three-aquifer case. An approximate formula can be obtained by assuming that there is no vertical flow through the part of the middle blanket that lies beneath the dam. In this case the formula derived for a single aquifer will apply when h and Q are replaced by h_2 and $-Q_2$, respectively.

$$h_2 = \frac{H}{2} + \frac{Q_2}{C_2} x, \quad \left(-\frac{L}{2} \leq x \leq \frac{L}{2}\right).$$

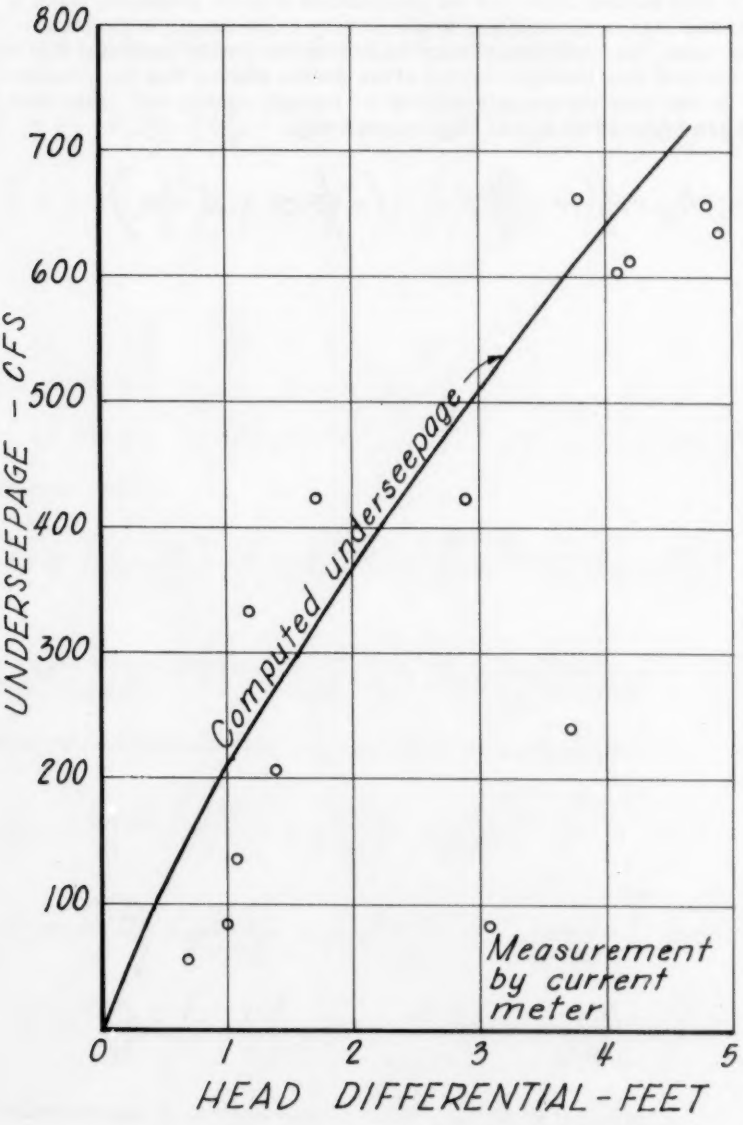

Levee 37
S-9 to S-32
Fig. 1

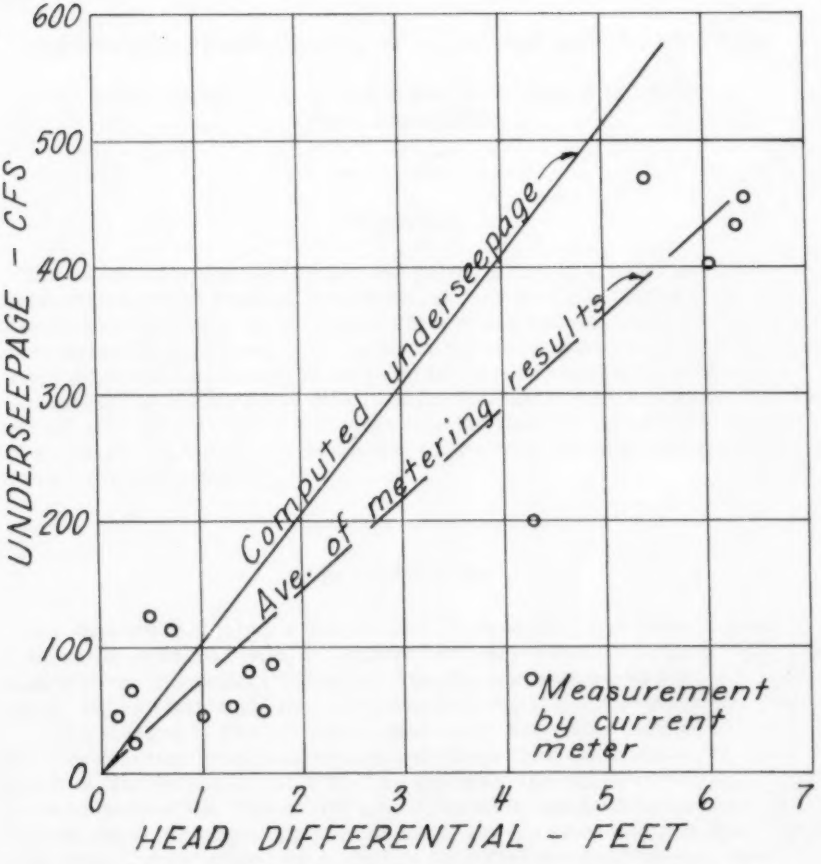

Levees 33 & 37
S-34 to S-9

Fig. 2

Paper 1728 August, 1958 SM 3

Journal of the
SOIL MECHANICS AND FOUNDATIONS DIVISION
Proceedings of the American Society of Civil Engineers

DESIGN AND PERFORMANCE OF VERMILION DAM, CALIFORNIA

K. Terzaghi,[1] Hon. M. ASCE and T. M. Leps,[2] M. ASCE
(Proc. Paper 1728)

SYNOPSIS

This paper describes the design and performance of a zoned earth dam located in the Sierra Nevada, California, on marginal glacial deposits. The pattern of stratification is so intricate that it was impracticable to determine all the essential geological features of the subsoil in advance of construction. Therefore, it was necessary to check on the design assumption during construction and to modify some details of the original design in accordance with the findings. As a result of this procedure the finished structure is as safe and satisfactory as if all the essential properties of the site had been known in advance of construction.

INTRODUCTION

The damsite is located at an elevation of about 7500 feet above sea level, in the valley of Mono Creek, a northern tributary of the South Fork of the San Joaquin River in central California. The site was investigated for the first time in 1918 to determine the watershed and capacity of the reservoir. Exploratory drilling in 1924 revealed unfavorable foundation conditions for the concrete dam then being considered, and the project was temporarily abandoned. It was reconsidered in 1940 on the basis that an earthfill dam could be shown to be feasible. The earthfill dam, as built, has a maximum height of 160 feet above the original ground surface, and the crest has a length of about 4,300 feet. Construction was started in May 1953 and the dam was completed at the end of 1954. The reservoir formed by the dam adds 125,000 acre feet to the total storage capacity of the reservoirs which have previously been built by the Southern California Edison Company in the San Joaquin basin. A

Note: Discussion open until January 1, 1959. To extend the closing date one month, a written request must be filed with the Executive Secretary, ASCE. Paper 1728 is part of the copyrighted Journal of the Soil Mechanics and Foundations Division, Proceedings of the American Society of Civil Engineers, Vol. 84, No. SM 3, August, 1958.

1. Prof. Emeritus, Harvard Univ., Cambridge, Mass.
2. Chf. Civ. Engr., Southern Calif. Edison Co., Los Angeles, Calif.

description of the entire hydroelectric power development utilizing the water resources of the basin, and a brief account of the construction of the Vermilion Dam have been presented by Mr. R. W. Spencer, Manager of Engineering Department, Southern California Edison Company, in the March 1955 issue of Civil Engineering.

Geology of the Damsite

Before the Pleistocene ice age, the present location of Mono Creek Valley was occupied by an erosion valley carved out of granite. Locally the surface of the granite was covered by the remnants of a flow of pre-Pleistocene basaltic lava. At the damsite, the bottom of the old riverbed is located at a depth of about 250 feet below the deepest point of the present valley. An outcrop of the basaltic lava is located a short distance upstream from the damsite, west of the old course of Mono Creek.

During the Pleistocene ice age, the valleys descending from the summit region of the Sierra Nevada were repeatedly invaded by valley glaciers descending to an altitude of a few hundred feet below that of the damsite. The glaciers deposited subglacial, marginal and fluvio-glacial materials in the valleys. At the damsite, the youngest member of the glacial deposits consists of a set of low, terminal moraines resting on a locally very impervious glacial till. At the west end of the damsite, the remnants of a kame terrace were encountered.

The upper portion of the fluvio-glacial sediments located beneath the youngest till sheet contains one large and several smaller lenses of silt with a very variable thickness. The continuity of at least the youngest fluvio-glacial and glacial lake deposits was disrupted by small erosion valleys carved out by streamlets emerging from the glaciers and subsequently backfilled with silty to clean sand and sand-gravel mixtures. Therefore, the pattern of stratification of the subsoil at the damsite is so erratic that it was impracticable to determine its average coefficient of permeability on the basis of the results of laboratory tests.

Upstream from the damsite, the subsoil consists of coarse-grained, somewhat silty, fluvio-glacial and post-glacial river deposits with an almost horizontal surface, underlying an area of the valley floor with a length of several miles and a width of several thousand feet. Formerly, Mono Creek meandered on this floor. In recent geological times, the meandering creek started to erode, forming incised meanders with steep side slopes. At the damsite, the creek has cut to a depth of about 40 feet below the old valley floor.

One of the important considerations indicating the reasonableness of constructing a dam on such a site was that the Sierra Nevada Mountains contain nearby many natural lakes and tarns formed entirely by glacial debris fills left across their outlets. These have stood for centuries without important water loss from percolation. Why then could not an artificial fill be made to approximate these natural fills and thereby obtain a sound structure, built entirely of country materials?

The details of the glacial geology of the damsite were investigated by Mr. J. H. Birman during the summers of 1950 and 1951, under the general supervision of Dr. Ian Campbell of California Institute of Technology. The location of the terminal moraines and the kame terrace at the west abutment are shown in Figure 1. Figure 2 is an idealized geological profile of the subsoil along the centerline of the dam. The results of the geological survey

Fig. 1. Glacial Geology of Vermilion Valley.

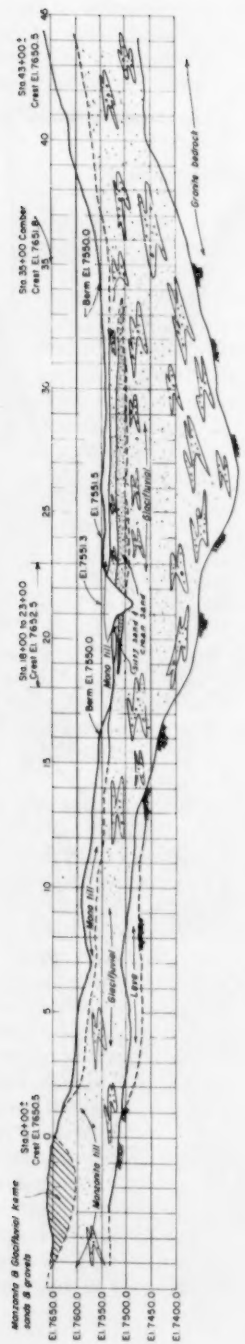

Fig. 2. Subsurface profile along axis of dam.

furnished the basis for a tentative interpretation of the boring records and for making reasonably realistic assumptions concerning the subsoil conditions for design purposes.

Subsoil Explorations

In 1924, 18 boreholes were made at and in the proximity of the present site of the dam. On the basis of the results, the project was temporarily abandoned. In 1946, the site exploration was resumed under the general direction of R. W. Spencer and under the direct supervision of the co-author, T. M. Leps. The exploratory work included 14 borings with an average depth of 100 feet and a maximum depth of 269 feet. The exploration also included the digging of 2 test pits with a depth of about 30 feet each, of 3 open cuts across terminal moraines and several bulldozer trenches on the steep slopes of the present erosion valley of Mono Creek. Eight of the 14 drill holes were located along the centerline of the dam and spaced abouy 600 feet apart. The other holes were drilled in the proximity of the toes of the dam.

The crest of the dam is about 4300 feet long and the base has a maximum width of 800 feet. If the drill holes had been spaced about 20 feet both ways, subsoil exploration would have required several thousand drill holes and a prohibitive amount of testing. Yet, judging from the pattern of stratification visible on the sides of open cuts, for instance on the exposure shown in Figure 3, the results would still have left a wide margin for interpretation. Therefore, at a site like that of Vermilion Dam, the exploratory drill holes merely serve the purpose of supplementing the results of the geological survey. At the site of Vermilion Dam, 14 borings sufficied to obtain all of the required information. Any additional exploratory work would have increased the cost of exploration without furnishing any significant contribution to our knowledge of the site.

The tests on the samples recovered from drill holes and test pits included grain size determination and permeability tests. Even within the fluvio-glacial deposits the value of the coefficient of permeability k was extremely variable. It ranged from between 10^{-1} and 10^{-6} cm/sec. On account of the silt content of the sediments, the average was rather low, and the coefficient of permeability in a vertical direction, k_v, was consistently smaller than the corresponding value k_h, for horizontal directions.

The results of the permeability tests made it possible to obtain at least an upper and lower limiting value for the loss of water, Q, due to seepage out of the reservoir, using the flow net method. Assuming:

1. $k_h = 9 \times 10^{-3}$ cm/sec and $k_v = 10^{-3}$ cm/sec, Q = 29 cfs and
2. $k_h = k_v \times 10^{-3}$ cm/sec, Q = 4 cfs

The observations described under a later heading entitled "Seepage Losses" will show that the total leakage at full reservoir is roughly equal to 6 cfs which is slightly greater than the foregoing estimated lower limiting value.

Construction Materials

Within the area surrounding the damsite, the following construction materials were available in significant quantities: stony till, fluvio-glacial sand

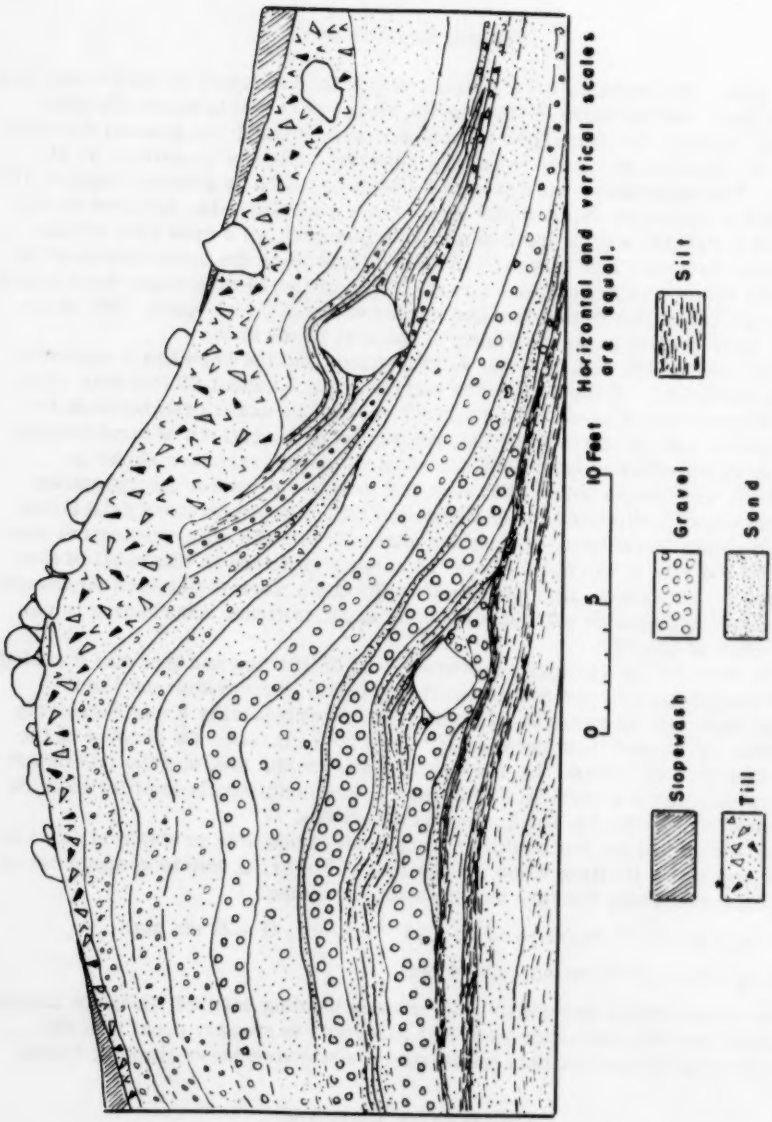

Fig. 3. Fluvio-glacial cored moraine.

and gravel, silty pond deposits, and the weathered top layer covering the unweathered river deposits upstream from the damsite. Clay deposits were conspicuously absent. Even the pond or lake deposits contained no more than a trace of clay. This is probably due to the steep gradient of the water courses which were fed by the glaciers. Most of the clay was removed in suspension.

Because of the absence of clay, all efforts were concentrated, in the earlier stages of the exploratory work, on locating suitable materials for the "impervious" section of the proposed earth dam and for the construction of an "impervious" blanket to be placed upstream from the dam. After the borrow pits were opened, it was found to be equally difficult to find very pervious material, because the bulk of the glacial outwash contained at least traces of silt or rock flour.

On the basis of the results of the geological survey, four general areas were selected as potential sources for suitable construction materials. The location of these areas with reference to the damsite are shown in Figure 4. Area #1, at a distance of about one mile west of the dam consisted of a marshy meadow covering the surface of a stratified to varved deposit of fine silty sand and silt which was laid down in a pond. In order to estimate the available quantity, auger borings with an average depth of 20 feet and a maximum depth of 90 feet, spaced about 400' both ways were made. It was found that the laboratory coefficient of permeability of the material which ranged between 10^{-6} and 10^{-2} cm/sec, averaged 10^{-5} cm/sec. The natural water content of the material was above optimum. Therefore, it was decided to lower the water table beneath the meadow about 5 feet by means of drainage trenches with a depth of about 10 feet (see Figure 4). Since the deposit contained more or less continuous layers of fine, clean sand, drainage was effective. Most of the material derived from Area #1 was classified as impervious and was used for constructing the blanket and core.

Borrow Areas #2 and #3 were close to and north of the eastern portion of the damsite. The water table was located at an average depth of 20 feet below the original ground surface. Most of the material encountered in these areas consisted of fluvio-glacial sand and gravel, containing scattered boulders with a diameter up to several feet. The coefficient of permeability, k, of the material ranged between 10^{-2} and 10^{-5} cm/sec, depending on the silt content. The most pervious material was placed in contact with the downstream face of the "impervious" core and on the base of the downstream portion of the dam. The remainder of the downstream portion and the upstream portion of the dam were made of the siltier varieties of the borrow material, with a permeability range of 10^{-3} to 10^{-4} cm/sec.

Area #4 was located on the wide and almost horizontal floor of the Mono Creek Valley upstream and within a distance of from two to four miles from the damsite. The deposit was explored by means of auger holes, 10 feet deep, spaced 700 feet in the direction of the valley and 500 feet at right angles to it. The borings showed that the area was underlain by pervious and semi-pervious fluvio-glacial deposits and river sand and gravel. The uppermost 3 ft. of the deposit were slightly weathered and relatively impervious. The water table was located at an average depth of 9 feet below the valley floor. By excavating the uppermost portion of the deposit to an average depth of 5 feet and mixing the pervious and impervious materials present within this layer, 1.3 million cu. yds. of compacted fill material with an average permeability of 10^{-5} cm/sec obtained. Such a blend of the top 5 feet of Area #4 furnished the bulk

Fig. 4. Plan showing location of borrow areas and drainage ditches.

of the "impervious" core of the dam. The mixing was satisfactorily performed by excavating the material along a vertical face with a height of about 5 feet, using Sierra Loaders. A portable sprinkler system was used to add moisture to the surface materials. The output averaged 20 cu. yd. per minute for each loader.

The material located beneath the 5 foot thick excavated layer was relatively pervious sand and gravel having an average coefficient of permeability of 10^{-3} cm/sec. Some 1.5 million cu. yds. of it was excavated and built into the upstream and downstream portions of the dam. Some of the borrow pit excavation for such material extended well below groundwater table, necessitating the excavation of the drainage ditch shown on Figure 4. The pervious materials were loaded by DW-20 scrapers assisted by two push-cats.

Design of the Dam

The design of the dam was governed by the following considerations. (1) Due to the scarcity of "impervious" materials, the construction of a zoned earth dam was indicated. (2) The average permeability of the substrata is high, and (3) the cost of a cutoff of over 200 feet to bedrock would be prohibitive. Therefore, it was necessary (1) to cover the ground surface upstream from the dam with an impervious blanket, and (2) to provide adequate drainage facilities along the downstream toe to eliminate the possibility of a failure due to piping.

Figure 5 is a plan of the dam, Figure 6a is a vertical section through the highest portion of the dam at about Station 21+00 and Figure 6b a section at about Station 28+00. The "impervious" core of the dam rises above the downstream fringe of the "impervious" blanket which covers the natural ground to some distance upstream from the dam. According to the original design, the fill upstream from the core was to be made of silty sand and gravel with an average coefficient of permeability k of less than 2×10^{-3} cm/sec, and the fill downstream from the core out of relatively clean sand and gravel with a k value of more than 2×10^{-3} cm/sec.

The water entering the pervious downstream section of the dam through its base flows into a toe drain installed in a trench with a maximum depth of 20 feet. Figure 7 is a typical section through the toe drain. Between Station 22 and 28 where the natural ground rises beneath the downstream slope to an elevation of about 70 feet above the toe trench (see Figure 6b) the toe drain was supplemented by an interior drain located between the core and the upper edge of the buried north slope of Mono Creek (see also Figure 5).

Because of the predominantly horizontal stratification of the subsoil and the presence in the subsoil of lenses and layers of silt with unknown horizontal dimensions underlain by very pervious sediments, it was conceivable that the hydrostatic pressure acting on the base of silty layers might lift the floor of the valley downstream from the dam. Therefore, it was decided to supplement the toe drain with relief wells as shown in Figures 7 and 10. At the maximum section of the dam, where the danger of heave was greatest, the wells were drilled to an average depth of 70 feet and the spacing ranged between 50 feet and 100 feet. Beyond the maximum section of the dam and the outer boundaries of the Mono Creek stream bed, the wells were drilled to a depth of about 50 feet and the spacing was increased to 200 feet (see Figure 10).

The stability computation for the dam was made by the Swedish Circle

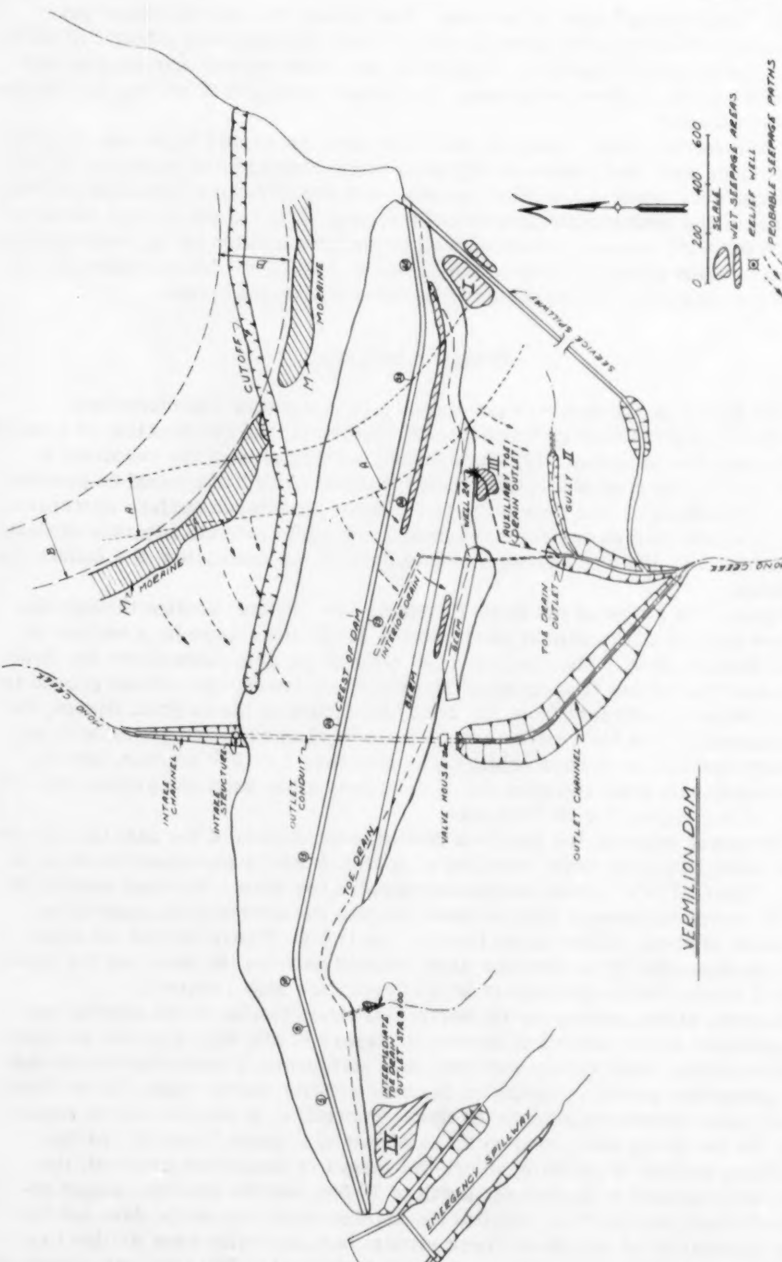

Fig. 5. General plan showing wet areas and probable subsurface seepage paths.

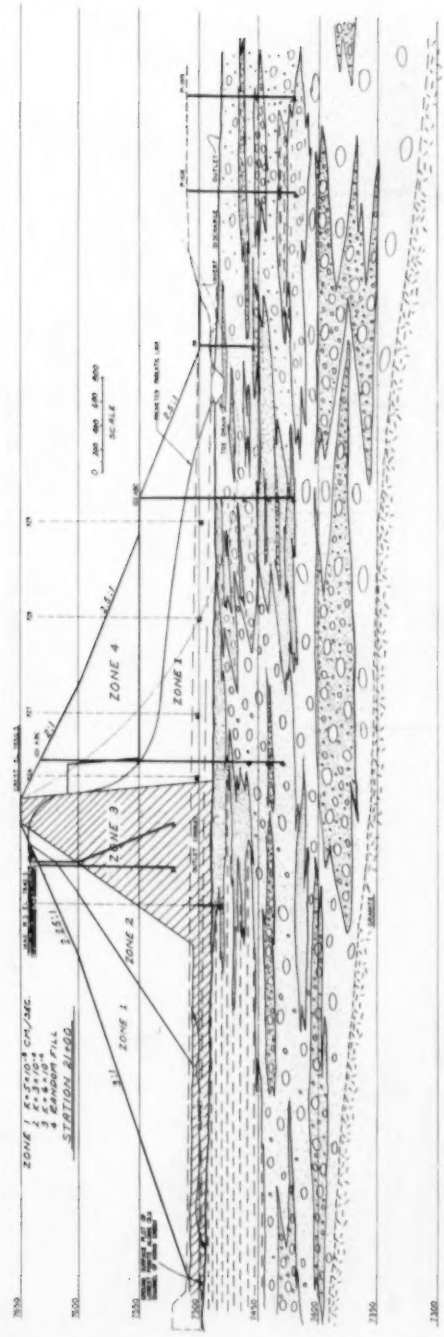

Fig. 6.a. Cross section of dam at maximum section.

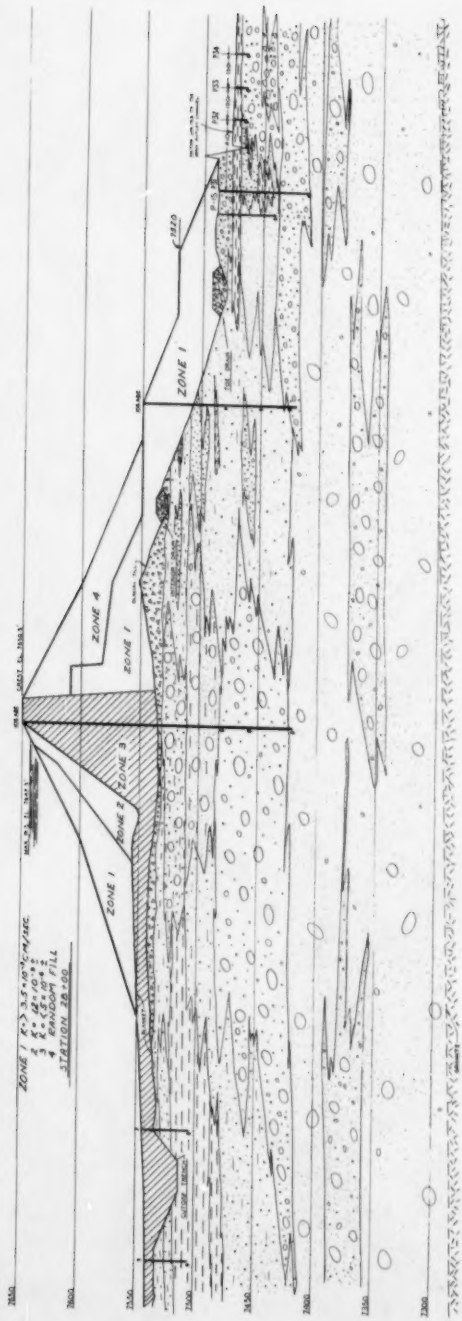

Fig. 6 b. Cross section of dam at Station 28+00.

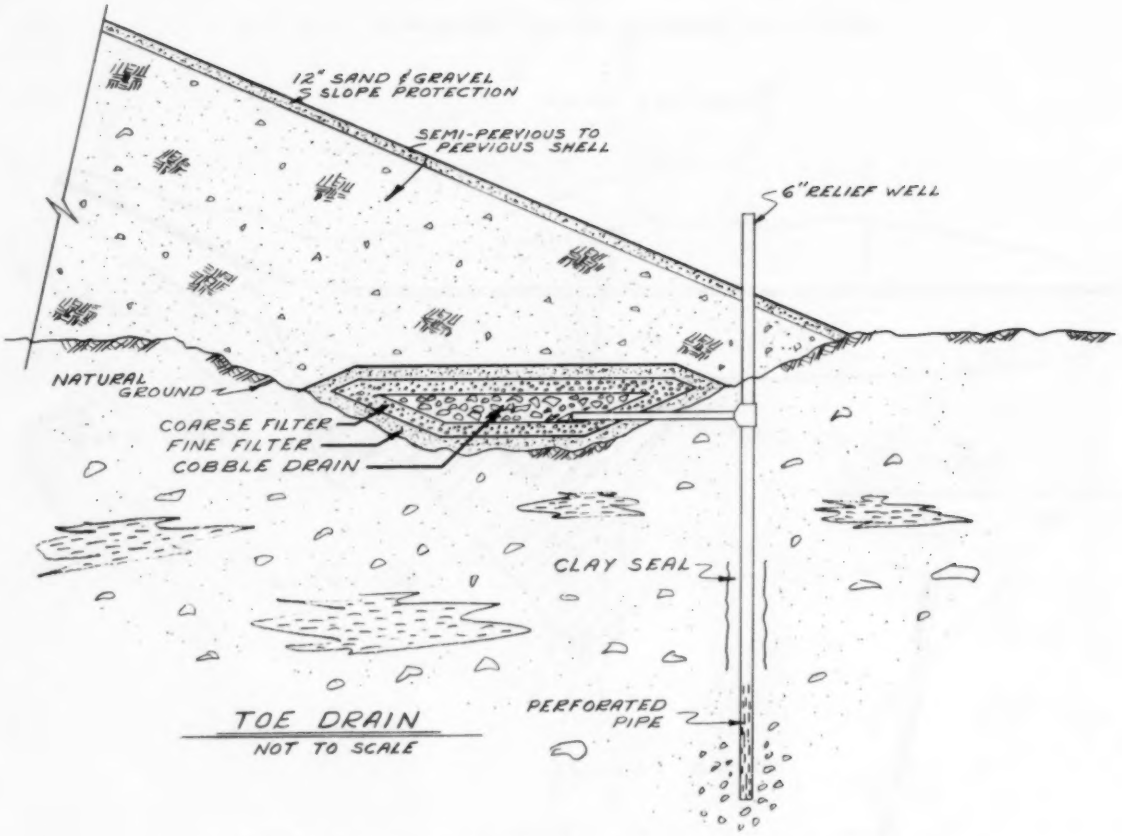

Fig. 7. Typical section through toe drain and relief well.

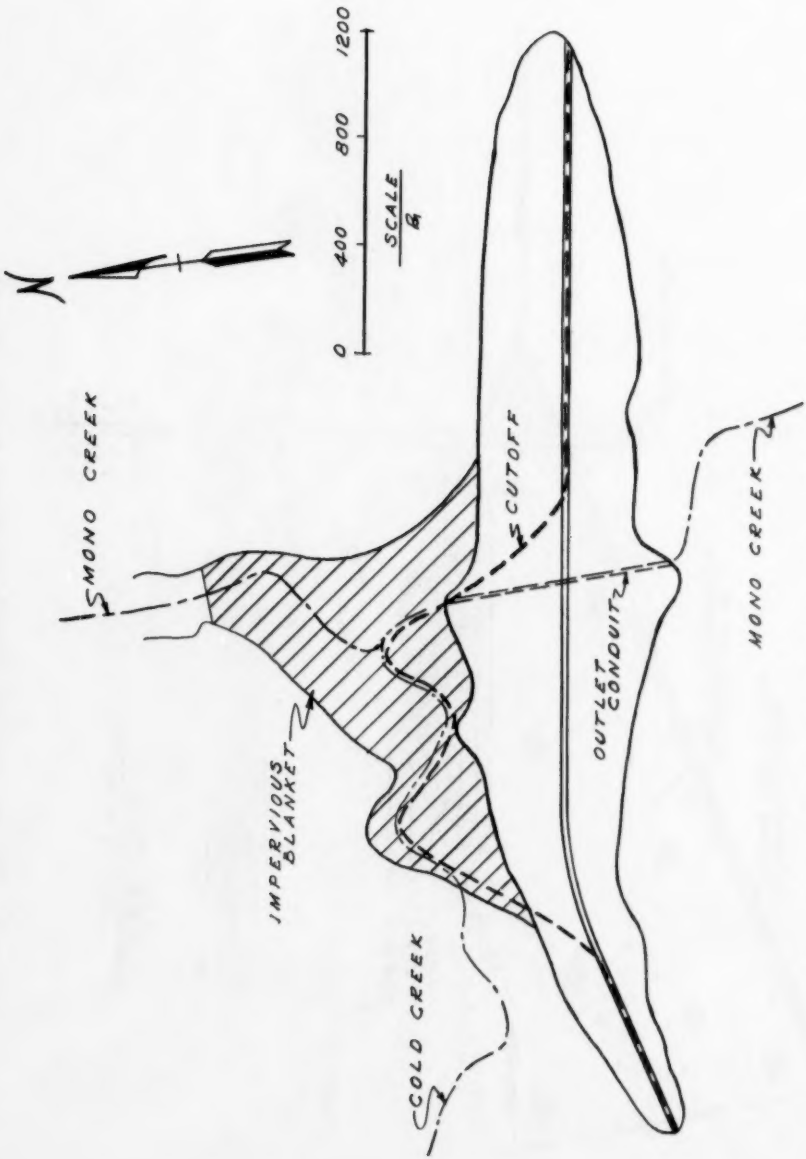

Fig. 8 a. Preliminary design of cutoff and blanket.

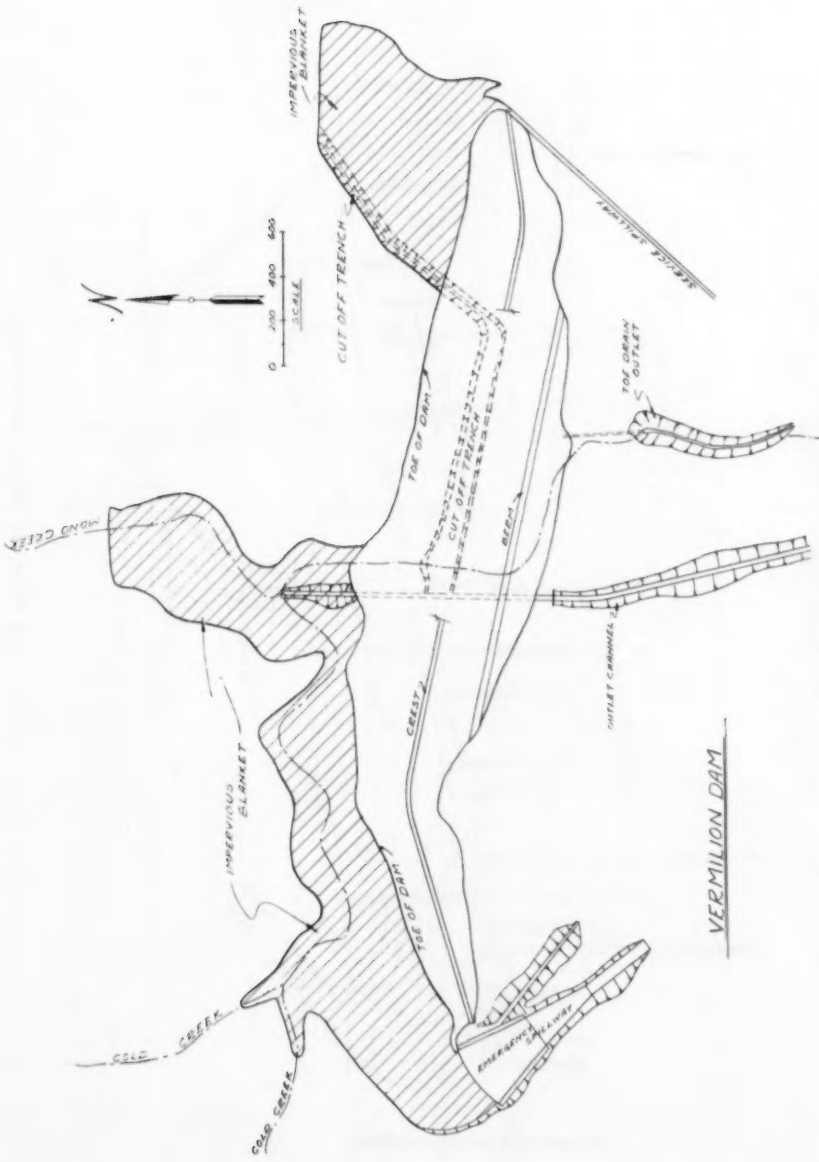

Fig. 8 b. Proposed construction of cutoff and blanket.

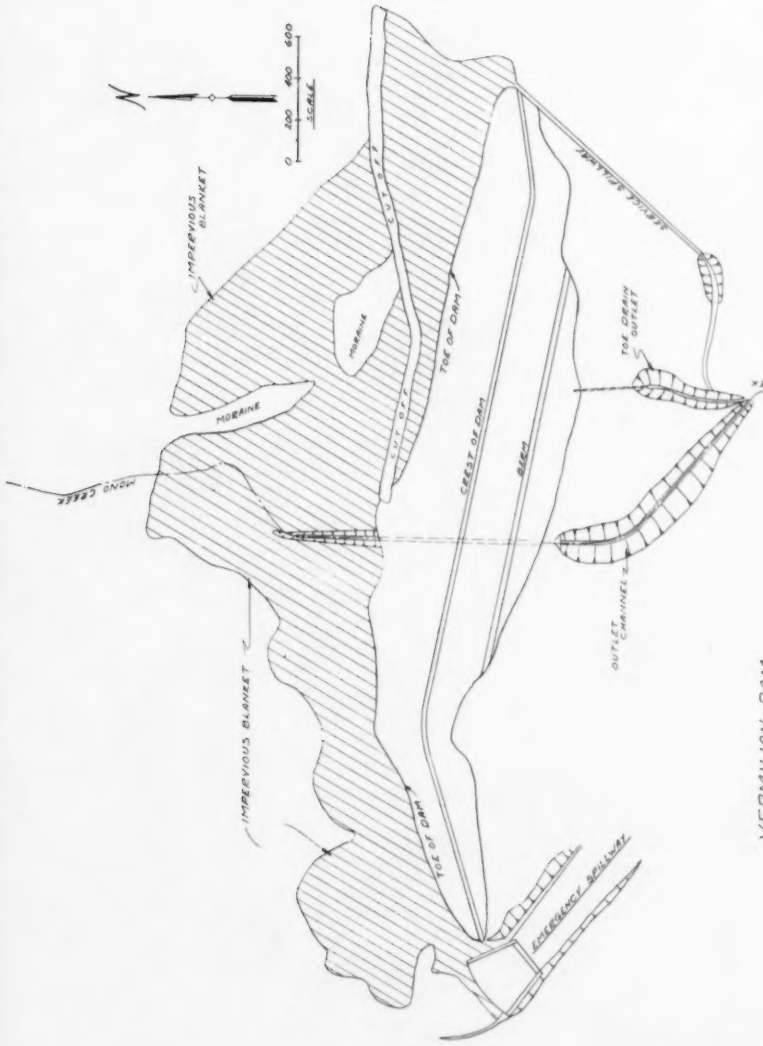

Fig. 8 c. Cutoff and blanket as constructed.

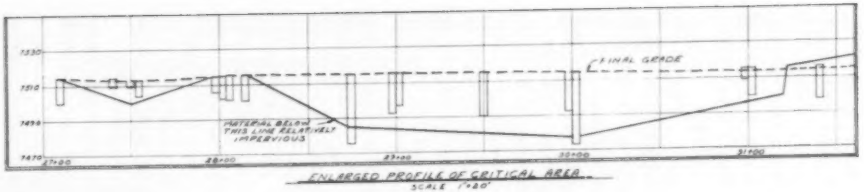

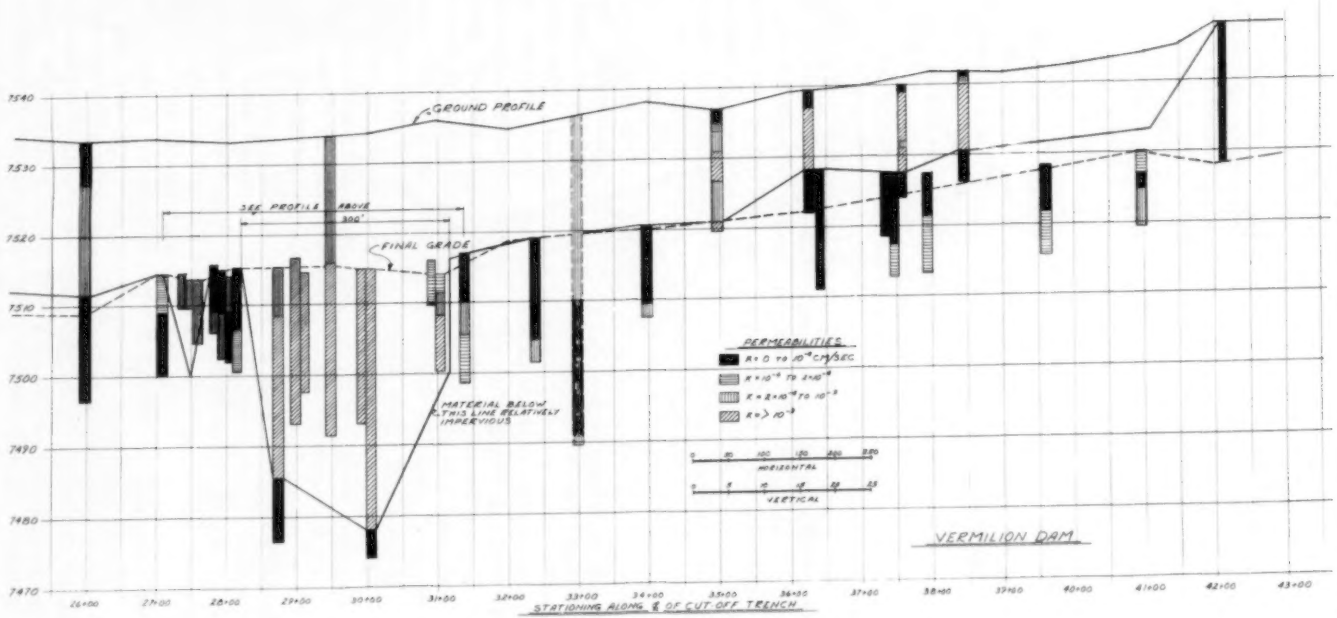

Fig. 9. Exploratory borings for cutoff trench east of Mono Creek.

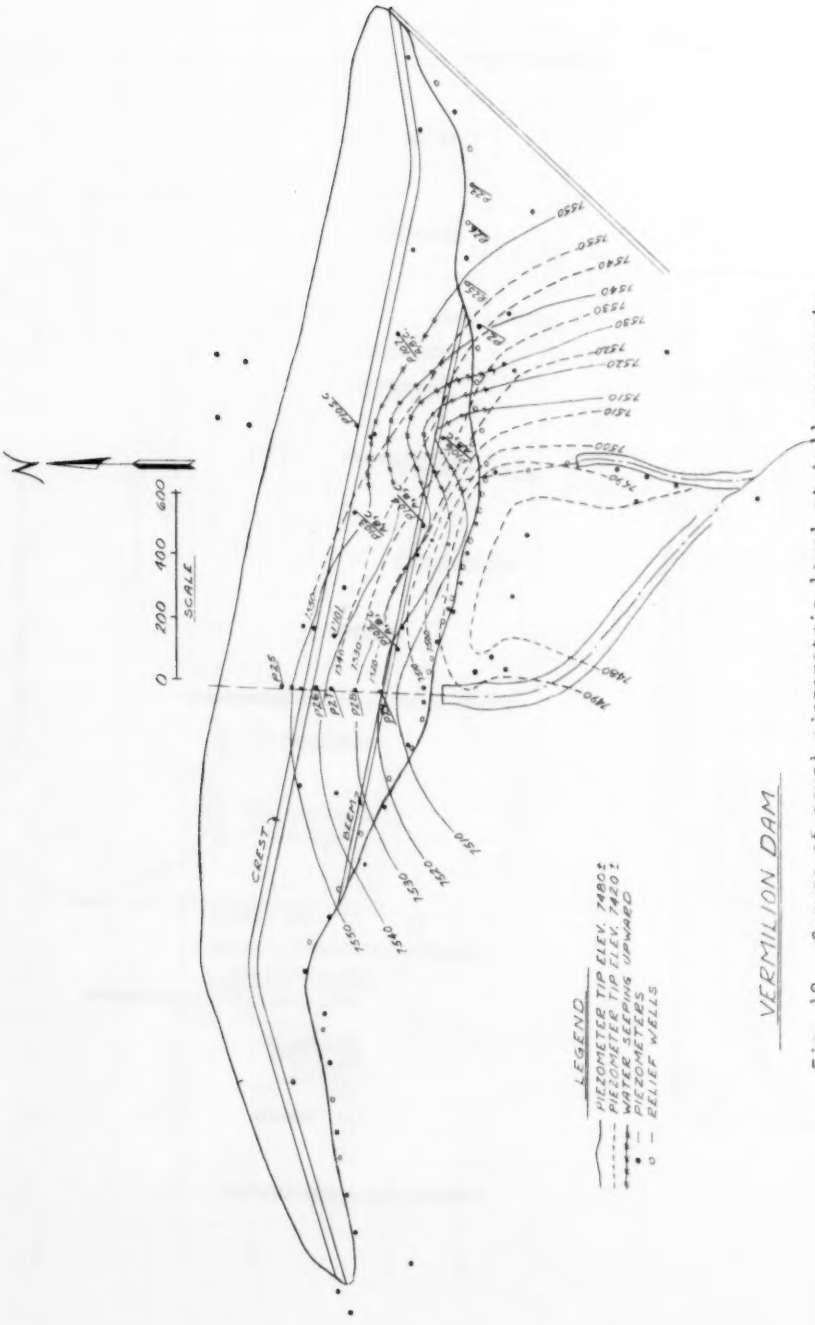

Fig. 10. Curves of equal piezometric level at full reservoir.

method. In any investigated section, a large portion of the critical circle was located in the natural ground, beneath the base of the fill. The factor of safety with respect to sliding along the potential surface of sliding depends to a large extent on the average intensity of the porewater pressures along the surface. Because of the relatively high permeability and low compressibility of the core material, it was justified to assume that the construction porewater pressures would be negligible. The porewater pressures due to leakage out of the reservoir are determined by the pattern of seepage through the subsoil. Such information was unknown until the reservoir was filled for the first time. Therefore, the stability computations were made on the basis of what appeared to be the highest porewater pressures compatible with general geological characteristics of the subsoil.

Trial computations showed that the loss of water due to seepage out of the reservoir could turn out to be prohibitive unless the core of the dam was supplemented by an "impervious" upstream blanket. Due to the presence of lenses and layers of silt in the subsoil, the foundation of the dam represents an irregularly stratified, layered system. Mono Creek and its western tributary, Cold Creek, have cut trenches into the system to a depth of about 40 feet, thus permitting the water to enter the highly pervious strata located between silty ones. Therefore, it was decided during the preliminary investigation to seal the bed and the slopes of Mono Creek by means of a blanket extending to a distance of about 1300 feet upstream from the core of the dam, and to seal in a similar manner the bottom and the south slope of Cold Creek between Mono Creek and the west abutment of the dam.

On the eastern slope of Mono Creek, a silt stratum with a variable thickness was exposed. The outcrop appeared to extend from a point about 1000 feet downstream from the damsite to a distance of more than 2000 feet upstream from it. The surface of the silt stratum was located at a depth ranging from 10 to 25 feet. When the preliminary design was prepared, it was believed that the silt stratum underlies the entire eastern half of the damsite. Therefore, it was proposed to construct east of Mono Creek, a cutoff extending from the base of the core into the silt stratum as shown in Figure 8a. Subsequently, the modification shown in Figure 8b was proposed to offset expected seepage through the east abutment area. However, before the construction drawings were prepared, exploration disclosed that the dam was located above a narrow but deep pervious gap in the silt stratum. Therefore, the location for the cutoff was shifted into the position shown in Figure 8c. Core and cutoff are connected with each other by an "impervous blanket." The thickness of the blanket is 13 feet from the core to the cutoff, whereas the thickness of the blanket in the valley of Mono Creek decreases from about 13 feet at the core to 6 feet at its upstream boundary.

The service spillway with a discharge capacity of 1200 cfs is located at the east abutment of the dam (see Figure 5). It is a concrete weir with a crest elevation of 7634.5, equipped with one 15 ft. x 8 ft. radial gate. Floods in excess of 1200 cfs can escape over a broad emergency spillway at the west abutment, through a gully and into Mono Creek.

The outlet structure was constructed in a cut in foundation soils near the maximum section of the dam. It follows the foot of the right hand slope of Mono Creek, from the upstream to the downstream toe of the dam. It consists of a reinforced concrete culvert, 800 feet long, housing a 54" diameter steel pressure conduit, controlled at the downstream end by a Howell-Bunger valve. The water is admitted into the steel outlet conduit through a reinforced concrete inlet structure. At the intersection between core and outlet conduit,

the base of the core is located at a minimum depth of 5 feet below the base of the outlet conduit. Therefore at that location the outlet conduit is entirely surrounded with impervious core material.

Construction of the Dam

The construction of the dam was started in May 1953. It required the following quantities of fill material:

1,236,824 cu. yds.	Core material and blanket under dam
1,027,208 cu. yds.	Upstream blanket material and cutoff
2,538,319 cu. yds.	Semi-pervious and pervious materials for the upstream and downstream portion of the dam
486,546 cu. yds.	Slope and blanket protection materials and filter materials
5,288,897 TOTAL	(Compacted Volume)

Prior to construction, the damsite was occupied by an old, high-altitude forest. The trees had diameters up to 48" and the ground was locally strewn with big boulders. Therefore, the stripping of the site was a major operation. The boulders were blasted and all stones larger than 6 inches were removed and stockpiled, to be used as riprap. The trees were either uprooted or cut at an elevation of one foot above ground level. All stumps and roots were removed to a distance of 20 feet beyond the outer boundaries of the dam. After this preliminary operation, the area to be occupied by the embankment was harrowed or disked to a depth of 6 inches and moistened by sprinkling to bring the water content of the processed layer up to optimum. Prior to placing the embankment the top layer was cross-compacted by 8 passes of a 50-ton rubber tired roller. The fill material was spread in 8 inch layers and compacted in the same manner as the aforementioned top layer.

Construction proper started in June 1953 by making the excavations for the toe drain, the outlet conduit, and for the outlet channel. In order to excavate for the outlet conduit, located in the normal course of the stream, it was necessary to divert Mono Creek at a point 1200 feet upstream from the upstream toe of the dam. The creek was diverted into an open cut channel excavated along the foot of the left hand slope of the riverbed. Since the bottom of the trench for the outlet conduit, at the site of its intersection with the core of the dam, was located about 5' below the water table, the trench was drained by pumping from well points.

In September 1953, the outlet conduit was concreted and the intake channel was provided with an "impervious" blanket. At that stage, Mono Creek was diverted from its artificial bed into the lined inlet channel and through a bypass pipe into the outlet conduit, thereupon the balance of the blanketing operations in the Mono Creek Valley upstream from the dam was completed. Henceforth, Mono Creek flowed through the outlet conduit into the outlet channel (see Figure 5), and entered the old stream at a point about 800 feet downstream from the downstream toe. None of its waters entered the toe trench.

In August 1953, the drilling of the relief wells was commenced. Figure 7 shows a typical relief well installation. In drilling the relief wells, it was noted that silts from higher strata would cave into the hole. To prevent this, a seal of bentonite, 6 to 8 feet thicker than the silt layer was placed around the well casing above the pervious strata. This confined the flowing water to

the casing, and prevented the fine sands and silts from washing down and into the pervious strata which is essential to the efficient operation of the well. The flow of water towards the pervious filter well produces a natural filter surrounding this section.

Modifications of Design During Construction

The excavation for the cutoff was started October 1953 at the upper edge of the eastern (left hand) slope of the creek channel. As excavation proceeded in an easterly direction, the depth of excavation to reach the silt stratum was generally about 22' below the broad flat floor of Vermilion Valley. At a distance of about 1400 feet from the east abutment, contact with the silt stratum was lost. In order to get reliable information concerning this unanticipated feature of the subsurface geology, subsoil exploration by borings was resumed in the Spring of 1954. It involved the drilling of 28 boreholes with depths up to 90 feet. In many holes, undisturbed samples were taken at points spaced 5 to 10 feet vertically. On each sample, mechanical analysis and permeability tests were performed.

Some of the 28 holes were drilled along the centerline of the proposed cutoff, east of the point where contact with the silt stratum was lost, and the others north of the centerline. The results of the borings along or close to the centerline are shown in Figure 9. The diagram also reveals the erratic character of the pattern of stratification of the fluvio-glacial deposits. The results of the borings, combined with those of the preceding geological survey, led to the conclusion that the cutoff, for a distance of about 300 feet, is located above a gap in the silt stratum, A in Figure 5. This gap was eroded by a meltwater stream and then backfilled with fluvio-glacial sediments before the youngest till sheet was deposited. During the last advance of the ice, the stream channel deposit A was buried beneath a till sheet and a set of terminal moraines.

After the ice retreated from the terminal moraine M in Figure 5, a stream channel B was eroded along the inner or northern edge of the moraine and backfilled with fluvio-glacial sediments. At a distance of about 600 feet north of the cutoff, the bottom of the younger stream channel deposit B intersects the top surface of the older one, A. Hence at that point, water can flow out of the reservoir through the deposit B into and through the deposit A under the dam towards the left hand slope of Mono Creek downstream from the dam.

Because of this geological situation, it was decided to excavate the cutoff trench to a maximum depth of 25 feet along the entire line indicated on Figure 5 in spite of the fact that over a length of 300 feet the base of the cutoff is located on fluvio-glacial sediments and not on silt. However, in order to reduce the quantity of water which will escape out of the reservoir into the stream channel deposit A, the section of the cutoff located above the gap was supplemented by a blanket extending from the cutoff in an upstream direction along B, Figure 5, to a point beyond the area where the stream channel deposits A, and B intersect. The resulting layout for cutoff and blanket is shown in Figure 8c.

Another modification of the original project became necessary when it was realized that the available quantity of highly pervious sand and gravel was smaller than anticipated. The cost of screening the silty embankment material would have been prohibitive. Therefore, it was decided to subdivide the

downstream section of the dam into a very pervious and a less pervious section. The very pervious material was placed on the base of the dam and against the lower part of the downstream face of the core of the dam as shown in Figures 6a and 6b Zone I. Since the estimated line of seepage is located entirely within the very pervious material, this modification of the design had no effect on the stability conditions.

Finally, the necessity of some minor modifications of the original design was realized when the observations during the first filling of the reservoir began to reveal the pattern of subsurface drainage. These modifications involved chiefly the installation of drains in the natural ground downstream from the dam.

Means for Observation

The performance of the dam has been observed by means of piezometers, discharge gages, and settlement reference points. The pattern of subsurface drainage and the performance of the relief wells is disclosed by the piezometer readings. The relationship between the water level in the reservoir and the amount of leakage out of the reservoir was determined by correlating the measured discharge at the outlets of the drains with the corresponding water level in the reservoir. The settlement of the different parts of the dam was measured by repeating from time to time the survey of the settlement reference points.

The design of the piezometers had to be adapted to the permeability of the soil surrounding the perforated tip and the location of the upper end of the piezometer with reference to that of the tip. Therefore, three different types of piezometers, A to C, have been used.

Type A: Observation wells, for measuring the pore water pressures in pervious material. They consist of 1 inch diameter tubes terminating in Stang well points, installed in 8-in. drill holes. Above the well points, the space between tubes and natural ground was filled with compacted clay.

Type B: Casagrande piezometers, for measuring pore pressures at multiple elevations in one well within the body of the dam and in the foundation soils.

Type C: Bourdon gages, attached to the outlet ends of tubes extending through the side walls of the outlet conduit into the surrounding fill material.

The initial piezometer installation consisted of 24 piezometers of Type A located midway between the relief wells; 7 triple piezometers of Type B with tips located below the base of the dam; 5 piezometers of Type B in the subsoil downstream from the dam between the outlet channel and the abandoned channel of Mono Creek; 4 piezometers of Type B with tips in the core; 8 Type A piezometers with tips in the downstream portion of the dam; and 5 Type C piezometers in the side walls of the outlet conduit. The total number of piezometers is 53. Their locations are shown on Figure 10.

Each of the 7 triple piezometers of Type B consists of three 1/2" O.D. plastic tubes installed in one 4-in. drill hole. The tips are located at about elevation 7420, 7450 and 7480. Between tips, the space between tubes and natural ground was sealed with clay. The uppermost tips at elevation 7480, are located about 15 feet below the level of the original bottom of the valley of

Mono Creek at its intersection with the centerline of the dam. During the first filling of the reservoir supplementary piezometers were installed at those few points where additional information concerning the pore pressure conditions was called for.

When the filling of the reservoir was started, the loss of water due to seepage was measured at two points. One of them was located in the short section of abandoned streambed of Mono Creek, about 310 feet downstream from the lowest point of the toe drain at Station 28. The second one is located at about Station 8 at the bottom of a gentle sag in the toe drain between the west abutment of the dam and about Station 10. The station 8 toe drain outlet consists of a 90° V-notch weir equipped with a staff gage. The outlet at Station 28 consists of an 18" rectangular weir plate and is equipped with an automatic recorder.

During the first filling of the reservoir, water seeped out of the ground at three points downstream from the dam. At these points the seepage was collected in drains and gauging devices were installed at the outlets of the drains.

In addition to the piezometers and gauging stations, settlement reference points were established. These are spaced at intervals of 300 feet and consist of brass markers inserted into the tops of cylindrical concrete blocks with a diameter of 12 inches. The base of each block is located 4 feet below the fill surface. Ten such points are on the crest of the dam and five on the downstream berm. Provisions have also been made for measuring the settlement of the invert of the outlet conduit.

Pattern of Seepage

As was expected on the basis of the geological history of the glacial substrata of the damsite, the piezometer readings disclosed an intricate, three-dimensional pattern of seepage. In some portions, the flow lines rise and in others they descend in the direction of the flow. Therefore, at different elevations the curves of equal piezometric pressure have a different shape. This is shown in Figure 10 representing the curves of equal piezometric heads at elevations 7420 and 7480 respectively for full reservoir. If the relief wells had not been drilled, the piezometric levels at elevations 7420, downstream from the highest portion of the dam, could have been very much higher than those shown in Figure 10, involving the possibility of the formation of boils on the valley floor, or even of a heave of the floor. Therefore, the installation of the relief wells was an essential precaution.

As the water level in the reservoir rises the piezometric levels in the observation wells rise approximately in simple proportion to the corresponding rise of the free water level. This relationship is illustrated by Figure 11 in which the abscissa represents the elevation, H, of the water level in the reservoir and the ordinates of the dash curves the corresponding piezometric levels, h, in representative observation wells. Under the following heading, it will be shown that the deviations from the straight-line relationship between h and H are due to changes in the hydrological conditions beyond the area occupied by the reservoir, such as heavy rainfalls or the melting of a snow cover, and not due to an erratic scattering from the fundamental relationship.

The slope of the h - H lines in Figure 11, is determined by the value of the ratio of the loss of head along the flow line through the piezometric tip

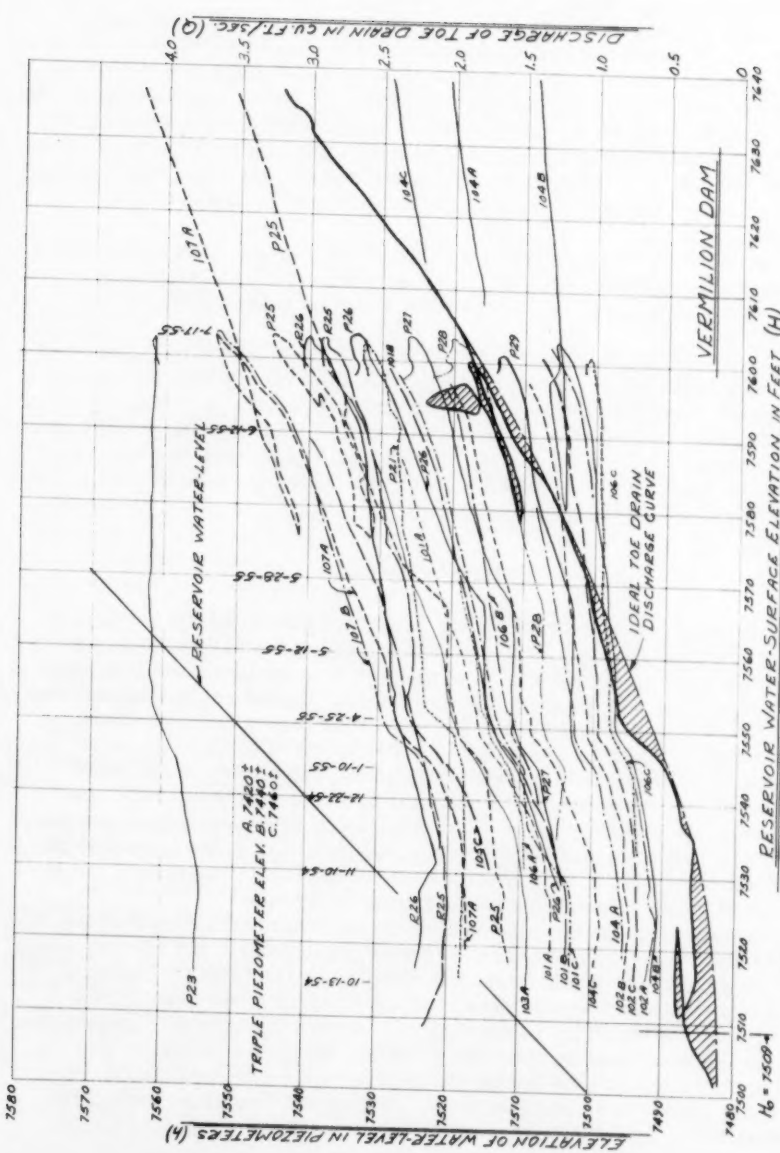

Fig. 11. Plot showing relationship of toe drain discharges and piezometric level vs. reservoir water surface elevation.

between the upper end of the line and the tip, divided by the total loss of head along the flow line. With increasing value of this ratio, the slope of the h - H line decreases. The slope of the h - H line for the downstream end of any flow line is zero.

Downstream from the core of the highest portion of the dam, the water table in the downstream section of the dam is located at an elevation of about 45 feet above the original ground surface (bottom of the valley of Mono Creek prior to the construction of the dam). The slope of the water table, disclosed by the piezometer readings indicates that the quantity of water percolating through the core is very small compared to the quantity entering the downstream section of this portion of the dam through the bottom and the sideslopes of Mono Creek.

The quantity of water entering the "interior drain" (see Figure 5 and 6b is negligible; this fact indicates that the drain serves no useful function. This however, could not be predicted. Therefore, the cost of constructing the interior drain, like that of installing the relief wells adjacent to the two abutments of the dam, is part of the price which had to be paid for the fact that the dam had to be designed and built before the pattern of subsurface drainage was known. However, this price was very moderate.

On the basis of the results of the piezometric observations, the stability computations of the downstream portions of the dam were repeated. The computations led to the conclusion that the factor of safety G_S of the downstream slope of the dam is consistently greater than the design value $G_S = 1.5$, except for a short section in the proximity of Station 28, where the value of G_S might have been slightly smaller than 1.5. Within this section, a small amount of fill was added to the downstream section.

Seepage Losses

The major portion of the water seeping through the foundation enters the toe drain. Originally the toe drain was equipped with two outlets, one at the lowest point of the drain, at about Station 28 and another one at about Station 8 at the foot of a short countergrade in the alignment of the drain. During the first filling of the reservoir, the toe drain became obstructed at about Station 32, probably by an accumulation of iron oxide (Fe_2O_3) which is apparently leached from the natural soils in the vicinity. This rust-colored, slimy sediment collects on the weir plates and in the stilling basins of the outlet weirs and therefore is believed to be the cause of the obstruction in the toe drain. Most of the water entering the toe drain east of the obstruction comes out of the natural ground adjacent to the point of obstruction, Area III, Figure 5. There the seepage water is collected in a drain leading to a gauging device. Hence, at the present time, the discharge from the toe drain is measured at three points. The outlet at Station 8 discharges the water entering the drain between Stations 0 and 10 (western section W) the outlet at Station 28, the water entering between Station 10 and 32 (middle Section M) and the unintentional outlet at Station 32 discharges the water entering between Station 32 and the east abutment at Station 43 (eastern Section E).

At full reservoir the discharge measurements at the three gaging points furnish the following information concerning the leakage Q into the three sections of the toe drain:

The Western section, W, 1000 feet long has a hydraulic head of 0 to 60 feet, Q_W = 0.5 cfs. The unusual features of this section will be discussed below.

The Middle section, M, 2200 feet long has a hydraulic head of 60 to 142 feet, Q_m = 3.8 cfs. Most of this water comes out of the floor and the side slope of the old stream channel. The contribution of the relief wells to this discharge amounts to 0.3+ cfs.

The Eastern section, $\bar{E}$, 1100 feet long, has a hydraulic head of 112 to 0 feet, Q_e = 0.7 cfs. In this section the downstream portion of the dam rests on a gentle morainal ridge located between the core and the downstream toe. Most of the seepage water flows between the ridge and enters the toe drain a short distance above the point of obstruction.

As the water level in the reservoir rises the rate of flow along the flow lines increases in simple proportion to the rise, because the hydraulic head increases in simple proportion to the rise of the water level. Furthermore, the area flooded by the reservoir also increases; the increase of this area involves an increase of the area through which water percolates out of the reservoir through the subsoil of the dam towards the drainage facilities on the downstream side of the dam. Therefore, the loss of water Q out of the reservoir should increase approximately in direct proportion to the square of the rise of the water level $H - H_0$ measured from the level of the bottom. The slope of the curve representing the relationship between Q and $H - H_0$ should be a curve, the slope of which steadily increases with increasing values of $H - H_0$. In Figure 11, the ordinates of the heavy plain curve represent the measured total discharge Q of the toe drain at different elevations H of the water level in the reservoir. According to the aforementioned simple relationship, the H-Q curve should be a smooth, roughly parabolic curve like the dash-dot ideal curve in Figure 11. The height of the shaded areas above the smooth curve represents the excess of the measured discharge over the corresponding discharge indicated by the ordinates of the smooth curve.

An investigation of the sources of the excess discharge indicated by the shaded areas led to the conclusion that most of the excess can be accounted for by a temporary increase of the quantity of water entering the ground adjacent to the toe drain and beyond the area occupied by the reservoir. The increase is caused by meteorological events such as heavy rainfall or snow melt. As a result of such events, water also enters the downstream portion of the dam through the downstream slope, whence it gets into the toe drain.

In addition to the leakage into the toe drain, seepage also comes out of the ground at four places downstream from the dam. Seepage Area I is located in the corner between the eastern portion of the dam and the concrete-lined spillway channel; Area II is on the bottom of a shallow gully descending towards Mono Creek from the east, about 500 feet downstream from the toe drain; Area III is at the downstream toe near the obstruction in the toe drain; and Area IV is in the corner between the emergency spillway and the westermost portion of the dam. The location of these places is indicated in Figure 5 by the shaded Areas I, II, III, and IV.

Seepage from Area I, west of the spillway channel did not start until the water level in the reservoir approached its highest position. The wet area was dried up by the installation of perforated drain pipes, forming a fish bone pattern. At the lower end of the drain, a V-notch weir was installed. At full reservoir, the maximum discharge is 0.2 cfs. Heavy rainstorms and thaws occurring at times of low reservoir stage increase the discharge as much as 50%. The foregoing facts indicate that the seepage through Area I depends not

only on the elevation of the water level in the reservoir but also on the elevation of the water table beneath the sloping natural ground downstream from the eastern portion of the dam.

Seepage Area II centers about the point where a small spring flowed out of the bottom of the shallow gully referred to above. Within this area seepage from the reservoir was anticipated. Therefore a stock pile of filter materials was established in the proximity before the construction of the dam was completed. As soon as the water level in the reservoir went up, the discharge of the spring increased. Considering the trend of the lines of equal piezometric level shown in Figure 10, the increase of the discharge can only be accounted for by the existence of a layer of exceptionally pervious sediments leading from the subsoil of the reservoir into the subsoil of the natural ground east of the spring. The buried stream channel deposit A in Figure 5 represents such a belt. Hence, the increase of the spring discharge accompanying the rise of reservoir level confirmed the conclusion derived from the boring records, shown in Figure 9, that the belt-shaped deposit A in Figure 5 exists.

As soon as the discharge of the spring started to increase during the first filling of the reservoir, a deep drain was installed on the bottom of the gully and the outlet end of the drainage conduit was equipped with a V-notch weir. At full reservoir, the maximum discharge of the drain is 0.5 to 0.7 cfs. During the winter months when the reservoir is at low stage, any unusually wet period or snow melt will cause the discharge temporarily to increase by as much as 10%. Furthermore, whenever water flows over the service spillway, the discharge also increases, indicating seepage from the unlined portion of the spillway channel towards Area II. Hence, at times a considerable portion of the discharge from Area II can come from sources other than the reservoir.

Seepage from Area III was discussed earlier in this section. The area receives most or all of the water which enters the toe drain between Sta. 32+00 and 43+00. The leakage from this area started as soon as the quantity of water flowing through the toe drain exceeded the amount which could be freely passed through the obstruction located at Sta. 32+00. The seepage from Area III, representing an overflow from the toe drain, is in simple proportion to the flow through the toe drain easterly from Sta. 32+00 and hence proportional to changes in reservoir level.

Seepage from Area IV was not appreciable until the water level in the reservoir rose above elevation 7634. However, a further rise of the water level was accompanied by a rapid increase of the discharge. In order to understand this peculiar phenomenon, the characteristics of the discharge from the outlet of the toe drain at Sta. 8+00 should be considered. This outlet is located at el. 7572. Yet the discharge from this outlet remained constant and equal to about 0.04 cfs. until the water level in the reservoir arrived at about el. 7610, which is the elevation of the base of the kame deposit underlying the west end of the dam (see Figures 1 and 2). Further rise of the water level was associated with rapid increase of the discharge at Sta. 8+00. This is shown by Curve $\underline{C}_2$ in Figure 12, representing the relation between the water level in the reservoir and the discharge at Sta. 8+00. As soon as the reservoir water level rose to about el. 7634, an appreciable amount of water also started to emerge from Area IV, and the discharge from this area increased rapidly with increasing elevation of the reservoir level. The relationship between the water level in the reservoir and the discharge from Area IV is shown by Curve $\underline{C}_3$ in Figure 12. The discharge from Area IV is represented by the shaded area between curves $\underline{C}_2$ and $\underline{C}_2+\underline{C}_3$ in Figure 12.

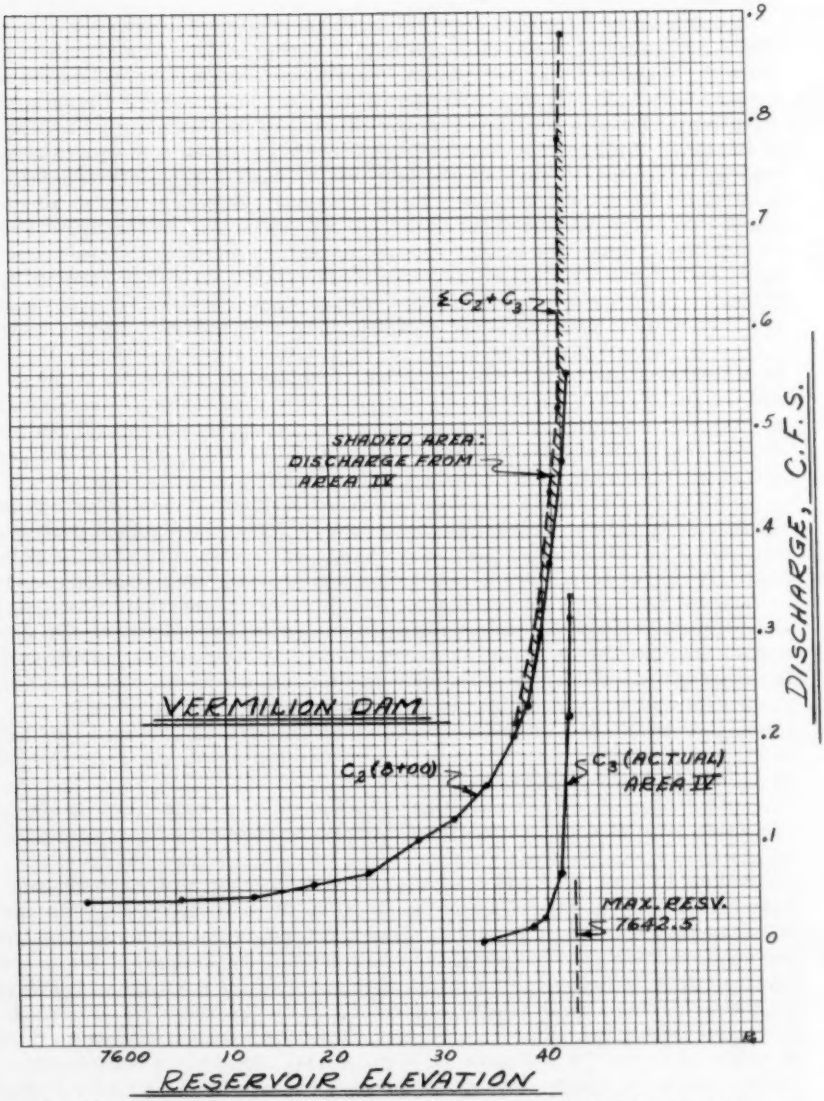

Fig. 12. Reservoir water surface elevation vs. discharge from Area IV.

Both the seepage from Area IV and the abnormal characteristics of the discharge of the toe drain at Sta. 8+00 can adequately be explained by assuming that the permeability of the kame deposit is very much higher than that of the fluvio-glacial deposits underlying the eastern part of the dam, including the section located between Sta. 32 and 43. Once the water level in the reservoir rises above el. 7634 the toe drain no longer suffices to unwater the kame deposit and, as a consequence, part of the water comes out of the adjacent ground downstream from the toe drain. While the water level in the reservoir rose from 7634 to its maximum level, 7642, during the first filling of the reservoir the discharge increased from 0 to 0.33 cfs.

The seepage from Area IV was brought under control by the installation of an inverted filter covering the area, supplemented by perforated drain pipes. The discharge is measured at the downstream end of the collector drain.

The following is a summary of the results of the discharge measurements made during the second filling of the reservoir prior to which time discharge from all seepage areas had been intercepted by collector drains and permanent gaging stations installed.

Let Q = discharge at full reservoir.

Toe drain, section W, Station 0-10	Q = 0.55
Toe drain, section M, Station 10-32	Q = 3.17
Toe drain, section E, Station 32-43	Q = 0.70
Seepage Area I (east abutment)	Q = 0.17
Seepage Area II (gully drain)	Q = 0.53
Seepage Area III (in section E above)	-
Seepage Area IV (west abutment)	Q = 0.39
TOTAL	Q = 5.51 cfs.

Before the water level reached its highest elevation for the first time, the fill material exposed on the downstream slope of the dam became moist along several horizontal lines between the highest portion of the dam and the east abutment, and at a few points in these lines minor sloughing over areas of 2 to 3 square feet occurred, but the quantity of seepage responsible for the sloughing was imperceptible. The bands were located in the random material and generally above the upper boundary of the highly pervious Zone 1 portion of the downstream section of the dam (see Figure 6A and 6B). Subsequent investigations showed that each one of the moist bands was located above an exceptionally silty layer of fill material. On account of the variable silt content of the borrow pit material, the formation of such layers was inevitable. The situation was easily brought under control by drilling vertical holes through the layers down to the pervious Zone 1 fill material and filling the holes with clean gravel; thereupon sloughing stopped.

Settlement

Settlements are very slight because the site was glacially preloaded, and the fill well compacted; and also because the well graded materials of the subsoil and the dam contain little or no clay.

The maximum settlement of the invert of the outlet conduit is 0.27 foot; and since the time when the dam was completed, the crest has settled a maximum of 0.12 foot.

CONCLUSIONS

1. If the pattern of stratification of the subsoil of an earth dam is as erratic as that of the subsoil of the Vermilion Dam information concerning the essential features of the subsoil conditions can only be obtained by a thorough geological survey supplemented by borings at points to be chosen on the basis of geological considerations and by soil tests on representative samples. The few borings which were made at the site of the Vermilion Dam fully served their purpose. Exploratory work in excess of what has been performed at that site would not have furnished any vital additional information to the knowledge of the site prior to construction.

2. The most complete information which can be obtained at a reasonable cost concerning significant features of a damsite on a subsoil with an erratic pattern of stratification still leaves a wide margin for interpretation. Therefore, the construction drawings accompanying the invitation for tenders are inevitably based on more or less arbitary assumptions concerning the character of the subsoil. While these assumptions are being made, the engineer in charge of design should consider, on the basis of the results of the geological survey, all the uncertainties involved, and he should make all the provisions which are necessary for detecting the errors in these assumptions before it is too late to modify the design during the construction in accordance with the findings. The procedure is illustrated by the contents of this paper.

3. Because of following the procedure described in this paper, the Vermilion Dam is as safe and almost as economical as it would have turned out to be, if all the significant features of the subsoil, including the pattern of seepage, had been known in advance of construction. The cost of the installation of those parts of the dam, such as the interior drain, which were afterwards found to be superfluous, were nominal. After the reservoir was filled for the first time, there was no gap in our knowledge of the performance of the dam, and every phase of its performance is clearly understood. This gives the owners and the State Engineer the positive assurance that the dam is satisfactory in every respect.

ACKNOWLEDGMENTS

For the Southern California Edison Company, W. L. Chadwick, Vice President, R. W. Spencer, Manager of Engineering Department and T. M. Leps, Chief Civil Engineer were in charge of investigations, design and construction of the dam. P. J. West, Engineering Geologist, with the extensive help of Dr. J. H. Birman of Occidental College, was responsible for development of the glacial geology of the area. O. N. Kulberg, Chief Construction Engineer, was in direct charge of construction activities, assisted by H. A. Barber, Resident Engineer and T. M. Leps. Consultants to the Company included K. Terzaghi, D. W. Taylor, Ian Campbell and Julian Hinds. Final engineering, construction drawings and construction management were provided by Bechtel Corporation under the direction of J. R. Kiely, Vice President.

Paper 1729 August, 1958 SM 3

Journal of the
SOIL MECHANICS AND FOUNDATIONS DIVISION
Proceedings of the American Society of Civil Engineers

PROCEDURE FOR RAPID CONSOLIDATION TEST

Hsuan-Loh Su[1]
(Proc. Paper 1729)

ABSTRACT

A rapid method for the consolidation test is suggested. A test of 10 load increments can be completed in a few hours instead of 10 days required by the conventional method. Precision of results is comparable to that from a conventional test and can be checked quantitatively.

INTRODUCTION

The standard procedure generally adopted for the consolidation test requires that each increment of load applied to the test sample is to act for a time (usually 24 hours) sufficient to allow the determination of the point of 100% completion of primary consolidation. Such a long period is inconvenient.

An alternative procedure for the consolidation test will be discussed in this article. The apparatus used for this procedure is the same as that for the conventional test. The time required to complete a test series of 10 load increments will not exceed one day.

The theoretical basis of the proposed procedure will be discussed in Part I and a suitable testing method is suggested in Part II. Some illustrations are included in Part III.

Notation

The nomenclature used in this article is in close agreement with that recommended in "Soil Mechanics Nomenclature" published by the ASCE in 1941. The only exceptions are as follows:

a,b - dial reading in A-type, B-type test respectively;
f - conformity factor;

Note: Discussion open until January 1, 1959. To extend the closing date one month, a written request must be filed with the Executive Secretary, ASCE. Paper 1729 is part of the copyrighted Journal of the Soil Mechanics Division, Proceedings of the American Society of Civil Engineers, Vol. 84, No. SM 3, August, 1958.

1. Engr., Ove Arup & Partners, 8, Fitzroy St., London, W.1. Eng.

h - difference of 2 intercepts, see Fig. 2;
s - the slope of the steepest tangent on the time compression curve.

Part I

Theoretical Basis of the Steepest Tangent Fitting Method

The equation governing primary consolidation based on Terzaghi's one-dimensional theory is

$$C_v \frac{\partial^2 u}{\partial z^2} = \frac{\partial u}{\partial t} \tag{1}$$

The solution of equation (1) can be found by means of Fourier's transform, and the average consolidation ratio can then be given as follows,

$$U = 1 - \frac{\int_0^{2H} u\,dz}{\int_0^{2H} u_0\,dz} = 1 - \sum_{m=0}^{\infty} \frac{2}{M} \epsilon^{-M^2 T} \frac{\int_0^{2H} u_0 \sin \frac{M}{H} z\,dz}{\int_0^{2H} u_0\,dz} \tag{2}$$

where $M = \frac{\pi}{2}(m + 1)$, m is an integer, and ϵ is the base of natural logarithms.

Assuming $u_0 = u_1 + u_2 \frac{H - z}{H} + u_3 \sin \frac{M}{H} z$ where u_1, u_2 and u_3 are constants (See Fig. 1.), we have

$$U = 1 - \sum_{m=0}^{\infty} \phi(M) \epsilon^{-M^2 T} \tag{3}$$

where $\phi(M)$ is a function of M only.

The residual of consolidation R is

$$R = 1 - U = \sum_{m=0}^{\infty} \phi(M) \epsilon^{-M^2 T} \tag{4}$$

The general expression for the slope of a tangent on the R-logT curve is

$$\frac{dR}{d(\log T)} = \frac{T}{\log \epsilon} \cdot \frac{dR}{dT} = -\sum_{m=0}^{\infty} \frac{\phi(M)}{\log \epsilon} M^2 T \epsilon^{-M^2 T} \tag{5}$$

The condition for the point of inflexion, through which the steepest tangent passes, is that

$$\frac{d^2 R}{d(\log T)^2} = 0 \tag{6}$$

i.e.,

$$\sum_{m=0}^{\infty} \frac{\phi(M)}{\log \epsilon} M^2 \epsilon^{-M^2 T} (1 - M^2 T) = 0 \qquad (7)$$

From eq. (7), we obtain T = 0.404 which corresponds to R = 0.298 or U = 0.702. Substitution of this T-value into eq. (5) with $\phi(M) = 2/M^2$ i.e., $u_3 = 0$ gives

$$S = \left. \frac{dR}{d(\log T)} \right|_{T=0.404} = 0.688$$

The values of T and R are practically independent of $\phi(M)$. But s can theoretically vary from 0.650 (with $u_3 = -\frac{u_1}{\pi}$) to 0.715 (with $u_3 = +\frac{u_1}{\pi}$). Matlock and Dawson gave s = 0.68, which presumably was obtained on the assumption of initial linear distribution of pore water pressure. (See Fig. 1 and Ref. 1) A detailed discussion of the s-value is beyond the scope of this paper. Its actual variation fortunately is within a smaller range than that mentioned above. The value of 0.688 may be taken as a standard value, although the use of a smaller and simpler value $s = \frac{2}{3}$ is preferable.

The dial reading, a_x, (or void ratio), corresponding to x% consolidation can be estimated by means of the following equation

$$a_x = a_o + \frac{h}{s} \cdot \frac{x}{100} \qquad (8)$$

where a_o is the corrected initial reading, s is the steepest slope of the time curve, and h can be obtained from the experimental results. The determination of h is illustrated on Fig. 2.

Log p vs e Curve for Partially Consolidated Soil

Suppose two different series of oedometer test are performed on a soil starting from identical conditions.

In series A, every load increment is applied when the consolidation process is only 90% completed under the previous load. In series B, the load increment is applied at the stage of 150% consolidation, which would be the 24-hour reading for a soft clay. (See footnote)

FOOTNOTE:

The orthodox division of consolidation into the primary and the secondary part is rather arbitrary and only suitable for Terzaghi's rheological model of soils. If a rheological model which can fully represent the real soil is found and adopted, there will be no "secondary" consolidation at all. Therefore, it is preferable to refer to the "secondary" consolidation in terms of a percentage of the "primary" part, which is defined by a mathematical theory.

The 150% consolidation therefore means a consolidation with a compression ratio r = 100/150 = 0.67, assuming that the corrected zero point coincides with the initial dial reading.

The curves shown in Fig. 3 have been constructed as follows:

A_o, B_o are curves representing the initial dial gauge (or void ratio) readings, a_o^i, b_o^i, respectively, where the superscript denotes the i-th increment of loa-d. A_{90}, B_{150} are curves representing the final readings, a_{90}^i, b_{150}^i, respectively.

These two series of tests were started under the same initial conditions. That is, $a_o^1 = b_o^1 = 0$ at pressure p_1. If the samples are identical and consolidate at the same time rates, then the following relation also exists

$$a'_{90} = b'_{90} \tag{9}$$

The second increment of load is applied in both cases. In series A, $a_o^2 = a_{90}^1$. In Series B, $b_o^2 = b'_{150}$. Obviously $b'_{150} > a'_{90}$, and $b_o^2 > a_o^2$ (a and b increase with decrease in sample thickness). And in general,

$$b_o^i \geq a_o^i \tag{10}$$

Relation (10) can be replaced by a more useful expression

$$1.6\,(a_{90}^i - a_o^i) = b_{150}^i - b_o^i \tag{11}$$

where the constant 1.6 is the ratio of 150% and 90%. The value of b_{150}^i can therefore be estimated from the results of test series A. As a consequence, the test series B which would have been performed to obtain a curve B_{150}, may be replaced by the test series A.

Part II

Suggested Procedure for Consolidation Test

In the following paragraphs, only those steps which depart from the conventional procedure are discussed. The major difference appear in the stage from application of load to the specimen until the plotting of load-compression curves.

The following recommendations are made:

1. Preparation for plotting dial readings directly on semi-log graph paper should be completed before the first load increment is applied. The size of the graph paper should be large enough for a precise construction of the steepest tangent.

2. Dial readings should be taken at the following time intervals:

   every 5 sec. for the first minute,
   every 30 sec. for the next 9 minutes, and then
   every minute till $t = t_{90}$ or $a = a_{90}$ whichever occurs later.

3. The corrected zero reading a_0 is determined by the parabolic method (See Ref. 2) while the test is proceeding. When the steepest tangent to the time-compression curve has been found, the difference in dial reading for one log-cycle, h, is determined. The dial reading corresponding to x% completion of consolidation is given by eq. (8). (In the following paragraphs whenever dial readings are mentioned, they refer to the change in dial reading from a_0.)

4. The last reading should be taken at time $t = t_{90}$ unless a_{90} has not yet been reached. The value for t_{90} can be estimated during the test by the following equation:

$$t_{90} = t_{50} \cdot \frac{T_{90}}{T_{50}} \cdot \frac{H_{90}^2}{H_{50}^2} \doteq 4.3\, t_{50} \tag{12}$$

where t_{50} can be located on the semi-log graph after finding a_{50} from eq. (8).

There is, however, another requirement to be satisfied when taking the last reading. This is that a must equal to a_{90} where a_{90} can be found from eq. (8). Theoretically, the point with an abscissa of log t_{90} should coincide with the point whose ordinate is a_{90}. If they do not coincide, another increment of load should not be applied until both these points have been recorded.

5. The conformity factor f should then be found. f_{90} is defined as the ratio of the actual dial reading to the predicted dial reading at 90% consolidation.

The actual dial reading is found on the time-compression curve by setting $t = t_{90}$ which is determined from eq. (12). The predicted dial reading is given by eq. (8).

6. The above procedure should be repeated for the following increments of load. For the last increment, the load may be left on to obtain the 24-hour "final" reading as in the conventional method.

7. Two laboratory curves A_0 and A_{90} can then be drawn. Other curves can be interpolated or exterpolated when required.

Comments on the Suggested Procedure

1. Advance preparation for plotting of the dial readings and for the construction of the steepest tangent as well as the subsequent calculation is necessary because the person performing the test will be fully occupied while the test is in progress.

2. Sufficient readings should be taken to provide a curve enabling a well defined tangent to be drawn.

3. The steepest tangent can be constructed when the path of the points on the semi-log graph paper indicates a slight decrease in slope.

4. The point of 90% consolidation is chosen as the last point only for the sake of convenience. The point of inflexion appears at about 70% consolidation, and the test can be stopped at any time after this. However, all the points around the 70% point appear to lie on a straight line, which extends over a range

equivalent to nearly 30% of the "primary" compression. The only means of ensuring that the steepest tangent point has been passed is to wait for the curve to turn the other way. The 80% point may still be in the lower reach of the straight portion on a small scale graph and the use of the 90% point is very much on the safe side.

The other advantage of using the 90% point is that the square root of time fitting method (See Ref. 3) can then be applied to the test results and a valuable comparison can be obtained. This is, however, not a necessity for a routine laboratory test.

5. The conformity factor is a measure of the discrepancy between the actual behaviour of the sample and its expected theoretical behaviour. Theoretically, this factor is constant for identical samples under identical conditions, and its variation in practice shows the error of observation. The mean square error can be found, thus giving a quantitative indication of the precision and uniformity of the experiment.

6. The 24-hour final reading provides further information on the conformity between behaviour of the test sample and the prediction made from the theory.

7. A_0 and A_{90} are two basic curves, from which other curves can be constructed.

Part III

Illustration of Steepest Tangent Fitting Method

A typical oedometer curve of dial reading vs time on a semi-log plot is shown in Fig. 4. The sample used was Wyoming bentonite with calcium as its exchangeable ion. The liquid limit was 240% and the coefficient of permeability was of the order of 1 micron per second, nearly 1000 times less than that of an ordinary clay.

It can be seen on Fig. 4 that a period of not less than five days was necessary for the determination of the 100% consolidation point by Casagrande's method (See Ref. 2) The point recorded at t = 110 minutes clearly indicates the existence of the steepest slope and the "rapid" test was therefore completed in less than two hours' time.

A. Steepest Tangent Fitting Method:

i) Corrected zero reading $d_0 = 6570$

ii) Intercepts of the steepest tangent for one log cycle,

$$h = 6438\ (t = 10) - 6175\ (t = 100) = 263$$
$$h = 6450\ (t = 9) - 6187\ (t = 90) = 263 \quad \text{Check.}$$

iii) Predicted dial reading for 90% consolidation

$$d_{90} = 6570 - 1.5 \times 263 \times 0.90 = 6214$$

iv) Actual dial reading for 90% consolidation

a) $d_{50} = 6570 - 1.5 \times 263 \times 0.50 = 6372$

b) from Fig. 4, t_{50} corresponding to d = 6372 was 17.8 min.

c) $t_{90} = 4.3\ t_{50} = 76.4$ min.

d) the dial reading at t = 76.5 min. was 6213.

v) Conformity factor $f_{90} = (6570 - 6214)/(6570 - 6213) = 1.003$

B. Casagrande's Method:

i) $d_0 = 6570$
ii) $d_{100} = 6161$

C. Comparison of values of d_{100}:

i) Method A, $d_{100} = 6570 - 1.5 \times 263 = 6175$
ii) Method B, $d_{100} = 6161$
iii) Discrepancy: $(6570 - 6153)/(6570 - 6161) = 1.02$

Illustration of the Use of A-Curves

Results of an oedometer test performed in accordance with the suggested procedure (except that the test was stopped at 80% consolidation instead of 90%) are shown in Table 1. The corresponding curves A_0 and A_{80} are shown in Fig. 5.

It should be noted that in this example, the initial value of the void ratio was equal to the final void ratio under a previous load. This occurred because the sample was prepared under a high vacuum, such that there was practically no air entrapped in the sample. If there had been air in the sample, there would have been instantaneous consolidation from compression of the air, which would have had to be included in the calculation.

The calculation used in development of Table 2 was as follows:

A. Rearrangement of Results. (Column 1 to Col. 5).

i) Col. 1 to 3 were taken from Table 1.
ii) Col. 4 = Col. 2 - Col. 3, i.e., $(\Delta e)^i_{80} = e^i_o - e^i_{80}$

Arithmetic check $e'_o - e^q_{80} = \sum(\Delta e)_{80} + \sum(\Delta e)_{AIR}$

$1.183 - 0.830 = 0.358$ Check.

iii) Col. 5 = $\frac{150}{80}$ (Col. 4) i.e., $(\Delta e)^i_{ISO} = \frac{ISO}{80}(\Delta e)^i_{80}$

Arithmetic Check $\sum(\Delta e)_{ISO} = \frac{ISO}{80}\sum(\Delta e)_{80}$

$358 \times 15/8 = 671$ Check.

B. Preparation of B-Test Data. (Col. 6 & 7).

i) The same sample was assumed to undergo a B-test. The initial condition was $b^1_o = e^1_o = 1.188$
ii) Col. 7 = Col. 5 - Col. 6 i.e., $b^i_o - (\Delta e)^i_{ISO} = b^i_{ISO}$

or, $\left(b^i_{ISO} + (\Delta e)^{i+1}_{AIR}\right) + (\Delta e)^{i+1}_{ISO} = b^i_o + (\Delta e)^{i+1}_{ISO} = b^{i+1}_{ISO}$

if $(\Delta e)_{AIR} \neq 0$

Arithmetic check: $b'_o - b^q_{ISO} = \sum(\Delta e)_{ISO}$

$1.188 - 0.517 = 0.671$ Check.

C. Construction of B-Curves

The construction of B-curves using the data in Col. 1, 6, and 7 was shown in Fig. 5.

In a case where the original oedometer data are not available, a graphical method comparable to the above calculation can be devised. However, it would be better to read off from the curves and derive data from them than to rely entirely upon the graphical method.

Table 1

A-Test Data. p vs e.

Applied Pressure	Initial Void Ratio	Final Void Ratio
0.1	1.188	1.184
0.2	1.184	1.179
0.4	1.179	1.173
0.8	1.173	1.161
1.6	1.161	1.107
3.2	1.107	1.037
	1.0	
6.4	1.037	0.969
12.8	0.969	0.899
25.6	0.899	0.820

Table 2

Column No.	1	2	3	4	5	6	7
	Appl. Pres.	e_o	e_{80}	$(\Delta e)_{80}$	$(\Delta e)_{150}$	b_o	b_{150}
	0.1	1.188	1.184	4	8	1.188	1.180
	0.2	1.184	1.179	5	9	1.180	1.171
	0.4	1.179	1.173	6	11	1.171	1.160
	0.8	1.173	1.161	12	23	1.160	1.137
	1.6	1.161	1.107	54	101	1.137	1.036
	3.2	1.107	1.037	70	131	1.036	0.905
	6.4	1.037	0.969	68	128	0.905	0.777
	12.8	0.969	0.899	70	131	0.777	0.646
	25.6	0.899	0.820	69	129	0.646	0.517
			Sum =	358	671		

CONCLUDING REMARKS

1. The "rapid" procedure can shorten the duration of a consolidation test, which unnecessarily long when the conventional method is used.

2. The reliability of the rapid procedure is not inferior to that of the conventional procedure. The rapid method can indicate the precision of a series of tests quantitatively, whereas the reliability of the results obtained by the conventional method can only be found qualitatively.

3. The steepest slope fitting method, although shown in this article to be based upon the classical rheological model of clay suggested by Terzaghi, can be applied to other complex models such as Biot's or Tan's generalised model. The only differences are in the s-value and in the coordinates of the tangent point. (See Ref. 4 and 5 for details of these models.)

4. After some slight modification, the square root of time fitting method, which also makes use of the steepest tangent, can be incorporated in the "rapid" method to provide a further check.

ACKNOWLEDGMENT

The writer would like to thank Mr. John Focht, Jr. for his valuable suggestions and Mr. Bruce Maisel for reading the original proof copy.

REFERENCES

1. Matlock & Dawson (1951), A.S.T.M. Special Technical Publication No. 126, June 1951.

2. Casagrande, A (1936), Proc. Int. Conf. Soil Mech. & F. Eng., v. 3. pp 60 - 64.

3. Taylor, D. W., (1942) M.I.T. Publ. Serial No. 82. (1948) "Fundamentals of Soil Mechanics" Wiley & Son, New York.

4. Biot, M. A. (1941), J. Appl. Phys. Vol. 12. (1956), J. Appl. Phys. Vol. 27.

5. Tan Tjong-Kie (1953), Proc. 3rd Int. Conf. Soil Mech. & F. E. (1954), Dr. Thesis, Delft Tech. Univ.

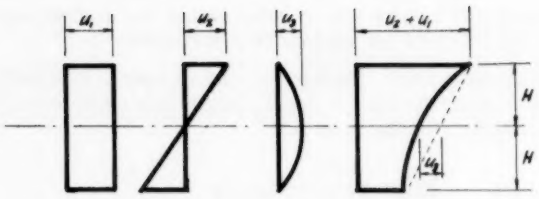

FIG. 1 Initial Vertical Variation Of Pore Pressure u_o

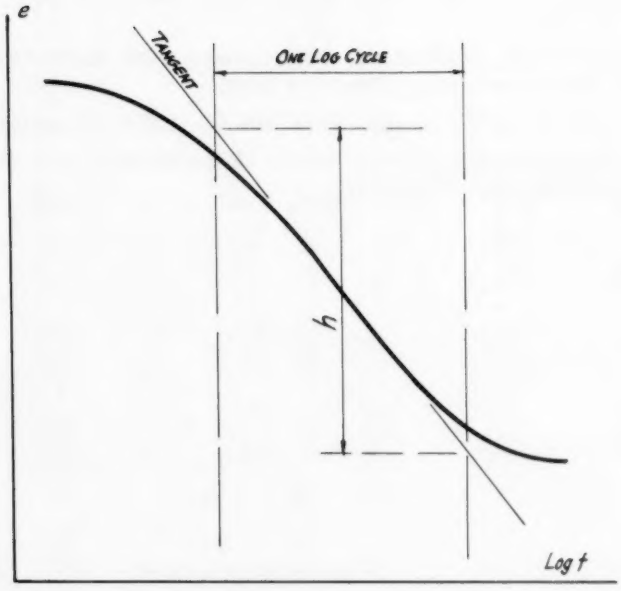

FIG. 2 Basis Of Log-Cycle Fitting Method

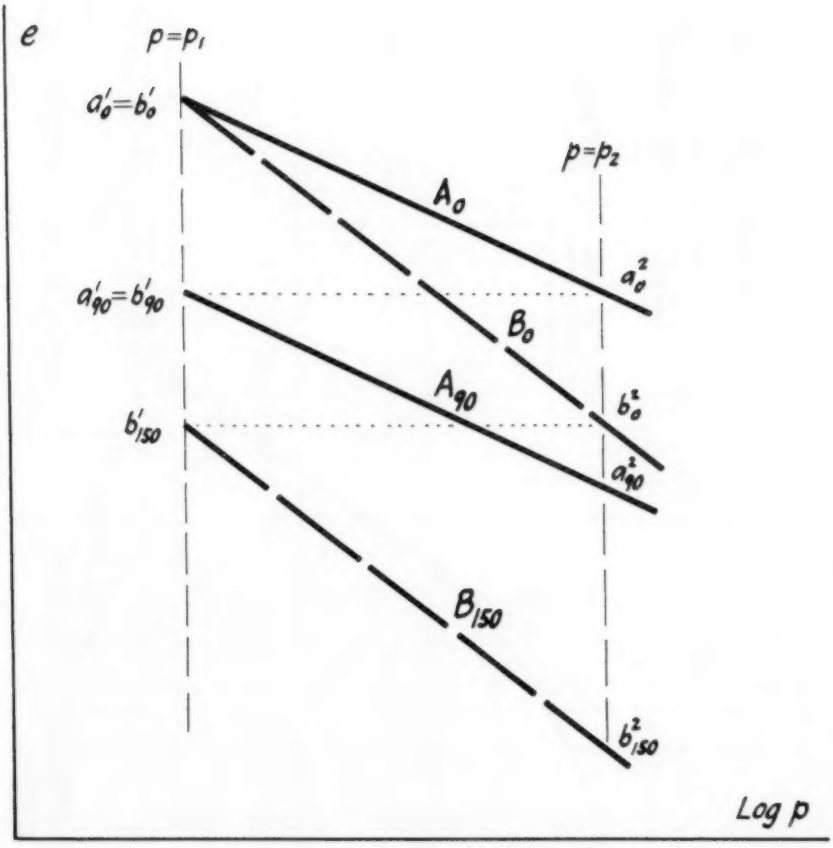

FIG. 3 LOAD-SETTLEMENT CURVES FROM A-TEST AND B-TEST

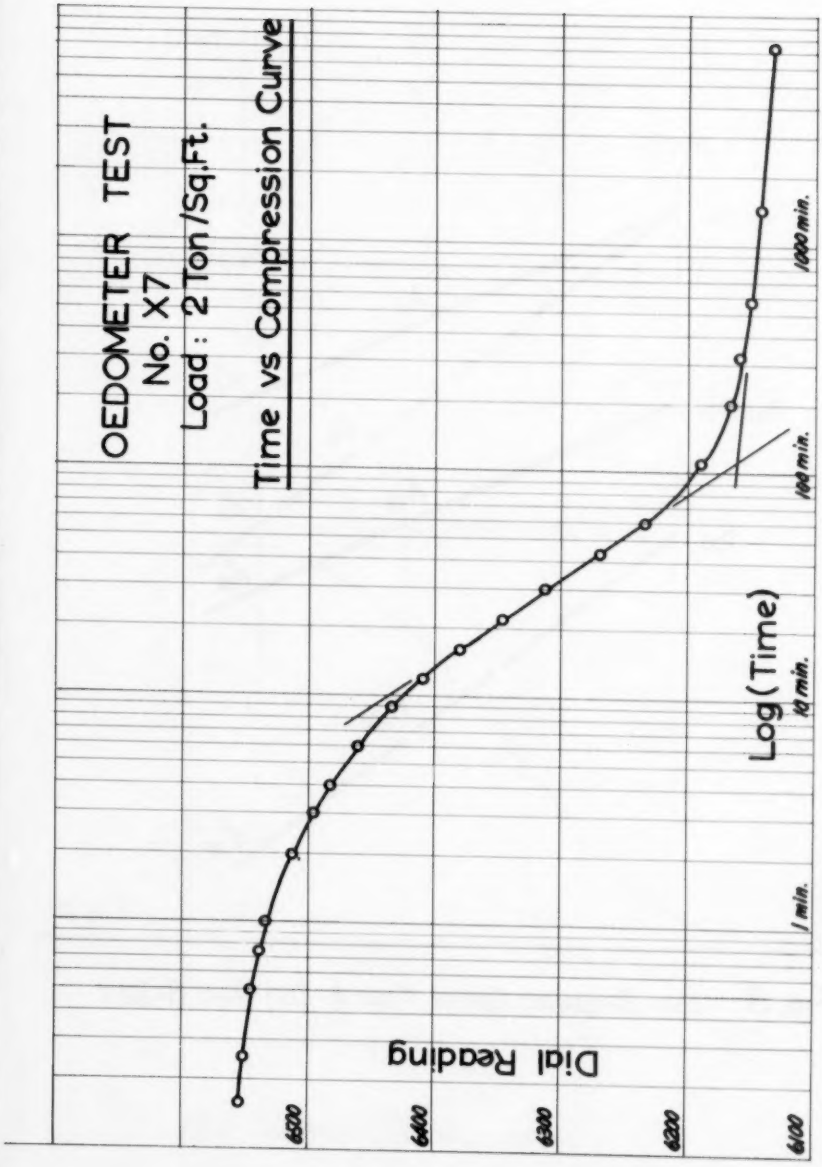
OEDOMETER TEST
No. X7
Load : 2 Ton/Sq.Ft.
Time vs Compression Curve
Dial Reading
6500
6400
6300
6200
6100
Log (Time)
1 min.
10 min.
100 min.
1000 min.

FIG. 4

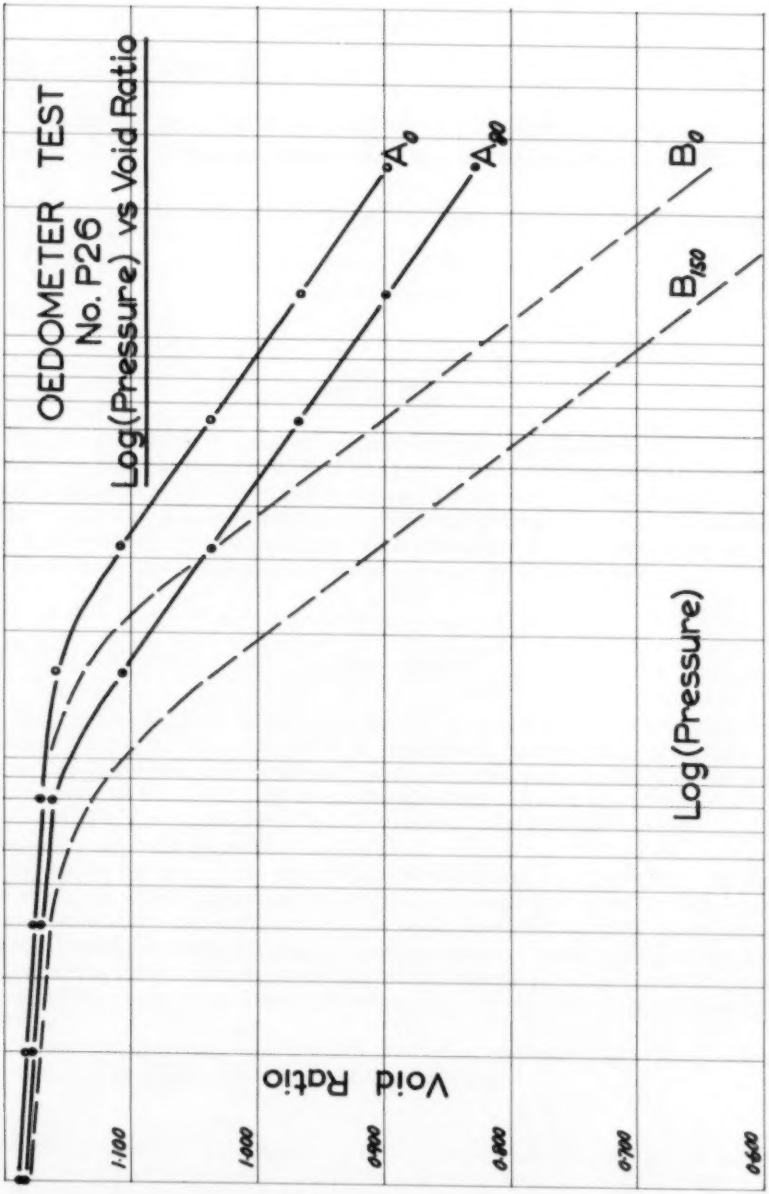
OEDOMETER TEST
No. P26
Log(Pressure) vs Void Ratio
Void Ratio
1.100
1.000
0.900
0.800
0.700
0.600
Log (Pressure)
A_0
A_{90}
B_0
B_{150}

FIG. 5

Paper 1730 August, 1958 SM 3

Journal of the
SOIL MECHANICS AND FOUNDATIONS DIVISION
Proceedings of the American Society of Civil Engineers

EFFECTS OF GROUND ON DESTRUCTIVENESS OF LARGE EARTHQUAKES

C. Martin Duke,[1] M. ASCE
(Proc. Paper 1730)

SYNOPSIS

The present state of empirical knowledge of the relation between ground conditions and earthquake damage to structures is presented in terms of observations in destructive earthquakes. Thirty-six earthquakes are cited for which a relation has been reported. Patterns of behavior exist for several kinds of building. Firm ground is much preferred to soft ground for most kinds of structure. Strong rigid buildings may be an exception.

INTRODUCTION

One of the major considerations facing the engineer who designs structures for seismically active regions is the question of how the ground under a structure influences the probability of damage in an earthquake. This question has interested the observers of earthquakes for at least three centuries. The earthquake-ground-structure system may be visualized as a circuit with a feedback loop from structure to ground.

Scientific investigations have taken three forms: the recording of relations between ground conditions and destruction in large earthquakes, field and laboratory studies using small natural and simulated earthquakes, and theoretical work. This paper summarizes the present state of knowledge gained from large earthquakes. The several figures presented are idealizations of the reports of the respective authors, to whose papers the reader is referred for details.

Thirty-six earthquakes for which a relation has been reported between damage and ground conditions are listed in Table I.

Note: Discussion open until January 1, 1959. To extend the closing date one month, a written request must be filed with the Executive Secretary, ASCE. Paper 1730 is part of the copyrighted Journal of the Soil Mechanics Division, Proceedings of the American Society of Civil Engineers, Vol. 84, No. SM 3, August, 1958.

1. Dept. of Eng., Univ. of California, Los Angeles, Calif.

TABLE I

THIRTY-SIX EARTHQUAKES FOR WHICH A RELATION HAS BEEN REPORTED BETWEEN BUILDING DAMAGE AND GROUND CONDITIONS

Year	Place	Bibliographic Citation
1692	Port Royal, Jamaica	2
1737	Lisbon, Portugal	2
1755	Lisbon, Portugal	3
1780	Messina, Italy	2
1783	Calabria, Italy	2, 3
1835	Talacahuano, Chile	2
1855	Tokyo, Japan	2
1855	New Zealand	2
1861	Mendoza, Argentina	4
1868	San Francisco, California	2, 5
1880	Yokohama, Japan	2
1880	Manila, Phillipine Islands	2
1886	Charleston, South Carolina	6
1891	Mino-Owari (Nobi), Japan	7
1897	Assam, India	3
1906	Valparaiso, Chile	4
1906	San Francisco, California	5
1907	Kingston, Jamaica	4
1911	Germany	8
1913	Freiburg, Germany	9
1923	Tokyo, Japan	10
1933	Long Beach, California	11
1935	Oberschwaben, Germany	12
1943	Tottori, Japan	13
1944	Tonankai, Japan	14, 15
1945	Mikawa Province, Japan	13
1946	Nankaido District, Japan	13, 16
1948	Fukui, Japan	17, 18
1949	Seattle, Washington	19
1949	Imaichi, Japan	20
1950	Assam, India	21
1952	Hokkaido, Japan	22
1952	Kern County, California	23
1954	Eureka, California	24
1955	Quetta, Pakistan	25
1957	Oaxaca, Mexico	26

History to 1886

The following quotation from John Milne, engineer and seismologist,[1] summarizes the early qualitative findings.

"That the nature of the ground on which a building stands is intimately related with the severity of the blow it receives is a fact which has often been demonstrated . . .

"In the great Jamaica earthquake of 1692, the portions of Port Royal which remained standing were situated on a compact limestone foundation; whilst those on sand and gravel were destroyed . . . According to the observations made at Lisbon, in 1737, by Mr. Sharpe, the destroying effects of this earthquake were confined to the tertiary strata, and were most violent on the blue clay, on which the lower part of the city is constructed. Not a building on the secondary limestone or on the basalt was injured.

"In the great earthquakes of Messina, those portions of the town situated on alluvium, near the sea, were destroyed, whilst the high parts of the town, on granite, did not suffer so much. Similar observations were made in Calabria, when districts consisting of gravel, sand, and clay became, by the shaking, almost unrecognizable, whilst the surrounding hills of slate and granite were but little altered. At San Francisco, in 1868, the chief destruction was in the alluvium and made ground.

"At Talacahuano, in 1835, the only houses which escaped were the buildings standing on rocky ground: all those resting on sandy soil were destroyed . . .

"Humboldt observed that the Cordilleras, composed of gneiss and micaslate, and the country immediately at their foot, were more shaken than the plains.

"Some writers have asserted that the wave-like movements (of the Calabrian earthquake in 1783) which were propagated through recent strata from west to east, became very violent when they reached the point of junction with the granite, as if a reaction was produced when the undulatory movement of the soft strata was suddenly arrested by the more solid rocks. Dolomieu when speaking of this earthquake says the usual effect was to disconnect from the sides of the Apennines all those masses of sand and clay which either had not sufficient bases for their bulk, or which were supported only by lateral adherence . . .

"When referring to the question as to whether buildings situated on loose materials suffered more or less than those on solid rocks, Mallet, in his description of the Neapolitan earthquake of 1857, remarked: 'We have in this earthquake, towns such as Saponara and Viggiano, situated upon solid limestone, totally prostrated; and we have others such as Montemarro, to a great extent based upon loose clays, totally levelled. We have examples of almost complete immunity in places on plains of deep clay as that of Viscolione, and in places on solid limestone, like Castelluccio, or perched on mountain tops like Petina.' . . .

"Professor D. S. Martin, writing on the earthquake of New England in 1874, remarks that in Long Island the shock was felt where there was gneiss between the drift. . . . generally the shocks were felt more strongly and frequently on rocky than on soft ground . . .

". . . a civil engineer, writing about the New Zealand earthquake of 1855, when all the brick buildings in Wellington were overthrown, says that it was most violent on the sides of the hills at those places, and least so in the centre of the alluvial plains . . .

". . . in the destructive earthquake of 1855, when a large portion of Tokio was devastated, it was a fact, remarked by many, that the disturbance was most severe on the low ground and in the valleys, whilst on the hills the shock had been comparatively weak . . .

"In Hakodadi, which is a town situated very similarly to Gibraltar, partly built on the slope of a high rocky mountain and partly on a level plain, from which the mountain rises, the rule is similar to that for Tokio, namely, that the low flat ground is shaken more severely than the high ground. At Yokohama, sixteen miles southwest from Tokio, the rule is reversed, as was very clearly demonstrated by the earthquake of February 1880, when almost every house upon the high ground lost its chimney, whilst on the low ground there was scarcely any damage done; the only places on the low ground which suffered were those near to the base of the hills. The evidence as to the relative value of hard ground as compared with soft ground, for the foundation of a building, is very conflicting. Sometimes the harder ground has proved the better foundation and sometimes the softer, and the superiority of one over the other depends, no doubt, upon a variety of local circumstances . . ."

Recent History

John R. Freeman, civil engineer,[27] has presented a good summary of worldwide experience, with emphasis on the early 20th century. The Report of the State Earthquake Investigation Commission,[5] the reports of the Imperial Earthquake Investigation Commission,[10] and the reports of the Japanese committees[17] and the U. S. Army,[18] give extensive information on the ground-intensity correlations of the earthquakes of San Francisco 1906, Tokyo 1923, and Fukui 1948, respectively. Hisada and Nakagawa[28] presented a detailed summary and bibliography of Japanese findings since 1945. The author[29] has compiled an annotated bibliography of worldwide experience.

The first detailed quantitative study was made by Wood on the 1906 San Francisco earthquake.[5] For most subsequent earthquakes such quantitative studies have been made, presenting comparisons of distribution of degree of damage to various kinds of buildings with distribution of ground conditions.

The recording of accelerations in strong earthquakes, initiated in 1932 in the United States and in 1952 in Japan, has helped clarify the effects of ground on intensity. Records have been obtained to date in a number of strong western United States earthquakes.

Japanese Houses

Extensive investigations of the relation between ground conditions and damage to wood houses have been conducted in Japan since 1923. The usual criterion of destructiveness was the "damage ratio" or ratio at a given locality of damaged houses to total houses. Ground parameters used by various investigators have been age of surface deposits, depth of alluvium, softness of ground, and seismic wave velocity.

The older Japanese houses, which constitute the majority of structures damaged in past earthquakes, are constructed of wood, usually with heavy roofs of tile or thatch, and usually with exterior walls of mud plaster over bamboo lath. Principal lateral force resistance comes from these walls, the timber framing and interior partitions being of such construction that they provide only very small lateral resistance. The buildings may be of one or two stories. Their average natural period is about 0.3 second, and they have been subjected in earthquakes to destructive accelerations of 0.3 to 0.4 of gravity.(30)

Aseismic properties of these houses may be compared with modern United States wood-frame construction on the basis of side-by-side performance of the two kinds in Fukui in the 1948 earthquake.(18) The latter were designed with special attention to earthquake resistance by the Office of the Chief of Engineers, Far East Command, U. S. Army, Tokyo. The U. S. style houses were damaged in all cases but none of them collapsed or suffered significant damage to the structural framing. In the same area of Fukui, the average percentages of light-roofed (newer) and heavy-roofed (older) Japanese houses collapsed were about 50 and 90, respectively. In the 1935 Formosa earthquake,(31) this kind of Japanese house was much less damaged than were adobe houses.

The great majority of buildings in Japan are located along the seacoast and in valleys in the very mountainous topography. The following kinds of foundations are common:

1. river deltas, drowned valleys, reclaimed lagoons, muddy alluvium, and made land;
2. littoral sand dunes, beaches, bars, spits, river flood plains, and diluvial volcanic formations;
3. firm tertiary formations, compact conglomerate, and rock.

The first kind is found most often and the third kind least often.

It is seen from Table II, where the several recent comparisons of damage with ground conditions are summarized, that the three kinds of foundation listed above are in the order of increasing desirability. Damage was always many times greater on kind 1 than on kind 3, with kind 2 being intermediate but usually closer to 3 than to 1 in desirability.

Certain investigators have made use of numerical ground parameters to study the distribution of damage ratio. Fig. 1 shows the influence of depth of alluvium found by Kawasumi(32) and Omote and Miyamura.(33,34) The wide divergence between the curves for Tokyo and Yokohama may be due to differences in quality of the alluvium or to the fact that Yokohama was much closer to the epicenter. At Fukui, 1948,(18) damage was roughly proportional to thickness of alluvium, with some exceptions.

Kitazawa(38) obtained a correlation, Fig. 2, between damage ratio and softness of ground. He utilized the logs of many borings in which standardized blow-count diagrams were obtained, and defined ground softness as the reciprocal of the area of the blow-count diagram down to a particular depth.

Omote and Miyamura(34) obtained approximate data on the effect of age of made land in Nagoya, Fig. 3. Kanai(20) also found at Imaichi that damage diminished with age of reclaimed land.

Seismic exploration was used by Tanabashi and Ishizaki(13) to find stratification and wave velocities in four cities which experienced destructive earthquakes in 1943-48. After finding no correlations between damage and several

TABLE II

SUMMARY OF EFFECT OF AGE AND TEXTURE OF GROUND ON EARTHQUAKE DAMAGE TO JAPANESE HOUSES

Year	Place	Ground	Damage Ratio, percent	Bibliographic Citation
1923	Tokyo (b)	Tertiary	0.8-1.4	32
		Diluvium	0.3-0.5	
		Alluvium	2.3-8	
	Yokohama (c)	Sand	Less than 50	33
		Other alluvium	50	
1944	Nagoya (c)	Hills	1	34
		Foothills	2	
		Plain	20	
	Totomi (a)	Rock	0.2	14
		Sand and gravel	1	
		Clayey alluvium	26	
	Mikawa	High ground	Least	35
		Lowlands	Greatest	
	Tonankai	Firm	Slight	15
		Alluvium	Severe	
		Made land	Extra severe	
1946	Kochi	Rock or gravel	Negligible	36
		Beach sand	Variable	
		Swampy ground	Severe	
1948	Fukui (a)	Hills	0.5	18
		Foothills, beaches	5-75	
		Alluvial plain	75-100	
1952	Hokkaido (b)	Beach sand	Small	37
		Peat beds	92	
	Kushiro	Shaly hill	Slight	37
		Peat beds	Great	
		Made land	Greatest	

Damage criteria were:
(a) Number of collapsed houses.
(b) Number of collapsed plus number of partially collapsed houses.
(c) Number of collapsed plus $\frac{1}{2}$ number of partially collapsed houses.

velocity parameters, they obtained a linear correlation, Fig. 4, with the ratio of adjusted depth of soft soil to velocity of surface wave. The slope is different for each earthquake, and it would be useful to attempt to reconcile these differences in terms of differences in mean intensity and ground quality.

Suspecting a pattern to the variability between damage rates based on collapsed and partially collapsed houses, Kanai,[39,40] studied the damage statistics of Japanese earthquakes from 1891 to 1947. He found that while the great majority of houses on firm ground were not materially damaged, those that were damaged were likely to collapse in over half the cases. Conversely, damage to houses on soft ground was widespread, but less than half of those damaged suffered collapse. He attributes this difference to the fact that differential settlement due to the earthquake plays an important role in damage on soft ground, while damage on firm ground is primarily due to vibrational forces. Such differential settlement has been identified at Hokkaido, 1952,[37] and Eureka, 1954,[24] as an important cause of damage on very soft ground. This suggests that ground softness, as measured by Kitazawa or by Tanabashi, may in some cases be better than depth of alluvium as a criterion of earthquake vulnerability.

Other Buildings

Stone and Earth Houses

Masonry houses of stone, mud, or burned brick, bonded with mud or with very weak lime mortar, and houses built wholly of earth, are common in many parts of the world.

The largest amount of information comes from Italy[2,27] from the earthquakes of 1780, 1783, 1860, 1883, 1887, 1894, 1909, and 1930. The typical Italian house was two stories in height with walls of stone rubble masonry set in weak lime-and-earth mortar, with arches of the same material supporting the second floor and with tile roofs on wood framing. In each earthquake listed, the superiority of rock or other firm ground over soft alluvium was noted. Unfortunately, no quantitative studies of this relation have been reported.

In the earthquakes of 1935 and 1955, the damage in Quetta, Pakistan, was greater in the southwestern section on water bearing alluvium than in the northeastern section on dry alluvium and gravel.[25] Most houses in 1935 were of sun dried or burned brick bonded with mud or lime mortar, but those erected subsequently were mostly of aseismic design.

Schlocher and Radbruch[23] made observations in the epicentral area of the Kern County, California, earthquake of 1952. Stone masonry and adobe buildings on rock or thin soil were undamaged or only slightly damaged, while those on thick soil were damaged severely, damage increasing with thickness of alluvium.

In Chilean earthquakes[41] the behavior of adobe construction has been good on rock and gravel ground and very questionable on sandy and clayey soils. The best of adobe buildings can not withstand intensities greater than 9 on the Sieberg scale.

Rigid Buildings

There is evidence that rigid brick and concrete buildings erected since about 1850, with strong materials and good workmanship, and in accordance

with engineering practice of the time, may be less damaged in earthquakes if they are on softer soils. Milne noted[2] that in the New Zealand earthquake, 1855, brick buildings suffered greatest damage when on hillsides, least when on alluvial plains. Also, in the 1880 Yokohama earthquake, almost every house on high ground lost its chimney while damage on the low ground was very slight. In the 1950 Assam, India, earthquake,[21] brick buildings suffered greater damage when on firm than when on soft ground.

The 1923 Tokyo earthquake has yielded the most quantitative information on this subject. In Tokyo there were, on the soft ground, 582 brick and 418 reinforced concrete buildings, and on the firm ground, 192 brick and 158 reinforced concrete buildings. They were generally of one to three stories. Suyehiro[42] reported that the damage to the brick buildings was more severe when they were on firm ground. Kanai[43] restudied the data in detail and confirmed this finding. In a later study,[44] Kanai showed that the damage ratio, based on completely plus partially destroyed brick buildings, was less where the thickness of alluvium was greater, as shown in Fig. 5.

Martel[11] obtained a similar result based on his study of damage to 1261 one- to four-storied brick buildings in the 1933 Long Beach, California, earthquake. Using the ratio of cost of repairs to original value of building as the damage criterion, he determined that damage to buildings on soft water-logged soil and on beach sand was somewhat less than to those on more firm ground.

Damage to the reinforced concrete buildings in Tokyo, 1923, has been analyzed by Kanai[43,44] and Kitazawa,[46] Fig. 6. Kanai found that damage diminished with thickness of alluvium, similarly to the case of brick buildings but at a lesser rate. Kitazawa plotted his ground softness parameter (see above) against damage ratio based on damage to structural elements only. It is seen that damage determined on this basis increased with ground softness.

Japanese experience with small rigid farm structures used for storage usually has been consistent with the above. These buildings, called godowns, are constructed of closely spaced strong wood pillars covered outside with thick mud plaster walls or soft stone and usually have stronger foundations than the houses. Small-motion period is about 0.2 second.[47] In the Northern Musashi earthquake of 1931, the walls of such structures on paleozoic formations were cracked to a greater extent than for those on alluvial ground.[42] However, in Fukui, 1948, an opposite trend was noted:[48] houses were damaged more than godowns when on firm soil, less when on sand dunes, and to the same degree when on alluvium. In the 1949 Imaichi earthquake,[20] 3174 relatively rigid soft-stone granaries were damaged. While the comparative damage ratios on various kinds of ground were not reported, it was determined that the granaries on soft ground suffered most damage in the upper 1/3 of their height, and those on hard ground were most damaged in the lower 1/3.

Buildings in General

Many other reports have been made of the effect of ground on intensity. When buildings in general are considered, the superiority of firm ground is nearly always proven. This trend appears in most of the reports of the earthquakes of the 18th and 19th centuries, Table I.

Kitazawa[46] found for steel frame buildings in Tokyo, 1923, the same trend in relationship between damage and ground softness as illustrated in Fig. 6 for reinforced concrete buildings. In the Mexico earthquake of 1957,[26]

flexible multistory buildings in Mexico City 200 miles from the epicenter suffered much greater damage than similar buildings in Acapulco which was 60 miles from the epicenter. Mexico City is on deep soft alluvium and Acapulco is on rock and beach sand.

Wood's study[5] of San Francisco, 1906, has become a classic. The San Andreas fault was close to the city, and damage had some relation to distance from the fault. However, the effect of kind of ground was more pronounced. He found the most severe damage on made land, with damage successively less severe on alluvium, conglomerate and shale, and rock. Damage was 5 to 10 times greater on made land than on rock. His findings were supported by other investigators.[49,50]

The same trend has been found for earthquakes in eastern Canada,[51] Germany,[12] Chile,[41] Turkey, Greece, and Algeria,[52] and China.[53]

Neumann[54,55] has provided ground-intensity data on several United States earthquakes by drawing envelopes of intensity versus distance from epicenter, such as in Fig. 7. He believes that in virtually all cases the points on the lower envelope are for locations on basement rock outcrops, giving a very uniform intensity-distance relation which depends only on the character of rock (igneous or sedimentary). Points on the upper envelope are believed to correspond with locations on soft overburden, with points between the two envelopes representing local geology of intermediate firmness. Neumann has found it possible to construct these envelopes from a small number of points using curve shapes determined from well-documented earthquakes.

Strong-Motion Accelerograms

The strong motion seismograph program of the United States Coast and Geodetic Survey has been in operation since 1932, and a large number of records has been obtained. In 1956 there were 71 accelerograph stations at 56 sites in the western United States and in Central and South America, the majority being in California. Most are located in the basements of buildings; a few are on higher floors, and two are on the ground away from buildings. Of the 37 U.S.C.G.S. sites in California, 27 are on unconsolidated sediments, 4 are on consolidated sediments, and 6 are on rock. However, no adequate investigation has been made of the ground conditions at these sites. In addition to the U.S.C.G.S. stations, other seismologists operate a few strong motion stations in California.

The Japanese strong motion program was initiated in 1952, but, to date there have been only relatively small earthquakes recorded. In 1956 there were 14 stations located in seven buildings in Tokyo. The number of instruments is being increased as rapidly as possible. Although records from the present instruments may be influenced by the vibrational properties of the buildings housing them, these buildings are situated on various kinds of ground, and a large earthquake should yield records with useful data on the effect of ground.

Engineers at California Institute of Technology[56,57] have obtained 88 spectra based on U.S.C.G.S. records in 11 western United States earthquakes. The spectra are of two kinds, velocity and acceleration, and were computed for various damping factors including zero damping.

The damped velocity spectra are consistent with the random disturbance hypothesis of earthquake motion[58] in that, above a certain minimum period,

velocity is distributed more or less randomly about a mean value of velocity which is independent of period. Such a shape suggests the equipartition of energy among the earthquake wave components at the surface. Kanai[59] shows from amplification theory that velocity spectra on very deep alluvium, such as exists at most of the stations, should be expected to be flat.

In several cases, two or more earthquakes were recorded at the same station, but examination of the spectra did not disclose any special features that could be attributed to the locality. Also, several earthquakes were recorded at two or more stations, but no characteristic resemblance attributable to the particular earthquake could be found in the spectra.

However, in two special cases, features associated with the locality were suggested. The station at Helena, Montana, was on rock; the 1935 acceleration spectra showed a predominance of short period waves. The station at Seattle, Washington, was on watersoaked filled land; the 1949 acceleration spectra showed a predominant period of 0.9 second, although the corresponding accelerations were much smaller than those recorded on firm alluvium at Olympia at about the same epicentral distance.

Damping was introduced so that the spectra might represent the response of typical real structures without further computation. However, for analyses treating the complete earthquake-ground-structure system, the undamped spectra will be needed.

Lateral Force Coefficients

Coefficients Based on Earthquake Experience

Only two cases were found where the variation in equivalent horizontal static force with kind of ground has been numerically computed from damage studies of particular earthquakes. Kawasumi[61] reconsidered the damage data reported by Wood for San Francisco, 1906, to correct for the effect of distance from fault. The relative foundation coefficients thus determined are:

Rock	1
Alluvium	1.5
Made land	5

Takahasi[17] obtained the following relative coefficients for Fukui, 1948:

Tertiary	0.4
Diluvium	0.7
Alluvial ground	1.0
Marshy land, approximately	1.5

Coefficients in Building Codes

In many places the building codes provide for variation in lateral force coefficient with kind of ground and kind of foundation. These code provisions have been arrived at by committees of engineers who have studied the earthquake experience in their own and other localities. Several examples are given below, the coefficients being expressed in fractions of gravity acceleration. These coefficients, which are to be applied to dead load and a fraction of live load, are listed here only to illustrate the present discussion. They must not be utilized in design without study of the detailed provisions in the referenced publications.

Japan[62,63]

	Wood Construction	Steel Frame Construction	Reinforced Concrete Construction
Tertiary	.12	.12	.16
Diluvium	.16	.16	.18
Alluvium 5-30 meters deep	.20	.20	.20
Alluvium over 30 meters deep, or made land	.30	.20	.20

Seismic zoning maps have been prepared for several Japanese cities.[28]

Chile[41]

	Rigid Construction, Period < 0.4 sec.	Semi-Rigid Construction, Period 0.4-0.75 sec.
Rock	.08	.05
Conglomerated or very compact soil	.12	.10
Sand and filled ground		
With mat or similar foundation	.10	.12
Without mat	.12	.15

Turkey[52]

	Best Ground	Worst Ground
Higher seismicity zone	.02	.04
Lower seismicity zone	.01	.03

California Schools[64]

Safe Bearing Capacity, tons/sq. ft.	Coefficient
4 or more	.06
2 to 4	.08
Less than 2	.10

CLOSURE

The type of soil on which a structure is founded, the structure and depth of underlying rock, the depth and type of foundation, and the features of surface topography including adjacent buildings all have been found to affect the damage done to buildings by large earthquakes. While in many of the cases cited the soil properties and configuration are quantitatively known, the present state of knowledge is such that terms such as "soft ground" must be used in generalizations.

The preponderance of evidence indicates that the majority of structures are least damaged when on firm ground. Damage has generally been greater on average ground. Soft ground has nearly always been associated with highest damage.

It must be emphasized that the mass of older damage data were obtained on the basis of residential construction, wood in Japan and wood or masonry

in the Mediterranean area. There are indications in the more recent data that strong rigid structures may be less damaged when on softer ground.

As noted in the introduction, this paper has considered but one of the three avenues of investigation. Such large earthquake studies in the future will be more productive if planned with full awareness of the previous work. But the experimental and theoretical work going on in this field, principally in Japan but also in other countries, is equally important and necessary. There remains much divergence of opinion among engineers and seismologists as to how the kind of ground affects the response of structures, and as to how the effects may be quantified.

The author desires to express his deep appreciation, for assistance and advice leading to the preparation of this paper, to Kiyoshi Kanai and Hirosi Kawasumi of the Earthquake Research Institute, Tokyo University, to Toshihiko Hisada and Kyoji Nakagawa of the Building Research Institute, Japanese Government, and to the many other Japanese engineers and seismologists who aided him.

BIBLIOGRAPHY

1. Milne, John. "Earthquakes and Other Earth Movements." D. Appleton and Co., New York, 1886, 363 pg.

2. Milne, John. "Construction in Earthquake Countries: a Compilation, with a Few Original Articles, Respecting Building in Earthquake Countries." Trans. Seis. Soc. Japan, v. 14, 1891, 228 pg plus plates.

3. Davison, Charles. "Great Earthquakes," Thomas Murby & Co., London 1936. 286 pg.

4. Branner, J. C. "Impressions Regarding the Relations of Surface Geology to Intensity in the Mendoza, Valparaiso, Kingston, and San Francisco Earthquakes." Bull. Seis. Soc. Amer., v. 1, 1911, pp 38-43.

5. Lawson, Andrew C. (Chairman). "The California Earthquake of April 18, 1906." State Earthquake Investigation Commission. Publication No. 87, Carnegie Institution of Washington, 1908. 2 volumes and atlas.

6. Dutton, C. E. "The Charleston Earthquake of August 31, 1886." Ninth Ann. Rept., U. S. Geol. Survey, 1887-88, pp 203-528.

7. Omori, F. "Macroseismic Measurement in Tokyo. I. II. III." Publ. Earthq. Inv. Com. in For. Lang., No. 10 and 11, 1902.

8. Seiberg, A. und R. Lais. "Das Mitteleuropäische Erdbeben vom 16, November 1911. Bearbeitung der makroseismischen Beobachtungen." Veröffentlichungen der Reichstanstalt für Erdbeben forschung, Jena, Heft 4, 1925, 106 pp, 2 maps.

9. Lais, R. "Die Wirkungen des Erdbebens vom 20, Juli, 1913, in der Stadt Freiburg." i. Br. Badische Geologische Landesanstalt, Mitteilungen, v. 7 (1914) pp 671-698, 1 pl.

10. Imperial Earthquake Investigation Committee. "The Great Kwanto Earthquake of September 1, 1923." (Japanese.) Reports 100A, 100B, 100C1, 100C2, 100D, 100E, of Imperial Earthquake Investigation Committee, Japan. 1925, 1926.

11. Martel, R. R. "A Report on Earthquake Damage to Type III Buildings in Long Beach." Spec. Pub. 201, U. S. Coast and Geodetic Survey, 1936, pp 143-162.

12. Hiller, Wilhelm. "Why Regulations for Structures in Earthquake Zones in Germany?" Proc. World Conf. Earthq. Engr., 1956, Paper 18, 4 pg.

13. Tanabashi, Ryo and H. Ishizaki. "Earthquake Damages and Elastic Properties of the Ground." Bull. No. 4, Disaster Prevention Research Institute, Kyoto University, May 1953, 70 pg.

14. Ooba, Syohachi. "Study of the Relation between the Subsoil Conditions and the Distribution of the Damage Percentage of Wooden Dwelling Houses in the Province of Tootomi in the case of the Tonankai Earthquake of Dec. 7, 1944." (Japanese.) Bull. Earthq. Res. Inst., v. 34, 1956, pp 201-295.

15. Minakami, Takeshi and Sadao Utibori. "The To-Nan-Kai Earthquake Damage and After-Shocks." (Japanese.) Bull. Earthq. Res. Inst., v. 24, 1946, pp 19-30.

16. Miyamura, Setumi. "Notes on the Geography of Earthquake Damage Distribution." Pacific Sci. Assoc., Proc. 7th Cong., v. 2, pp 653-661, 1953.

17. Tsuya, H. (Chairman). "The Fukui Earthquake of June 28, 1948." Report of the Special Committee for the Study of the Fukui Earthquake, 1950, 197 pg.

18. Office of the Engineer, U. S. Army. "The Fukui Earthquake, Hokuriku Region, Japan." General Headquarters, Far East Command, U. S. Army, 1949, 2 vol., 300 pg.

19. Edwards, Harlan H. (Chairman). "Discussion of Damage Caused by the Pacific Northwest Earthquake of April 13, 1949." Report of Earthquake Committee, Seattle Section, ASCE, 1950. Also published in Western Construction News, Feb., Mar., Apr., 1951.

20. Kanai, Kiyoshi and Teiji Tanaka. "On the Damage to Buildings by the Imaichi Earthquake of December 26, 1949." Bull. Earthq. Res. Inst., v. 28, 1951, pp 461-464.

21. "A Compilation of Papers on the Assam Earthquake." Central Board of Geophysics, Calcutta, India, 1953, p. 7.

22. Special Committee for the Investigation of the Tokachi-Oki Earthquake. "Report on the Tokachi-Oki Earthquake, Hokkaido, Japan, March 4, 1952." (Japanese.) Published by the Committee, Sapporo, 1954, 1018 pg.

23. Schlocker, J. and Dorothy H. Radbruch. "Arvin-Tehachapi Earthquake—Structural Damage as Related to Geology." Bull. 171, Div. of Mines, Calif. Dept. of Natural Resources, 1955, pp 213-220.

24. Steinbrugge, Karl V. and Donald F. Moran. "An Engineering Study of the Eureka, California, Earthquake of December 21, 1954." Bull. Seis. Soc. Amer., v. 47, 1957, pp 129-154.

25. Khan, Abdual Quadir. "Earthquakes and Aseismic Designs in Pakistan." Proc. World Conf. Earthq. Engr., 1956, Paper 23, 9 pg.

26. Duke, C. M. and D. J. Leeds. "Effect of Soil Conditions on Damage in the Mexico Earthquake of July 28, 1957." Bull. Seis. Soc. Amer. In press.

27. Freeman, John R. "Earthquake Damage and Earthquake Insurance." McGraw-Hill, 1932, 904 pg.

28. Hisada T. and K. Nakagawa. "Recent Japanese Developments in Engineering Seismology and their Application to Buildings." Pub. of Bldg. Res. Inst., Japan, 1958. In press.

29. Duke, C. Martin. "Effects of Soil Conditions on Earthquake Damage—A Bibliography." Publ. Earthq. Engr. Res. Inst. In press.

30. Seismic Research Group, Architectural Institute of Japan. Discussion of paper, "Lateral Forces of Earthquake and Wind" by Rinne et al, Trans. Am. Soc. Civ. Engrs., v. 115, 1952, pp 755-764.

31. Takahasi, R. "Intensity Distribution of the Formosa Earthquake of April 21, 1935, and the Strength of Dokaku Structures." (Japanese.) Bull. Earthq. Res. Inst., Supp. v. III, March 1936, pp 120-140.

32. Kawasumi, H. "On the Earthquake-Stricken Areas and their Underground Formation in Tokyo." (Japanese.) Jour. Arch. Inst. Japan, No. 773, 1951.

33. Omote, Syun'itiro. "The Relation between the Earthquake Damages and the Structure of the Ground in Yokohama." Bull. Earthq. Res. Inst., v. 27, 1949, pp 63-68.

34. Omote, Syun'itiro and Setumi Miyamura. "Relations between the Earthquake Damage and the Structure of the Ground in Nagoya City." Bull. Earthq. Res. Inst., v. 29, 1951, pp 183-196.

35. Omote, Syun'itiro. "Comparison of the Vulnerability Rates of the Ground Revealed in Tonankai and Mikawa Earthquakes." (Japanese.) Bull. Earthq. Res. Inst., v. 24, 1946, pp 87-98.

36. Miyamura, S., Y. Saizyo, and S. Kaizuka. "Geographical Distribution of Earthquake Damages with Special Reference to the Effects of the Nankaido Earthquake, Dec. 21, 1946, in Kochi Prefecture, Shikoku, Japan." (Esperanto.) Jour., Phys. of the Earth, v. 1, no. 2, 1952, pp 83-93.

37. Ohno, K. and others. "Discussion of Effects of Soil Conditions on Damage in the Tokachi-oki Earthquake of 1952." March 22, 1957, unpublished.

38. Kitazawa, G. "On the Relation between Earthquake Damages and the Hardness of the Ground." (Japanese.) Jour. Seis. Soc. Japan, Series 2, v. 1, 1948, pp 48-49.

39. Kanai, Kiyoshi. "On the Damages to Buildings due to Earthquakes." Bull. Earthq. Res. Inst., v. 25, 1947, pp 61-64.

40. Kanai, Kiyoshi. "On the Damage to Japanese-style Buildings due to Earthquakes." (Japanese.) Bull. Earthq. Res. Inst., v. 29, 1951, pp 215-222.

41. Bertling, H. "Development of Earthquake-Proof Construction in Chile." Proc. World Conf. Earthq. Engr., 1956, Paper 20, 10 pg.

42. Suyehiro, K. "Engineering Seismology—Notes on American Lectures." Proc. ASCE, v. 58, May 1954, 110 pg.

43. Kanai, Kiyoshi. "Relation between the Earthquake Damage of Non-Wooden Buildings and the Nature of the Ground." Bull. Earthq. Res. Inst., v. 27, 1949, pp 97-100.

44. Kanai, Kiyoshi and Shizuyo Yoshizawa. "Relation between the Earthquake Damage of Non-Wooden Buildings and the Nature of the Ground. II." Bull. Earthq. Res. Inst., v. 29, 1951, pp 209-213.

45. Kitazawa, G. "Distribution of Seismic Intensity in the Downtown of Tokyo." (Japanese.) Jour. Seis. Soc. Japan, Series 2, v. 3, 1950, pp 32-40.

46. Kanai, Kiyoshi. "Destruction System of Building by Earthquake." Bull. Earthq. Res. Inst., v. 29, pp 393-401.

47. Special Investigation Committee of Fukui Earthquake. "Report of Damage Investigation at Fukui, 1948. Volume II, Building Division." (Japanese.) 1951, 288 pg.

48. Gilbert, G. K., R. L. Humphrey, J. S. Sewell and F. Soule. "The San Francisco Earthquake and Fire of April 18, 1906 and their Effects on Structures and Structural Materials." Bull. 324, U. S. Geol. Survey, 1907, 170 pg, 54 pl.

49. Special Committee. "The Effects of the San Francisco Earthquake of April 18th, 1906, on Engineering Constructions." Trans. ASCE, v. 59, 1907, p 208.

50. Hodgson, Ernest A. "Industrial Earthquake Hazards in Eastern Canada." Bull. Seis. Soc. Amer., v. 35, 1945, pp 151-174.

51. Pinar, Nuriye. "Historical and Modern Earthquake Resistant Construction in Turkey." Proc. World Conf. Earthq. Engr., 1956, Paper 22, 8 pg.

52. Hsieh, Yu-Show. "Intensity and Ground in China." Personal Communication, Feb. 28, 1957.

53. Neumann, Frank. "Some Generalized Concepts of Earthquake Ground Motion." Proc. Symp. Earthq. and Blast Effects on Structures, 1952, pp 8-19.

54. Neumann, Frank. "Earthquake Intensity and Related Ground Motion." Univ. of Washington Press, 1954, 77 pg.

55. Alford, J. L., G. W. Housner, and R. R. Martel. "Spectrum Analysis of Strong Motion Earthquakes." Report, Aug. 1951, Calif. Inst. of Tech.

56. Housner, G. W., R. R. Martel, and J. L. Alford. "Spectrum Analysis of Strong Motion Earthquakes." Bull. Seis. Soc. Amer., v. 43, 1953, pp 97-119.

57. Housner, G. W. "Characteristics of Strong-Motion Earthquakes." Bull. Seis. Soc. Amer., v. 37, 1947, pp 19-31.

58. Kanai, Kiyoshi. "Semi-empirical Formula for the Seismic Characteristics of the Ground." Bull. Earthq. Res. Inst., v. 35, Part 2, 1957, pp 309-326.

59. Kanai, Kiyoshi, Ryutaro Takahasi and Hirosi Kawasumi. "Seismic Characteristics of Ground." Proc. World Conf. Earthq. Engr., 1956, Paper 31, 16 pg.

60. Kawasumi, Hirosi. "Relations among Soil Conditions, Intensity, and Distance from Fault in the San Francisco Earthquake of 1906." Unpublished analysis. 1950.

61. Minister of Construction, Japanese Government. "Ministry of Construction Notification No. 1074, July 25, 1952." Mimeographed, 4 pg.

62. Japanese Government. "Building Standard Law Enforcement Order. Cabinet Order No. 338, Nov. 16, 1954." Published by Housing Bureau, Ministry of Construction, Jan. 1954, 55 pg.

63. State of California. "Title 21, California Administrative Code." Div. of Admin. Proc., State of Calif., Sacramento, 1948, 145 pg.

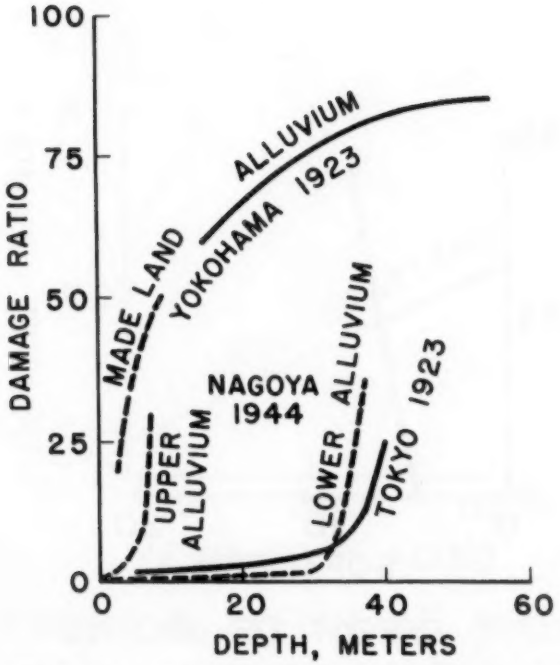

FIGURE 1 EFFECT OF ALLUVIUM DEPTH ON HOUSE DAMAGE IN TOKYO, YOKOHAMA, AND NAGOYA. (AFTER KAWASUMI, OMOTE, AND MIYAMURA.)

DAMAGE CRITERIA:

TOKYO: NUMBER OF HOUSES WHICH WERE MORE THAN HALF DESTROYED

YOKOHAMA AND NAGOYA: NUMBER OF COLLAPSED PLUS 1/2 NUMBER OF PARTIALLY COLLAPSED HOUSES

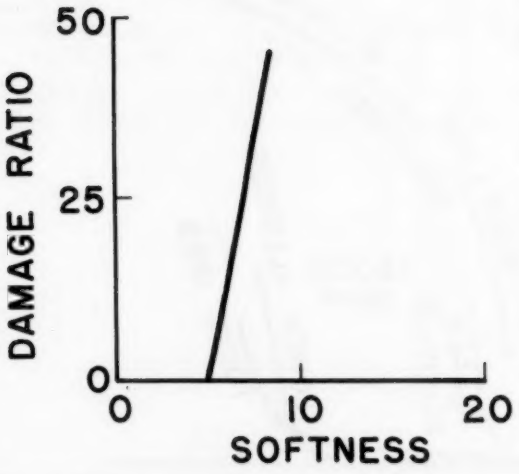

FIGURE 2 EFFECT OF GROUND SOFTNESS ON HOUSE DAMAGE IN TOKYO, 1923. (AFTER KITAZAWA)

DAMAGE CRITERION:
NUMBER OF COLLAPSED HOUSES

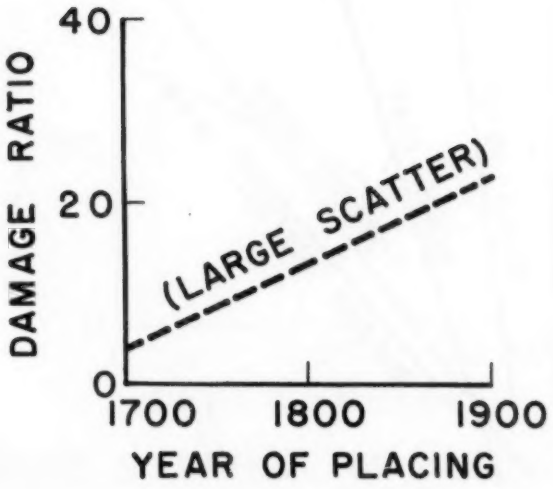

FIGURE 3 EFFECT OF AGE OF MADE LAND ON HOUSE DAMAGE IN NAGOYA, 1944. (AFTER OMOTE AND MIYAMURA.)

DAMAGE CRITERION: SEE FIGURE I

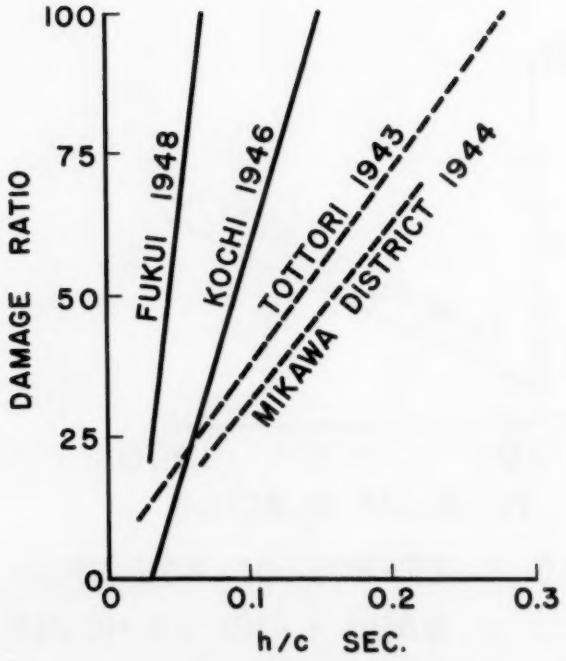

FIGURE 4 EFFECT OF GROUND ON DAMAGE IN FOUR JAPANESE EARTHQUAKES. (AFTER TANABASHI AND ISHIZAKI.)

DAMAGE CRITERION: NUMBER OF COLLAPSED HOUSES
h = ADJUSTED DEPTH OF TOP LAYER
c = PROPAGATION VELOCITY OF SURFACE WAVE

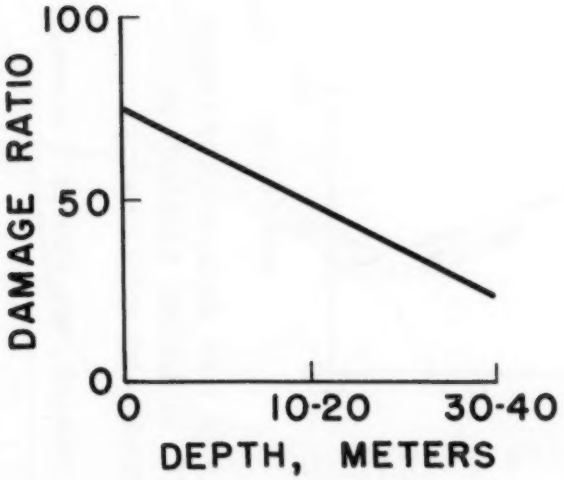

FIGURE 5 EFFECT OF ALLUVIUM DEPTH ON BRICK BUILDING DAMAGE IN TOKYO, 1923. (AFTER KANAI.)

DAMAGE CRITERION: NUMBER OF DESTROYED PLUS NUMBER OF PARTIALLY DESTROYED BUILDINGS

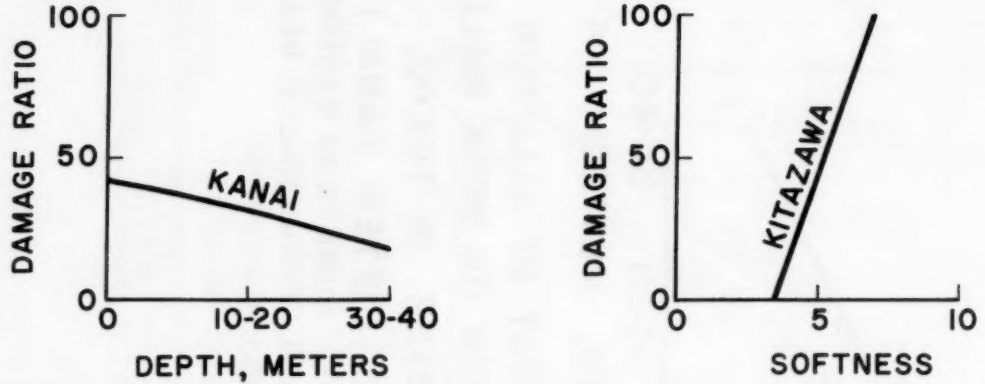

FIGURE 6 EFFECT OF ALLUVIUM DEPTH AND GROUND SOFTNESS ON REINFORCED CONCRETE BUILDING DAMAGE IN TOKYO, 1923. (AFTER KANAI AND KITAZAWA.)

DAMAGE CRITERIA: KANAI: SEE FIGURE 5.
KITAZAWA: 50, LARGE DAMAGE; 100, COMPLETE DESTRUCTION

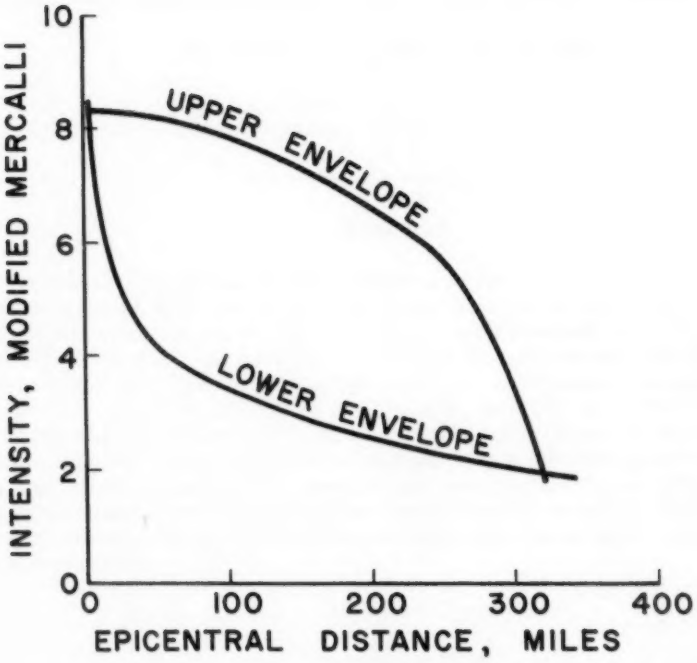

FIGURE 7 EFFECT OF GROUND ON INTENSITY-DISTANCE RELATION, SEATTLE EARTHQUAKE, 1949. (AFTER NEUMANN)

Paper 1731 August, 1958 SM 3

Journal of the
SOIL MECHANICS AND FOUNDATIONS DIVISION
Proceedings of the American Society of Civil Engineers

PRESSURE GROUTING FINE FISSURES

Thomas B. Kennedy[1]
(Proc. Paper 1731)

SYNOPSIS

Standard field equipment and methods were used in grouting fine fissures between specially prepared concrete slabs in a laboratory study with various grout mixtures and pressures. The lowest water-cement ratio that could be used in grout with neat cement, cement plus fly ash, cement plus fly ash plus an intrusion aid, cement plus an intrusion aid, and cement plus calcium lignosulfonate, to penetrate fissures of 0.01, 0.02, and 0.03 in. width at 25, 50, and 100 psi was determined. The penetration characteristics and the quality of hardened grout films were determined with seven different grout compositions, neat cement, cement plus fly ash, cement plus fly ash plus calcium lignosulfonate, cement plus calcium lignosulfonate, cement plus finely ground water-quenched slag, cement plus pumicite, and cement plus finely ground calcined shale.

INTRODUCTION

Purpose of Investigation

It is recognized that the strength and impermeability of a grout film follows the water-cement ratio law as do mixtures of other materials containing water and cement. Because of this fact it is desirable, where important work is concerned, to use grouts containing as low water contents per unit volume as possible. Since the lower the water content the thicker the grout, it is also important to determine the thickest consistencies that will penetrate cracks of various widths at given pressures.

Note: Discussion open until January 1, 1959. To extend the closing date one month, a written request must be filed with the Executive Secretary, ASCE. Paper 1731 is part of the copyrighted Journal of the Soil Mechanics and Foundations Division, Proceedings of the American Society of Civil Engineers, Vol. 84, No. SM 3, August, 1958.

1. Chf., Task Committee on Cement Grouting, Concrete Div., U. S. Army Engr. Waterways Experiment Station, Jackson, Miss.

In sealing fine seams, grouts having water contents as high as 20 to 1 (20 cu ft of water per bag of cement) are sometimes used, and grouts of a consistency as thin as 10 to 1 are not uncommon. The assumption has been that thin grout placed under sufficient pressure to force out the excess water used to obtain such a consistency will form a hard durable film. Whether it is always possible to exert enough pressure to squeeze out this excess water is questionable, and for this reason a knowledge of the physical nature of the grout films produced by fairly high water-cement ratios would be valuable. Such grouts are believed to be extremely pervious and, in time, susceptible to leaching that will transform an impervious area into a pervious one.

The purpose of the program was to obtain information on the degree to which the penetration of fine fissures by grout was influenced by surface texture of specimen, pumping pressure, water-cement ratio, chemical fluidifiers, and finely divided mineral additives. It was also desired to determine the effect of these factors on the quality of the hardened grout films.

Description of Investigation

The study was conducted in three phases during which the ability of grouts, of various compositions, to penetrate fine fissures at several pumping pressures was observed. Observations were also made of consistency, bleeding characteristics, and setting time of the grouts. Hardened grout films were examined for apparent quality and solubility of selected grout films in distilled water was measured.

The information in the report has been grouped so that all data bearing on one condition are presented together rather than discussed under the separate phases.

Materials, Equipment, and Specimens

Materials

Cement

Type II cement was used throughout the investigation and was obtained from the same mill but in three different shipments. The chemical and physical data for each shipment, designated by the numbers RC-183, RC-186, and RC-233, are shown below:

	Stage 1 (RC-183)	Stage 2 (RC-186)	Stage 3 (RC-233)
Chemical Properties			
Constituents, %			
SiO_2	22.8	22.5	22.2
Al_2O_3	4.3	5.3	4.8
Fe_2O_3	3.8	3.2	3.7
CaO	63.2	64.0	63.9
MgO	3.3	3.0	3.1
SO_3	1.5	1.5	1.5
Ignition loss	0.55	0.68	0.52
Insoluble residue	0.24	0.18	0.19
Na_2O	0.17	0.21	0.13
K_2O	0.48	0.34	0.41
Total alkalies as Na_2O	0.49	0.44	0.40

Calculated compounds, %			
C_3S	45	46	50
C_2S	32	30	26
C_3A	5	9	6
C_4AF	12	10	11
$CaSO_4$	3	3	3
Physical Properties			
Normal consistency	25.2	24.2	25.0
Setting time, Gilmore, hr-min:			
Initial	4:00	3:25	3:15
Final	6:20	6:25	4:15
Autoclave expansion, %	0.09	0.07	0.10
Air content of mortar, %	4.9	7.3	3.5
Compressive strength of mortar, psi:			
3 days	1540	1260	1625
7 days	2390	2010	2875
28 days	4025	3300	5035
Fineness, cm^2/g:			
Wagner	1805	1720	1840
Blaine	3170	2965	3080
Sieve analysis, dry:			
No. 50 (% retained)	0.2	0.0	0.0
No. 100 (% retained)	0.1	0.1	0.0
No. 200 (% retained)	2.4	4.3	1.3

Fly Ash

The fly ash used in all three stages came from the Chicago region but in different shipments. A chemical analysis was not made of the fly ash used in stages 1 and 2. The chemical analysis of the fly ash used in stage 3 is shown in the following paragraph. The physical characteristics of the fly ash used in the respective stages are listed in the following tabulation:

Sieve Analysis, Dry				
	Opening	Per Cent Retained		
Sieve No.	in.	Stage 1	Stage 2	Stage 3
50	0.0117	0.4	0.2	0.9
100	0.0059	1.3	1.1	0.9
200	0.0029	6.2	6.0	2.5
Fineness, cm^2/g:				
Blaine		2795	2795	--
Fisher		--	--	3335
Specific gravity		2.43	2.43	2.48

Other Mineral Admixtures

The following mineral admixtures were used in stage 3 only:

a. Slag, water-quenched, ground, laboratory No. RC-216.
b. Pumicite, laboratory No. AD-6.
c. Opaline shale, calcined, laboratory No. AD-13.

Data on these materials and on the fly ash used in stage 3 follow:

	Fly Ash AD-3 %	Slag RC-216 %	Pumicite AD-6 %	Opaline Shale AD-13 %
Chemical Properties				
Constituents, %				
Moisture loss	0.20	--	0.83	1.2
SiO_2	47.2	35.8	68.8	70.1
Al_2O_3	19.5	15.8	14.8	19.3
Fe_2O_3	18.2	1.2	1.4	5.9
Mn_2O_3	0.07	0.62	0.05	0.05
P_2O_5	0.23	--	0.02	0.14
CaO	5.3	35.5	0.65	0.22
MgO	1.2	10.4	0.33	0.85
Sulfide sulfur	0.05	--	0.00	0.00
SO_3	2.2	0.1	0.03	0.10
Ignition loss	0.8	0.23	3.9	1.26
Insoluble residue	70.4	0.52	94.6	86.9
Na_2O (gravimetric)	0.69	--	--	--
K_2O (gravimetric)	1.16	--	--	--
Total Na_2O (gravimetric)	1.45	--	--	--
Na_2O (flame)	1.62	0.11	1.38	0.40
K_2O (flame)	1.98	0.65	4.96	0.61
Total Na_2O (flame)	2.92	0.54	4.64	0.80
$CHCl_3$ sol	--	--	--	--
Total carbon	0.43	0.54	0.02	0.07

		Fly Ash AD-3 %	Slag RC-216 %	Pumicite AD-6 %	Opaline Shale AD-13 %
Physical Properties					
Fineness, cm^2/g:					
Wagner		--	3,430	--	--
Blaine		--	5,795	--	--
Fisher		3,335	5,470	4,640	15,020
Specific gravity		2.48	2.85	2.35	2.35
Sieve No., and sieve opening (in.)					
50	0.0117	0.9	0.8	0.0	0.1
100	0.0059	0.9	0.4	0.4	0.9
200	0.0029	2.5	1.3	1.5	13.9

Chemical Admixtures

The intrusion aid causes slight expansion of the grout and is purported to prevent agglomeration of the solids and aid penetration of fissures. It was used in all tests at the rate of one per cent of the weight of cement or cement plus fly ash whenever fly ash was used in the grout.

Calcium lignosulfonate, cls, was added for the same purposes as intrusion aid. It did not, however, cause expansion of the grout. It was used in all cases at the rate of 0.23 per cent of the weight of cement.

Grouting Equipment

The grout pump was a single-cylinder, reciprocating 3-3/4- by 2-1/2- by 5-in. steam pump with rubber piston and valves, air-driven for these tests. The grout mixer was a paddle-type machine powered by a motor from an electric drill. A photograph of the grouting assembly, including a typical specimen, as used in stage 1 of the program is shown on Fig. 1. An important change in the equipment setup was made at the conclusion of stage 1 and was used throughout the remainder of the program. This change is shown schematically on Fig. 2 and consisted of connecting the delivery line and a return line with a corresponding control valve immediately adjacent to gage A (gage O on Fig. 2). It was suspected that the velocity of flow in the riser of the delivery line would be so low in some cases as to allow settlement of the coarser particles and thus result in a variable grout passing through the fissure. This supposition was confirmed by observing the flow of grout through a vertical lucite tube. This difficulty was largely overcome by opening the valve on the return line, as shown on Fig. 2, sufficiently to insure a relatively constant rate of grout flow through the riser under all grouting conditions. In addition, three additional gages were installed along the specimen so that variations in pressure gradient could be determined during grouting operations.

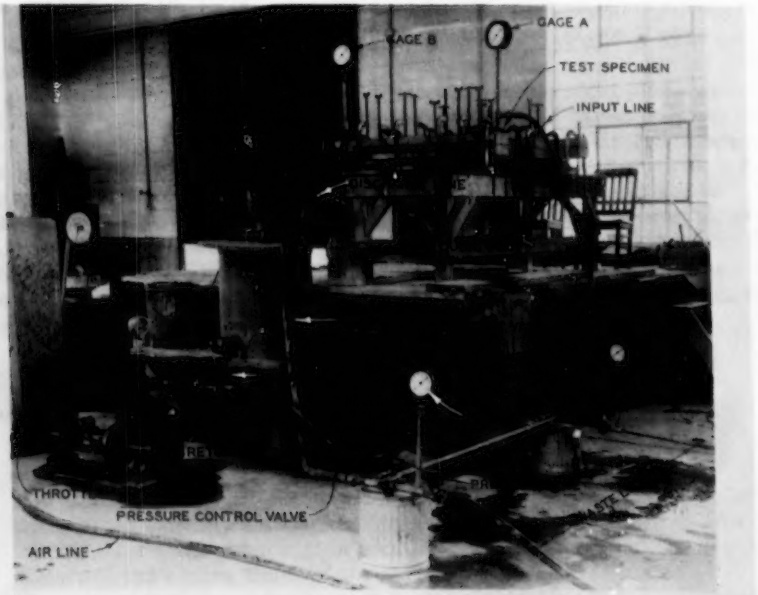

Fig. 1. Equipment setup for stage 1 grouting tests

Specimens

A specimen consisted of a pair of matching prisms of high-strength reinforced concrete. Each half was 7 in. wide by 3 in. thick by 52 in. long. Two prisms were cast at the same time in the same form with a piece of 1/4-in. plate glass as a separator between them to assure matching surfaces. Half of the prisms were without pipe connections. Half of those in the first stage tests contained two 3/4-in. pipe nipples 48 in. apart embedded along the center line normal to and in contact with the glass separator. Half of those in the second and third stage tests contained five nipples 12 in. apart.

A pair of matching prisms was separated by a ribbon of shimstock 1/2 in. wide of the required thickness around the edges and ends between the halves to form a fissure 6 in. wide and 48 in. long between the end nipples. The two halves were held together by C-clamps. The specimens were pumped in a horizontal position for the following reasons:

a. The most dangerous conditions in grouting under a dam are caused by extensive open passages such as horizontal bedding planes. It was desired to learn something about grout flow and pressure distribution under such conditions.
b. It was hoped to learn something concerning the validity of the assumption that excess mixing water can be forced out of the grout by the application of pressure. It was believed that if this did occur a good bond would be made with the top as well as the bottom half of the specimen; if not, bleed water would prevent bond with the top half.

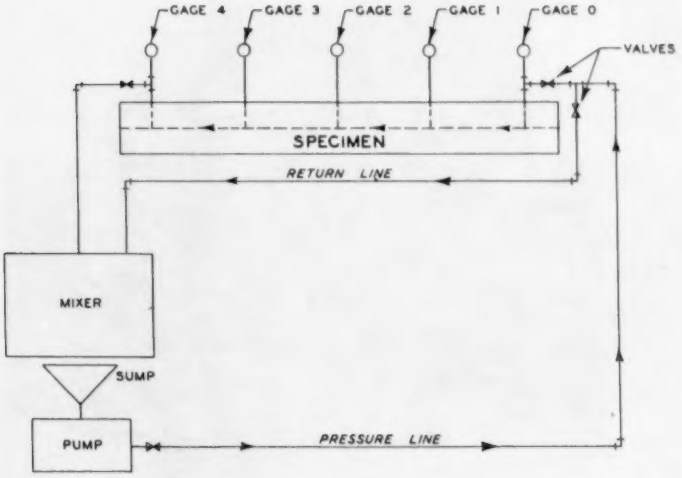

FIGURE 2 SCHEMATIC DIAGRAM, GROUTING TESTS-FINE FISSURES
NOT TO SCALE

Grout Pumping Tests

General Procedures

Treatment of Grout

Dry materials were all sieved through a 30-mesh sieve and the mixed grout was passed through a 30-, 50-, or 100-mesh sieve depending upon the water-cement ratio. The thinnest grouts were passed through a 100-mesh sieve, thicker grouts through a 50-mesh sieve, and the thickest grouts through a 30-mesh sieve.

Grout Injection

Grout injection was started by pumping water through the specimen followed by thin grout which was gradually thickened by the addition of solids. The desired pressure was maintained on the specimen by operating the bypass valve so that only a controlled portion of the total flow of grout was shunted through the specimen. The pump was operated at a speed of approximately 72 strokes per minute for the major portion of the tests. At the lowest water-cement ratio for a given test more than one hour of pumping was usually required to discharge one cubic foot of grout through the fissure of a specimen. Grout flow stopped at any given pressure when the grout became too thick. In stage 1 operations, pressure was maintained on specimens for 10 to 15 min after all flow had stopped with the valve at B (Fig. 1) open at all times. Water continued to drip very slowly from the discharge line during final application of pressure, being squeezed out after separating from the grout film in the specimen. When gage B assembly was removed the short pipe nipple cast in the test specimen was invariably found to be full of hardened grout into which a pencil could be forced only with difficulty. This was the case regardless of the consistency of the grout being pumped. In stage 2 operations the valves at the entrance and discharge ends of the specimen were closed as soon as all flow had stopped and the pressure within the specimen was allowed to equalize insofar as internal conditions would permit. Pumping for stage 3 was in most instances conducted as in stage 1 although for some tests the valves were closed at cessation of pumping on both ends of the specimens, as in stage 2.

Test Conditions

The study was conducted in three separate stages as follows:

a. The first stage furnished data on the lowest water-cement ratios of grouts that could be pumped through fissures of 0.01-, 0.02-, and 0.03-in. thickness at 100 psi pressure, with the following grout conditions: (1) neat cement; (2) cement plus fly ash; (3) cement plus fly ash plus the admixture, intrusion aid. A study of consistency, bleeding characteristics, and setting times of the various grouts was also made.
b. The second stage provided data on grout penetration obtained at pumping pressures of 25 and 50 psi using the three grout conditions of the first stage and the additional condition of cement plus intrusion aid. Tests were also made of neat-cement grout plus calcium lignosulfonate, hereinafter abbreviated as cls, at 25, 50, and 100 psi, and of neat-cement grout plus intrusion aid at 100 psi.

c. The third stage consisted of: pumping tests through an 0.03-in. thick crack at 50 psi using the seven grout conditions listed below; tests of the grouts themselves for consistency, bleeding, setting time; and tests to determine the apparent solubility of hardened grout films in distilled water.

Grout Conditions

(1) Neat cement
(2) Cement plus fly ash
(3) Cement plus cls
(4) Cement plus fly ash plus cls
(5) Cement plus slag
(6) Cement plus pumicite
(7) Cement plus opaline shale

Some of the above materials were used in various proportions of one to the other so that a total of 17 different grout mixtures were pumped. These are described in detail later in the report.

Observations were made during and after pumping for:

a. The effect of specimen surface on the water-cement ratio and pumpability of the grout (stage 1 only).
b. Lowest water-cement ratio of grout that would penetrate the three different fissure thicknesses.
c. Pressure drop along the specimen.
d. Rate of grout flow at a given pressure, water-cement ratio, and crack thickness.
e. Relationship between pumping pressure and lowest water-cement ratio grout that a fissure would take.
f. Relationship of particle size of grout solids to the width of crack that could be grouted.
g. Effect of chemicals (intrusion aid and cls) on the penetration qualities of grouts.
h. Quality of hardened grout films, from visual observation.
i. Strength of grout film as judged by shear tests (for stage 2 only).
j. Special observations and tests were made in stage 3 for consistency of the grout at each change in water-cement ratio by measuring change in unit weight of the grout and the torque imparted to a piano-wire consistency meter.

Discussion of Pumping Tests

Ninety-seven pumping tests were made. The detailed data, because of their voluminous nature, are not tabulated in this report. They are presented and analyzed in the figures and discussion. In most instances the lowest water-cement ratio shown for a given grout mixture and test condition was the lowest water-cement ratio that could be pumped. It is considered, however, that the water-cement ratio at which the flow equals 0.1 cu ft per min (6 cu ft per hr) is the stiffest grout practical for field pumping.

Throughout this report water-cement ratio is expressed by weight of water to cement or to cement plus other solids when materials such as fly ash were added to the grout. All references in text or figures to cement-fly ash grout, or cement-slag grout, etc., refer to grout having equal parts of cement to fly ash or other material by weight unless specifically stated otherwise.

Effect of Surface Texture of Specimen on Grout Penetration

Pumping tests 2 through 12 were made using specimen surfaces from which the glaze, due to casting against the glass, was removed by light rubbing with a carborundum stone. Tests 13 through the end of the program were made using specimen surfaces from which the glaze had not been removed. The effects of type of specimen surface, fineness (maximum grain size) of the grout, and crack thickness on the water-cement ratio of the grout are shown on Fig. 3 and discussed below:

a. The combination of smooth surfaces and grout strained through a No. 50 sieve permitted the use of lower water-cement ratios for the 0.03- and 0.02-in. fissures than for the combination of rubbed surfaces and grout strained through a No. 30 sieve, for both neat grout and grout containing fly ash.
b. The combination of smooth surfaces and grout strained through a No. 50 sieve permitted the passing of neat grout with a water-cement ratio of 1.34 by weight through the 0.01-in. opening as contrasted with a

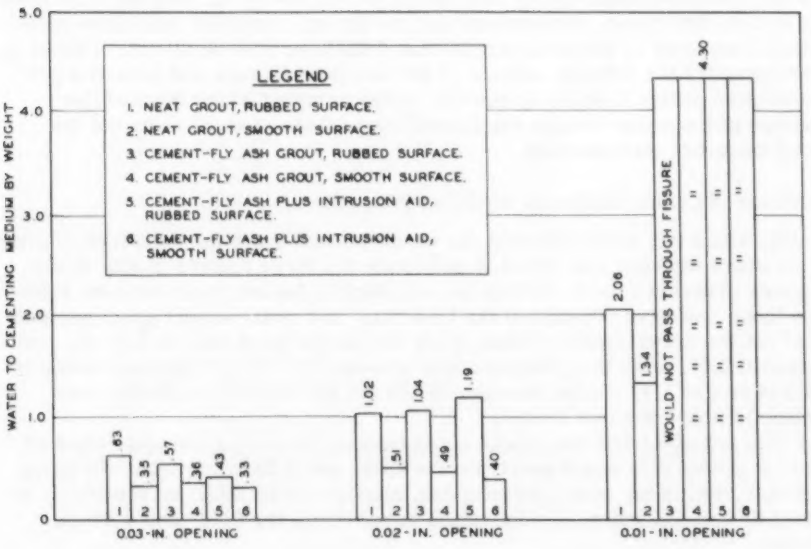

Fig. 3. Effect of crack thickness, surface texture, and fineness of grout on water-cement ratio

water-cement ratio of 2.06 with the rubbed surfaces and neat grout strained through a No. 30 sieve.

c. Grout containing fly ash could not be pumped through the 0.01-in. opening regardless of the type of surface or when strained through the No. 50 sieve even with a water-cement ratio of 4.30, the highest water-cement ratio used in the tests. The reason for the poor pumpability of the fly ash grout is discussed in the following paragraph.

d. The use of one per cent of intrusion aid by weight of the cement plus fly ash permitted a slight reduction in water-cement ratio when grouting the 0.03-in. fissures with rubbed surfaces as compared to the grout containing fly ash and no intrusion aid, but did not help when grouting the 0.02- and 0.01-in. fissures with rubbed surfaces.

e. The use of intrusion aid permitted a slight reduction in water-cement ratio when grouting the smooth-surfaced 0.02- and 0.03-in. fissures but was ineffective in promoting penetration of the 0.01-in. fissures.

The physical data on the materials used in stage 1 showed the cement to have a greater specific surface (Blaine 3172 cm^2 per g, 97.3 per cent passing the No. 200 sieve) than the fly ash (Blaine 2795 cm^2 per g, 92.1 per cent passing the No. 200 sieve), and showed that the fly ash contained somewhat more than 0.4 per cent of material larger than 0.0117 in. (No. 50 sieve). This grain size exceeded the 0.01-in. opening of the smallest fissure and caused a grid of oversize grains to build up quickly during pumping which blocked the passage of the grout through the fissure regardless of whether or not the grout contained intrusion aid.

Influence of Crack Thickness on Grout Penetration

Fig. 4 is a bar graph showing the water-cement ratio for each type of grout at the stage where it just failed to penetrate the three fissure widths at the pumping pressures used. Grouts of only slightly higher water-cement ratios than those indicated penetrated the fissures. For neat-cement grout pumped at 25 psi the lowest water-cement ratio that would penetrate an 0.01-in. crack exceeded 2.67, when this pressure was increased to 50 psi the water-cement ratio exceeded 1.33 but an increase to 100 psi did not permit further reduction in water-cement ratio.

Little practical difference was noted between the water-cement ratios of the neat grouts that would penetrate the 0.02- and 0.03-in. cracks. Pumping pressure, within the range investigated, also had little effect on the ability of grouts of various water-cement ratios to penetrate the 0.02- and 0.03-in. cracks.

Grouting of any of the 0.01-in. cracks with grouts containing fly ash was found impracticable for the reasons previously stated.

The use of fly ash was of no benefit in grouting the 0.02-in. crack, since it permitted no practical reduction in water-cement ratio over neat grout. Pumping pressure, within the range used, was of little value in improving the penetration of the 0.02-in. crack with a cement and fly ash grout.

Grouts of cement and fly ash that would penetrate the 0.03-in. crack were of slightly lower water-cement ratio than the neat grouts that would penetrate cracks of similar width at 25 and 50 psi, but practically the same at 100 psi.

Use of intrusion aid in the neat-cement grout permitted a slight reduction in water-cement ratio of the grouts that would penetrate both the 0.02- and 0.03-in. cracks at the pressures tested.

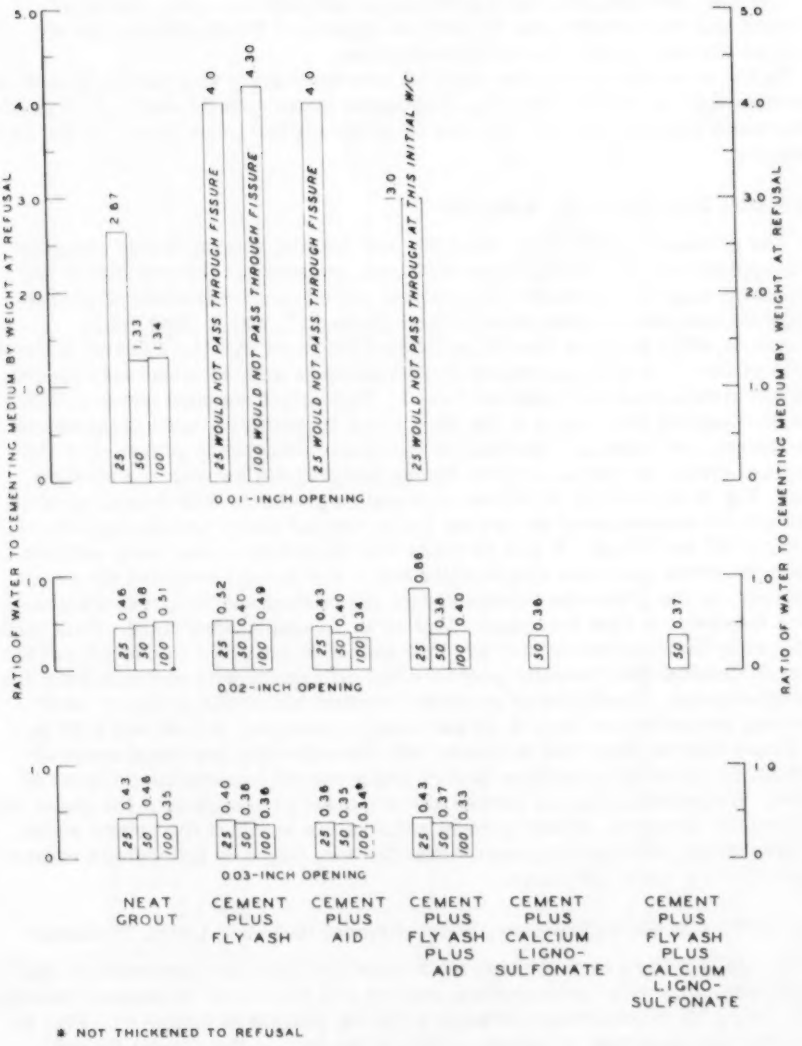

FIGURE 4. MINIMUM WATER-CEMENT RATIO AT REFUSAL AS INFLUENCED BY CRACK THICKNESS

Cls was used only at 50-psi pressure on the 0.02-in. crack with neat cement and with cement plus fly ash but appears to be as effective as intrusion aid with respect to grout penetration.

In the above discussion the effect of maximum grain size should be kept in mind as well as the fact that Fig. 4 indicates water-cement ratios at refusal, whereas a rate of flow of 6 cu ft per hr is the stiffest grout practical for field pumping.

Pressure Drop Along the Specimen

The pressure gradient for the 0.02- and 0.03-in. cracks during pumping was approximately a straight line with zero pressure at the exit end of the specimen (gage 4), maximum pressure at the entrance end of the specimen (gage 0), and intermediate pressures at gages 1, 2, and 3. The static pressure, after pumping was stopped when the grout was thick (water-cement ratio of less than 0.5) and valves at both entrance and exit ends were closed, did not always equalize from end to end. This may have been due to a thixotropic condition developing in the thick grout immediately upon cessation of movement, and causing a blocking of the specimen between gages. For the 0.01-in. crack, the pressure drop during pumping did not follow a straight line. Fig. 5 is a series of curves of pressure gradients that developed when neat grouts were pumped at various water-cement ratios through an 0.01-in. crack at 25 and 50 psi. It will be noted that the gradient was fairly uniform along the whole specimen length while water was being circulated through it; however, as the grout was thickened flow diminished and the pressure gradient between the first two gages (first 12 in. of length) increased. This would apparently indicate that in the very fine seams as the grout thickened and the flow diminished the hydraulic pressure fell off rapidly with distance from the intrusion point. Conditions of pressure gradient and static pressure after pumping are shown on Figs. 6-14 for crack thicknesses of 0.02 and 0.03 in.

These figures show that in cracks with smooth walls and thicknesses of 0.02 in. or more the conditions of flow and pressure are similar to those of water. Irregularities in the curves are due to faulty operation of the gages occasioned by plugging. Water-cement ratio values at which the grouts would act like water, relative to pressure distribution, might be different in nature where fissure walls are rough.

Rate of Flow at Given Pressure, Water-Cement Ratio and Crack Thickness

Fig. 15 is a bar graph showing the amount (in cubic feet per hour) of various grouts, all with a water-cement ratio of 0.5, that could be pumped through 0.02- and 0.03-in. cracks at the three pumping pressures employed. Fig. 16 presents the same data in curves, omitting the data on the cement fly ash plus intrusion aid grout, which are anomalous and inconclusive.

Increasing pressure caused proportionately increasing flow. Apparently the flow of the cement fly ash grout was greater at equivalent pressures and crack openings than that of neat grout.

The use of intrusion aid in the neat grout increased flow at equivalent pressures and crack thicknesses over plain neat grout and caused greater flow than did the use of fly ash. Data on the effect of intrusion aid on the cement fly ash grout were inconclusive.

The rate of flow provides a realistic measure of the viscosity of a grout. Figs. 15 and 16 show that the rate at which a grout can be injected into a

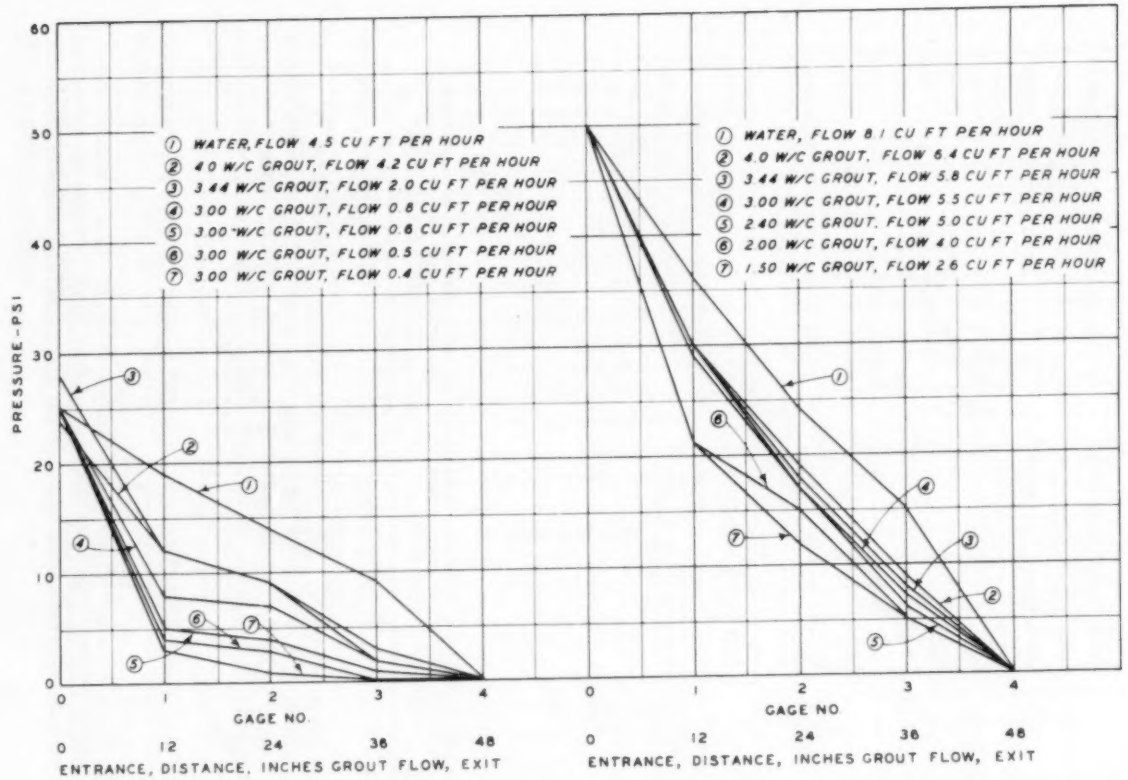

FIGURE 5 PRESSURE GRADIENTS DURING GROUTING OF 0.01-IN CRACK WITH NEAT GROUT

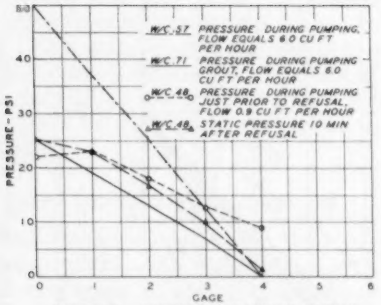

FIGURE 6 - PRESSURE GRADIENT DURING AND AFTER GROUTING 0.02-INCH CRACK, NEAT GROUT

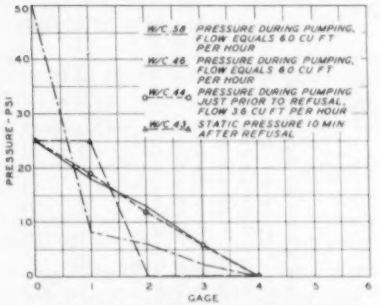

FIGURE 7 - PRESSURE GRADIENT DURING AND AFTER GROUTING 0.03-INCH CRACK, NEAT GROUT

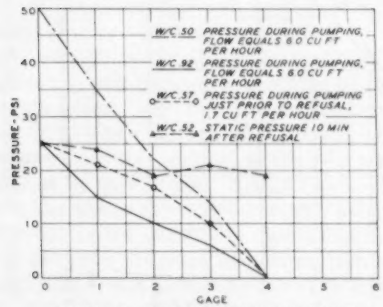

FIGURE 8 - PRESSURE GRADIENT DURING AND AFTER GROUTING 0.02-INCH CRACK, 1:1 CEMENT-FLY ASH GROUT

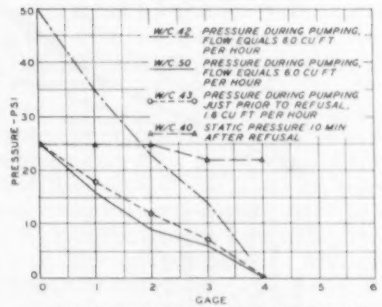

FIGURE 9 - PRESSURE GRADIENT DURING AND AFTER GROUTING 0.03-INCH CRACK, 1:1 CEMENT - FLY ASH GROUT

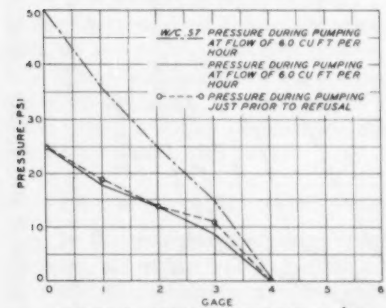

FIGURE 10- PRESSURE GRADIENT DURING GROUTING 0.02-INCH CRACK, NEAT GROUT + INTRUSION AID (1%)

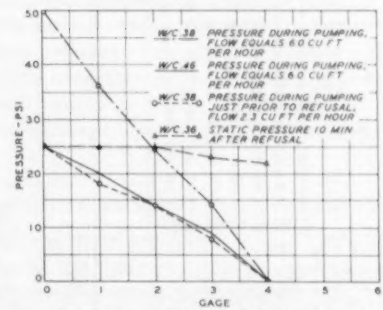

FIGURE 11- PRESSURE GRADIENT DURING AND AFTER GROUTING 0.03-INCH CRACK, NEAT CEMENT + INTRUSION AID GROUT

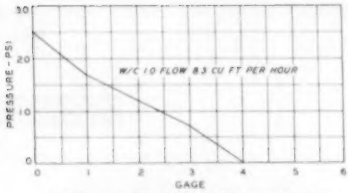

FIGURE 12- PRESSURE GRADIENT DURING GROUTING 0.02-INCH CRACK, 1:1 CEMENT-FLY ASH-INTRUSION AID GROUT

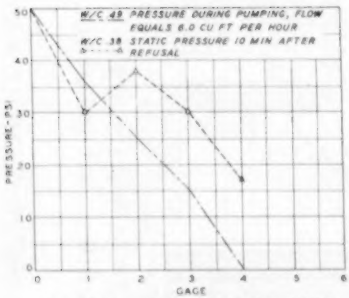

FIGURE 13- PRESSURE GRADIENT DURING AND AFTER GROUTING 0.02-INCH CRACK, 1:1 CEMENT - FLYASH - CL S GROUT

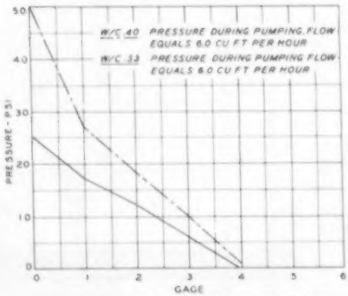

FIGURE 14- PRESSURE GRADIENT DURING GROUTING 0.03-INCH CRACK, 1:1 CEMENT-FLY ASH- INTRUSION AID GROUT

crack is influenced by pressure and composition. Rate of flow is an index to the distance a grout can be pushed at a given pressure before friction causes the flow to cease. Under conditions dictating the use of low-pressure grouting, greater density of drilling than ordinary or the use of fluidifiers is indicated.

Relationship Between Pumping Pressure, Water-Cement Ratio, and Crack Thickness

An examination of Fig. 4 shows that the crack thickness had a great effect on the lowest water-cement ratio grout that could be pumped through a crack. The pressure had little practical effect, since water-cement ratios lower than 0.5 are seldom employed.

Relationship Between Particle Size of Grout Solids and Width of Crack Penetrated

It will be noted that the lowest water-cement ratio neat grout that could be forced through the 0.01 crack (Fig. 4) was approximately 1.33 by weight. This is a dilute material of dubious quality and is believed to be neither durable nor impermeable. Grout containing fly ash could not be forced through the

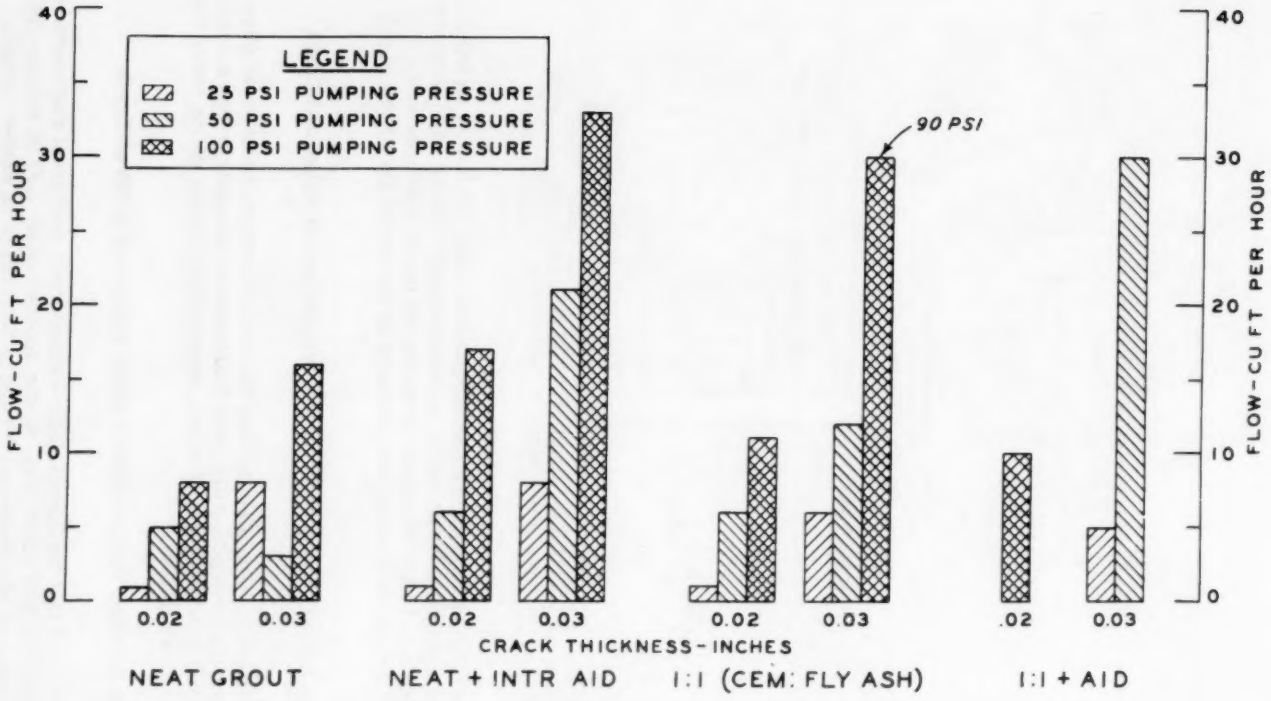

FIGURE 15 FLOW OF 0.5 WATER-CEMENT RATIO GROUT AT 25, 50, AND 100 PSI PUMPING PRESSURES

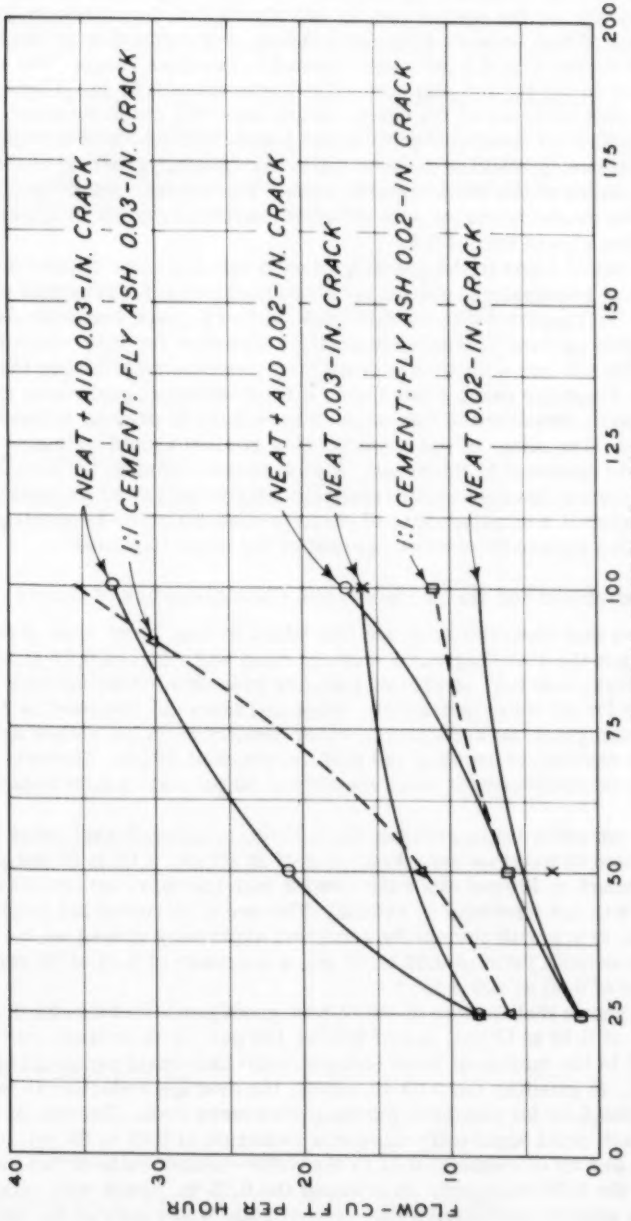

FIGURE 16 FLOW OF 0.5 WATER-CEMENT RATIO GROUTS AT PRESSURES AND THROUGH CRACKS SHOWN.

0.01-in. crack even at considerably higher water-cement ratios. Examination of the physical data on the cement and fly ash shows that the maximum grain size of the cement was between 0.01 and 0.006 in., corresponding to the 50- and 100-mesh sieves with 0.1 per cent retained in this size range. The maximum grain size of the fly ash was somewhat in excess of 0.01 in. These results indicate that stoppage of the crack occurs when the crack-opening: grain-size ratio is 1.7 even with quite dilute grouts, and that with fly ash, where the maximum grain size exceeds the crack opening, grouting is impossible regardless of the water-cement ratio. The critical crack-opening: grain-size ratio probably varies with different materials, and it is believed that a safe value should exceed 3.0.

Alfred Machis[1] found in the grouting of sand that the ratio of pore diameter to grain size necessary to permit penetration of cement slurry was at least five. A. F. Taggart,[2] in his handbook, shows a graph that indicates the ratio of filter opening to maximum particle diameter for filter-cake formation. The fly ash had a maximum grain diameter somewhat larger than 250 microns. From the curve cited above, a filter-opening: grain-size ratio somewhat greater than three is indicated as necessary to prevent formation of a filter cake. The shape of the opening being grouted should influence the ratio of particle diameter to thickness. A slot-shaped opening, as used in the tests being reported, because of its relatively infinite width and no restricting sides, should permit a smaller ratio of particle-size diameter to opening to pass grout than a square or rounded opening of the same thickness.

Effect of Intrusion Aid and cls on Penetration Characteristics of Grouts

Fig. 4 shows that when intrusion aid was added to neat grout when grouting an 0.02-in. crack the resulting water-cement ratio was reduced 0.03 at 25-psi, 0.08 at 50-psi, and 0.17 at 100-psi pumping pressure, or an average reduction of 0.09 for all three pressures. When intrusion aid was used in 1 cement: 1 fly ash grout, no reduction in water-cement ratio but rather an increase of 0.43 resulted in grouting the 0.02-in. crack at 25 psi. However, an 0.02 reduction in water-cement ratio resulted at 50 psi and an 0.09 reduction at 100 psi.

The use of intrusion aid in grouting the 0.03-in. crack with neat grout allowed a reduction in water-cement ratio of 0.07 at 25 psi, 0.11 at 50 psi, and an unknown amount at 100 psi since the cement plus intrusion aid grout at this pressure was not thickened to refusal. The use of intrusion aid in grouting the 0.03-in. crack with cement fly ash grout apparently caused an increased water-cement ratio of 0.03 at 25 psi, a decrease of 0.01 at 50 psi, and a decrease of 0.03 at 100 psi.

Fig. 4 also shows that the use of cls in neat grout permitted a reduction of 0.01 at 25 psi, of 0.12 at 50 psi, and of 0.09 at 100 psi, or an average reduction of 0.07 in the minimum water-cement ratio that would penetrate an 0.02-in. crack. In grouting the 0.03-in. crack, the average reduction in water-cement ratio was 0.04 for the three pumping pressures used. The use of cls in cement fly ash grout apparently allowed a reduction of 0.07 at 25 psi, of 0.03 at 50 psi, and an increase of 0.01 in the water-cement ratio at 100 psi when grouting the 0.02-in. crack. In grouting the 0.03-in. crack with cement fly ash grout a slightly increased water cement ratio was required for penetration at all three pressures used.

For penetration of a given crack thickness, intrusion aid seemed to be a little more efficient in lowering the water content of grout than cls. That is,

intrusion aid was slightly more efficient than cls as a fluidifier. However, little appears to be gained from use of either material except where it might be desirable to inject low water-cement ratio grout under low pressure.

Quality of Hardened Grout Films from Visual Observation

The two halves of the grouted specimen were opened and examined approximately 24 hr after pumping. The following tabulation summarizes these observations with the evaluations arranged in order of increasing water-cement ratios for each type of grout.

Type Grout	Water-cement Ratio, wt	Appearance	Bond Judged from Appearance
Neat	0.32-0.38	Good	Good to poor
	0.46	Good	Fair
	0.48	Fair	Poor
	0.51	Fair	Poor
	1.33	Poor, stringy	Poor
	1.34	Poor, stringy	Poor
Neat + intrusion aid	0.34	Good	Good
	0.34	Good	Fair
	0.35	Good	Good
	0.36	Good	Poor
	0.40	Good	Fair
	0.43	Good	Fair
	4.0	Poor, stringy	Poor
Neat + cls	0.36	Good	Fair to poor
1:1 (cement:fly ash)	0.36	Good	Poor
	0.38	Good	Poor
	0.40	Good	Poor
	0.45	Fair, stringy	Poor
	0.49	Good	Poor
	4.0	Poor, stringy	Poor
	4.3	Poor, stringy	Poor
1:1 + intrusion aid (cement: fly ash + aid)	0.33	Good	Poor
	0.37	Good	Poor
	0.40	Good	Poor
	0.43	Good	Fair
	0.43	Fair	Poor
	3.0	Poor, clumped	Poor
	4.3	Poor, stringy	Poor
1:1 + cls (cement:fly ash + cls)	0.035 to 0.038	Good	Good to poor
1.5:1 (cement:fly ash)	0.45	Fair, stringy	Poor
2:1 (cement:fly ash)	0.42	Fair, stringy	Fair
1.5:1 (cement:fly ash + cls)	0.36	Good	Good
2:1 (cement:fly ash + cls)	0.36	Good	Good
1:1 (cement:slag)	0.36	Good	Poor
1.5:1 (cement:slag)	0.38	Good	Poor

Type Grout	Water-cement Ratio, wt	Appearance	Bond Judged from Appearance
2:1 (cement:slag)	0.38	Good	Poor
1:1 (cement:pumicite)	0.56	Fair (soft)	Fair
1.5:1 (cement:pumicite)	0.50	Good	Fair
2:1 (cement:pumicite)	0.50	Good	Poor
1:1 (cement:opaline shale)	0.60	Fair (soft)	Poor
1.5:1 (cement:opaline shale)	0.55	Good	Poor
2:1 (cement:opaline shale)	0.55	Good	Poor

A grout film designated "good" in the tabulation was one which was hard to the fingernail, filled the cavity completely, and showed "none" to a "moderate" amount of bleeding as evidenced by channels cut by "bleed water" as it moved under slight residual pressure from the pumping process, or under gravity, toward points of lesser pressure or lower elevation. Fig. 17 shows a film designated "good". A film was designated "fair" when the grout could be scratched with the thumbnail or was traversed by numerous bleeding channels. It was called "poor" when it was quite soft or when the film occurred in lenses or streaks and could not be considered a continuous sheet of material. Fig. 18 shows a close-up of a poor-quality film.

Bond was considered "good" when approximately 40 per cent or more of the film adhered to the upper slab when the specimen was opened; "fair" when the adherence was approximately 25 to 40 per cent; and "poor" when the adherence was less than approximately 25 per cent.

It will be noted that the appearance of all the grouts having a water-cement ratio of 0.6 or less was "good" to "fair," and that where "poor" grout was encountered the ratio was 3.0 or higher. There are no intermediate values with the water-cement ratios ranging from 0.6 to 3.0, but it is only logical to assume that the quality of such films would have been "fair" to "poor." A direct comparison of the quality of different types of grout having the same water-cement ratio is not possible from the present data. However, judging from the bond evaluations, the use of intrusion aid appeared to be of some slight benefit in increasing adherence of the film to the top slab; but for grouting a horizontal opening between two nonabsorbent surfaces where a high-quality grout would be required, which would assuredly adhere to the top as well as the bottom of the cavity, a water-cement ratio not exceeding approximately 0.46 and neat grout should be used. The use of fly ash, judging from these qualitative data, may have had an adverse effect on the bond between top and bottom slab, although the quality of the films, from visual observation, was usually good. There was an apparent tendency toward clumping of the solids in some cases.

Cls in the cement fly ash grouts tended to make them softer at 24 hr, but appeared to counteract to a large extent the tendency to agglomerate, and improved the bond to the top slab.

The use of slag, pumicite, and opaline shale tended to improve the appearance of the grout films to a marked extent. Visual evidence of bleeding

Fig. 17. Good quality neat-cement-grout film, water-cement ratio 0.32 in., crack thickness 0.03 in., pumping pressure 100 psi. Note white streaks caused by passage of water that was squeezed from the grout under the shim

Fig. 18. Closeup (X2) of poor quality neat-cement-grout film, water-cement ratio 1.34, crack thickness 0.01 in., pumping pressure 100 psi

was entirely lacking with all the pumicite and opaline shale grouts and with the 1 slag: 1 cement grout. The 1.5 cement: 1 slag grout showed slight bleeding and the 2 cement: 1 slag grout showed moderate bleeding. All three slag-grout films were hard to the fingernail at 24 hr; however, the 1 cement: 1 pumicite grout could be dented by a fingernail at 24 hr and the 1 cement: 1 shale grout could be slightly scratched by a fingernail at 24 hr. Bonding to the top slab did not seem to be improved by use of slag, pumicite, or opaline shale.

Strength of Grout Films Judged by Shear Tests

An attempt was made, during stage 2 of the tests, to measure the bond strength developed between top slab and the grout by making shear tests at 120 days age on sections of grouted specimens cut to 10-in. lengths. Three 0.01-in. cracks were grouted at 50 psi with various grouts as listed below, all with a water-cement ratio of 0.45 and with pressure maintained on the specimens for 15 min after pumping:

Type Grout	Test No.	Remarks
Neat + intrusion aid	46A	
Neat	48	
1 cement: 1 fly ash	49	Came apart in handling
1 cement: 1 fly ash	54	Came apart in handling
1 cement: 1 fly ash + aid	50	Came apart in handling

The following results were obtained:

Specimen Section	Shear Resistance, psi
46(1)	50
46(2)	Came apart in handling
46(3)	180
46(4)	70
48(1)	65
48(2)	30
48(3)	50
48(4)	60

Test values were quite low for the neat-grout and neat-grout plus aid specimens tested, indicating very little bond. Those specimens containing fly ash did not develop enough bond to permit making a test.

Tests of Grout Characteristics

Consistency

A satisfactory device for measurement of consistency is highly desirable and would enable the grouting crew to suit the quality and "pumpability" of the grout to the grouting conditions encountered. Consistency measurements were made on the grout itself by means of a piano-wire, pendulum-type viscosimeter, Fig. 19, by a flow cone, and by a unit-weight device.

The viscosimeter was developed by Professor R. E. Davis of the University of California, Berkeley, and the Bureau of Reclamation. The viscosity or

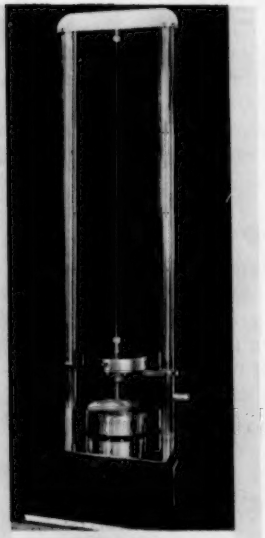

Fig. 19. Piano-wire viscosimeter

consistency of a slurry is measured by placing a sample in a shallow metal container mounted on a motor-driven turntable. A wire spider is suspended from a piano wire and is submerged in the sample of grout. A weight holds the piano wire taut. Torque is imparted to the spider and piano wire by the turning container of grout. The number of degrees of torque varies with the consistency of the sample being tested.

The flow cone is simply, as its name implies, a cone with a specified orifice from which a known volume of liquid flows in a certain length of time, depending upon its consistency. The flow cone contained 1725 ml which were discharged through a pipe orifice, 1-1/2 in. long by 1/2-in. inside diameter, in the bottom of the cone. Flow was timed with a stop watch. In some of the tests the discharge pipe was modified to 6 in. in length and 3/8-in. inside diameter.

The unit-weight device for consistency determinations was designed for use with neat-cement grout and consisted of a measure and specially graduated beam for translating unit weight into water-cement ratio.

The piano-wire torque meter provided the most satisfactory means of measuring consistency in the laboratory. It was calibrated against the Stormer viscosimeter in connection with another investigation so that the readings obtained could be translated into standard units of viscosity (poises). This calibration is shown on Fig. 20. Consistency meter readings at fixed water-cement ratios for grout combinations used in the third-stage work are tabulated below:

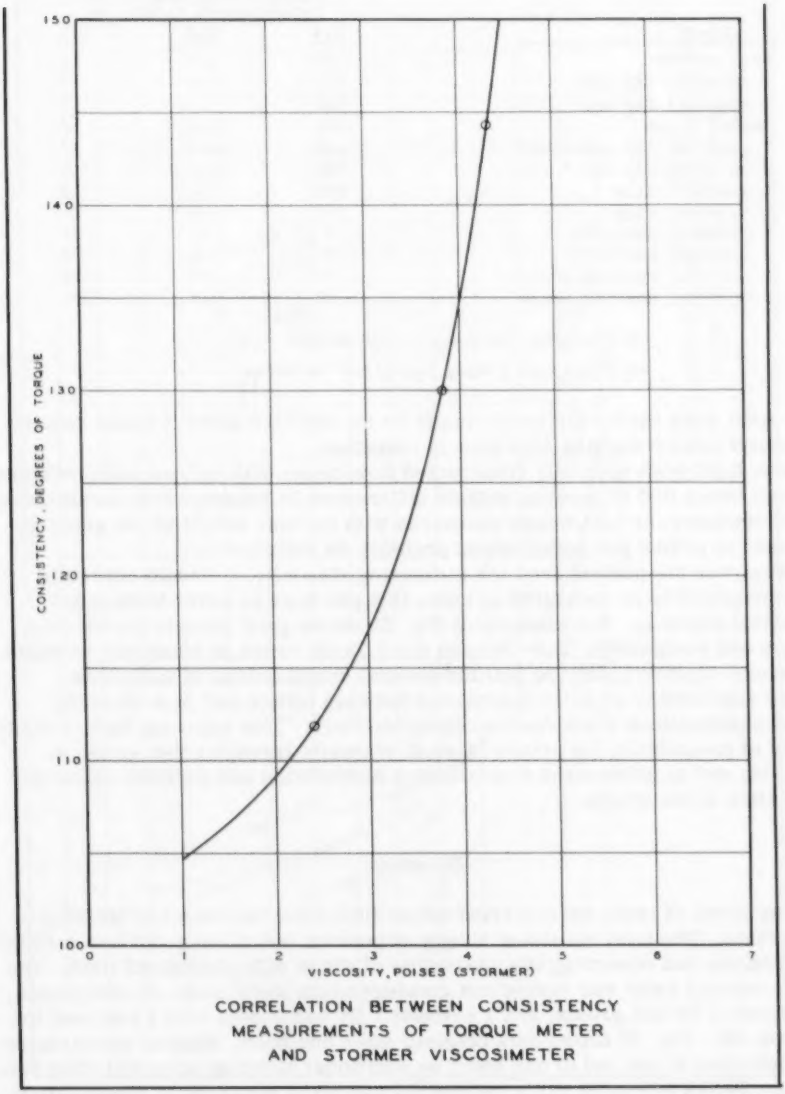

CORRELATION BETWEEN CONSISTENCY MEASUREMENTS OF TORQUE METER AND STORMER VISCOSIMETER

FIGURE 20

Grout	Consistency, deg Torque Water-cement Ratio, wt 0.4	0.6	0.8
Neat cement	350	---	15
1 cement:1 fly ash	332	---	19
2 cement:1 fly ash	337	---	17
Cement + cls	374	---	10
1 cement:1 fly ash + cls	258	---	17
2 cement:1 fly ash + cls	263	---	12
1 cement:1 slag	378	---	23
2 cement:1 slag	355	---	26
1 cement:1 pumicite	*	---	32
2 cement:1 pumicite	*	---	24
1 cement:1 opaline shale	**	787	86
2 cement:1 opaline shale	**	244	38

* Exceeded the capacity of meter.

** Not fluid grout, too stiff to test.

For field work the torque meter might be too delicate since it would require a special indoor working area free of vibration.

For field work specially constructed flow cones with volume and discharge orifice integrated to produce sizable differences in readings with small changes in viscosity, or unit weight measures with the unit weight of the grout expressed in grams per gallon would probably be satisfactory.

Whatever the method used for measuring viscosity, it should correlate with pumpability as measured in cubic feet per hour in order to have any practical meaning. Examination of Fig. 21 shows good correlation between torque and pumpability (flow through the 0.03-in. crack at relatively constant pressure, approximately 50 psi) for several combinations of materials. There appeared to be little correlation between torque and flow when the grout combinations were considered collectively. This apparent lack of similarity of pumpability for grouts of equal viscosity through a thin crack is probably due to differences in grain-size distribution and particle shape of the solids in the grouts.

Bleeding

Two kinds of tests were carried out to determine the extent of bleeding of the grouts. The first consisted simply of pouring 500 ml of grout into a 1000-ml graduate and observing the separation of water with passage of time. The water-cement ratio was varied and measurements were made on neat grouts, 1 cement: 1 fly ash grouts, and 1 cement: 1 fly ash grouts with 1 per cent intrusion aid. Fig. 22 shows data obtained after one hour. Most of the bleeding had occurred at the end of one hour; no additional bleeding occurred after two hours. Use of intrusion aid in cement fly ash grout appeared to reduce slightly its bleeding below that of neat and cement-fly ash grouts.

The second kind of bleeding test was performed according to ASTM C 243-52T insofar as practicable.

A water-cement ratio of 0.4 was used in all cases except for the grouts containing opaline shale, which were too thick for use at 0.4, so 0.6 was used for these. Placing the grouts on approximately the same water-cement ratio

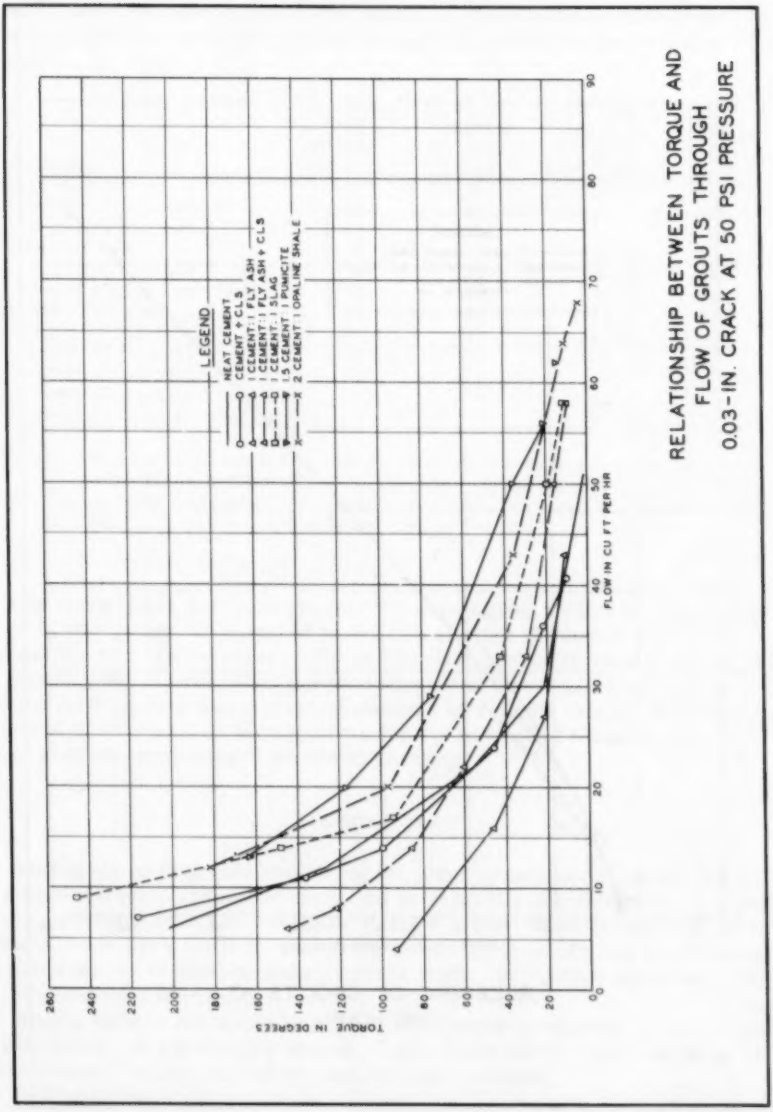
RELATIONSHIP BETWEEN TORQUE AND
FLOW OF GROUTS THROUGH
0.03-IN. CRACK AT 50 PSI PRESSURE
LEGEND
NEAT CEMENT
1 CEMENT : 1 CLS
1 CEMENT : 1 FLY ASH
1 CEMENT : 1 FLY ASH + CLS
1 CEMENT : 1 SLAG
1.5 CEMENT : 1 PUMICITE
2 CEMENT : 1 OPALINE SHALE
TORQUE IN DEGREES
FLOW IN CU FT PER HR

FIGURE 21

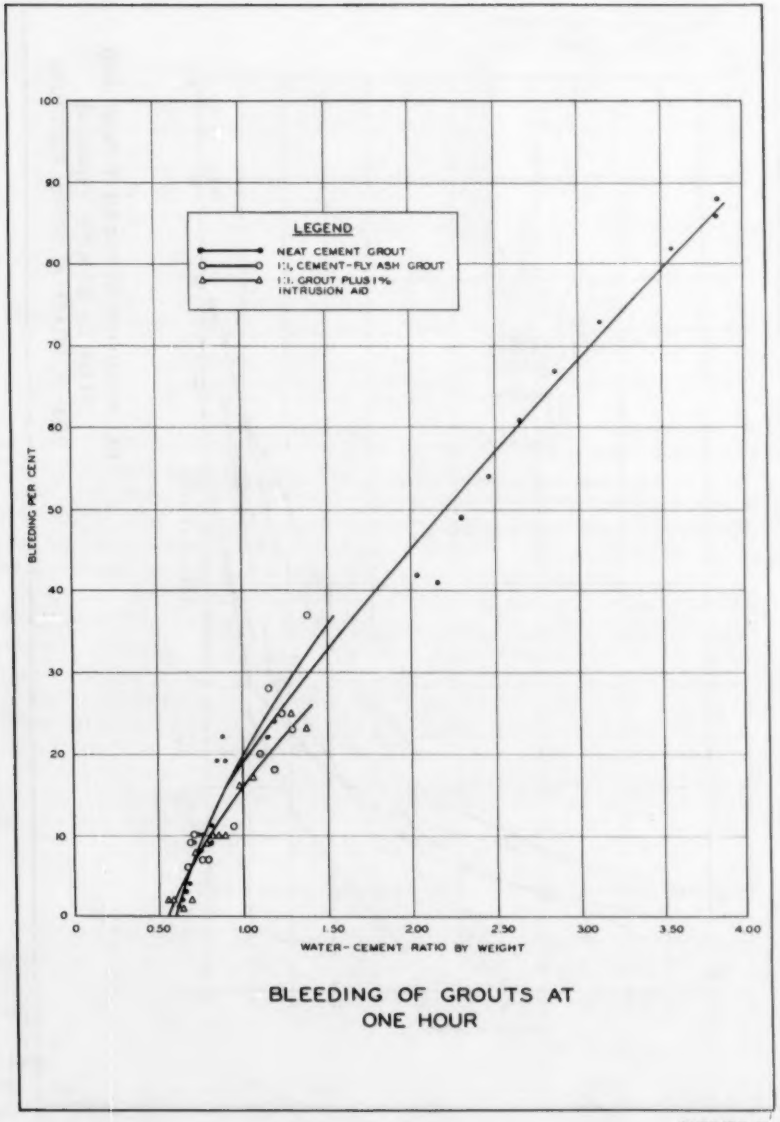

BLEEDING OF GROUTS AT ONE HOUR

FIGURE 22

basis regardless of solid material composition permitted evaluation of the effects of the constituents, other than water, on their bleeding characteristics. The combinations used and results obtained are shown in the following tabulation:

Grout	W/C, 0.4, wt Rate cm^3/cm^2/ sec X 10^6	W/C, 0.4, wt Capacity cm^3/cm^3 X 10^3	W/C, 0.6, wt Rate cm^3/cm^2/ sec X 10^6	W/C, 0.6, wt Capacity cm^3/cm^3 X 10^3
Neat cement	80	37	--	--
1 cement:1 fly ash	65	38	--	--
2 cement:1 fly ash	65	45	--	--
Cement + cls	38	6	--	--
1 cement:1 fly ash + cls	50	20	--	--
2 cement:1 fly ash + cls	55	36	--	--
1 cement:1 slag	73	28	--	--
2 cement:1 slag	69	33	--	--
1 cement:1 pumicite	53	18	--	--
2 cement:1 pumicite	40	14	--	--
1 cement:1 opaline shale	*	*	34	5
2 cement:1 opaline shale	*	*	72	18

Note: The rate indicates how rapidly the cement grains settle and the water rises and collects on the top surface of the paste. The capacity indicates the amount of water, per unit volume of paste, that collects on the surface during the test.

* Not fluid, too stiff to test.

Cls appeared to decrease sharply the rate and amount of bleeding when used in neat grout. It appeared to act in a similar manner in the grouts with fly ash but to a lesser extent. Fly ash itself appeared to slow down the rate of bleeding but did not affect the total amount of bleeding. Slag appeared to lessen both the rate and amount of bleeding to a small extent. Both the pumicite and opaline shale sharply decreased the amount of bleeding and, to a somewhat lesser degree, the rate of bleeding.

Setting Time

Setting times of grouts containing the same constituents, except for the addition of intrusion aid in two cases, as used for the second series of bleeding tests, and made with several water-cement ratios, were determined. The determinations were made by use of the 1-mm Vicat needle and small samples of grout placed in shallow wide-mouthed vials. The data obtained are shown in the tabulation following.

Setting time is obviously important when grout is expected to cut off percolating water. In grouting by stages, it also controls the time that must elapse before holes can be cleared out and drilling resumed.

Setting times could not be determined exactly because of hours-of-work limitations. Cls appeared to lengthen setting time. Setting time was also influenced by water content. It is conceivable that grouts could have water contents so high that the cement grains would be separated to such an extent that setting and development of strength could never occur.

Grout	Water-cement Ratio, wt	Approximate Setting Time, hr
Neat cement	0.33	7-1/4
Neat cement	0.4	Exceed 4, under 18
Neat cement	0.8	Exceed 4, under 19
Neat cement	2.06	233
1 cement:1 fly ash	0.4	Exceed 6, under 22
1 cement:1 fly ash	0.44	16-1/2
1 cement:1 fly ash	0.80	Exceed 5, under 21
1 cement:1 fly ash + 1% intrusion aid	0.36	20
1 cement:1 fly ash + 1% intrusion aid	4.32	Not set in 336
Cement + cls	0.4	Exceed 7, under 23
Cement + cls	0.8	72
1 cement:1 fly ash + cls	0.4	Exceed 22, under 46
1 cement:1 fly ash + cls	0.8	Exceed 22, under 46
1 cement:1 slag	0.4	Exceed 6, under 22
1 cement:1 slag	0.8	30
1 cement:1 pumicite	0.4	Exceed 4, under 20
1 cement:1 pumicite	0.8	Exceed 6, under 22
1 cement:1 opaline shale	0.6	Exceed 3-1/2, under 18
1 cement:1 opaline shale	0.8	30

Solubility

Two 50-ml portions of grouts, listed in Fig. 23, were placed in stoppered 200-ml flasks and one was cured for 7 days, the other for 90 days. At the end of the curing age, the samples were leached with 50 ml of distilled water for periods of 2, 7, 28, and 90 days. Leach water was then tested for pH, total solids, and calcium ion. The amount of total solids and calcium removed by leaching is shown graphically in Fig. 23.

Unfortunately reaction occurred between the Pyrex glass flasks in which the grouts were cured and the alkalies in the grouts, causing many to crack after several weeks storage permitting the water to leak out. No test results are plotted from specimens which were in the cracked flasks.

Conclusions drawn from the unspoiled tests are:

a. Grouts exposed to leaching after only 7 days curing appeared to be somewhat more susceptible to leaching than those cured 90 days.
b. About one-half of the dissolved material that leached out of the 0.4 water-solids ratio grouts was calcium, whereas about one-third of the dissolved material from the 0.8 water-solids ratio grouts was calcium.
c. Increasing the water-solids ratio from 0.4 to 0.8 approximately doubled the amount of calcium and more than doubled the total solids in the leach water.
d. Cls did not materially affect the solubility of the grouts made with a water-solids ratio of 0.4. Total solubility was increased and calcium solubility was decreased for the cls grouts at a water-solids ratio of 0.8.
e. Fly ash did not appear to materially affect solubility of the 0.4 ratio grouts. Solubility of the 0.8 ratio grouts seemed to be increased by use of fly ash.
f. Behavior of cls in the fly ash grouts was the same as in the neat-cement grout.
g. Slag reduced the solubility of all constituents. The effect on decreasing solubility was more marked at the higher water-solids ratio and was

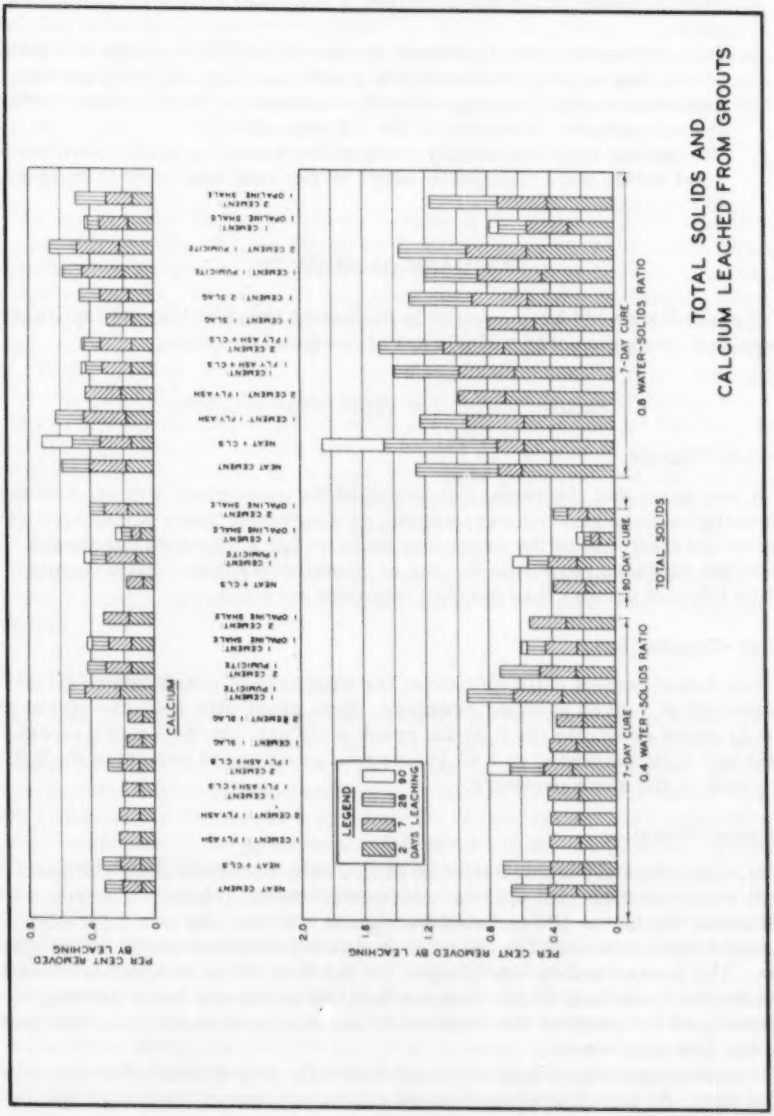
TOTAL SOLIDS AND
CALCIUM LEACHED FROM GROUTS
PER CENT REMOVED BY LEACHING
2.0
1.6
1.2
0.8
0.4
0
LEGEND
2
7
28
90
DAYS LEACHING
0.4 WATER-SOLIDS RATIO
7-DAY CURE
90-DAY CURE
0.8 WATER-SOLIDS RATIO
7-DAY CURE
TOTAL SOLIDS
CALCIUM
NEAT CEMENT
NEAT + CLS
1 CEMENT : 1 FLY ASH
2 CEMENT : 1 FLY ASH
1 CEMENT : 1 FLY ASH + CLS
2 CEMENT : 1 FLY ASH + CLS
1 CEMENT : 1 SLAG
1 CEMENT : 2 SLAG
2 CEMENT : 1 POZZOLITE
1 CEMENT : 1 POZZOLITE
1 CEMENT : 1 OPALINE SHALE
2 CEMENT : 1 OPALINE SHALE
NEAT CEMENT
NEAT + CLS
1 CEMENT : 1 POZZOLITE
2 CEMENT : 1 OPALINE SHALE
1 CEMENT : 1 OPALINE SHALE
NEAT + CLS
2 CEMENT : 1 POZZOLITE
1 CEMENT : 1 POZZOLITE
1 CEMENT : 1 OPALINE SHALE
2 CEMENT : 1 OPALINE SHALE
2 CEMENT : 1 SLAG
1 CEMENT : 1 SLAG
1 CEMENT : 1 FLY ASH + CLS
2 CEMENT : 1 FLY ASH + CLS
1 CEMENT : 1 FLY ASH
2 CEMENT : 1 FLY ASH
NEAT + CLS
NEAT CEMENT
PER CENT REMOVED BY LEACHING
0.8
0.4
0

FIGURE 23

more pronounced for the 2 cement: 1 slag than for the 1 cement: 1 slag grout.

h. Pumicite appreciably increased the overall solubility of the 0.4 ratio grouts, but slightly decreased the solubility of the 0.8 ratio grouts. Calcium solubility was appreciably increased in the 0.4 ratio grouts and only slightly increased in the 0.8 ratio grouts.

i. The opaline shale materially reduced the solubility of all constituents. Total solids were reduced by about 50 per cent and calcium by about 40 per cent.

SUMMARY OF RESULTS

The reader should keep in mind in evaluating the data that the investigation described comprises only a single set of tests per condition.

Factors Influencing Penetration of Grouts

Surface Texture

It was found that the surface condition of the specimens, that is, whether the surfaces to be grouted were smooth or roughened, had a pronounced effect on the thickness of the grout that could be forced through the cracks. The smoother surfaces permitted the use of considerably lower water-cement ratios (thicker grouts) than did the roughened surfaces.

Water-Cement Ratio

The water-cement ratio influenced the thickness of crack that could be penetrated at a given pumping pressure. Neat grout with a water-cement ratio of 0.43 would penetrate the 0.03-in. crack at 25 psi, but the water-cement ratio had to be increased to 2.67 before neat grout would penetrate the 0.01-in. crack at the same pressure.

Pumping Pressure

An approximately straight-line pressure drop occurred along the specimens while the 0.02- and 0.03-in. cracks were being grouted. The pressure was either 25, 50, or 100 psi where the grout entered, and was 0 psi where it emerged with intermediate pressures measured along the length of the specimen. The pressure drop was steeper for the first 12 in. of specimen length than for the remaining 36 in. when the 0.01-in. crack was being grouted. The steepness of the gradient for the first 12 in. increased as the grout thickened and the flow decreased.

Increased pumping pressures caused directly proportionate increases in grout flow. At identical water-cement ratios, pressures, and crack thicknesses the neat-cement grout had least flow, cement fly ash grout had more flow, and neat grout plus intrusion aid had still more flow. However, the flow was not greatest, as might be expected, with cement fly ash grout plus intrusion aid. Data on the cement fly ash intrusion aid grout were anomalous and inconclusive.

When the crack width was 0.02 or 0.03 in. the minimum water-cement ratio (thickness of grout) the crack would accept was little affected by the grouting

pressure, however, the thickness of the grout that would penetrate the 0.01-in. crack depended somewhat on pressure. At 25 psi, the thickest grout that would penetrate the 0.01-in. crack had a water-cement ratio of 2.67. When the pressure was increased to 50 psi, grout with a water-cement ratio of 1.33 would penetrate, but a further increase in pumping pressure to 100 psi did not permit use of still thicker grout.

Grain Size

The use of a No. 50 sieve cloth for straining the grout seemed beneficial and probably the use of a No. 60, or even a No. 100 cloth, if vibrated, would be practical in removing oversized particles which cause trouble in grouting the tightest seams. The fly ash contained grains of material larger than 0.01 in. and grouts containing fly ash would not penetrate the 0.01-in. fissures. Based on the maximum grain size of the cement, 0.006-0.01 in., and the thinnest cracks grouted, 0.01 in., the ratio of crack thickness to grain size should not be less than 1.7, and probably safer ratios would be 3.0 or more.

The use of fly ash appears limited to grouting larger cracks unless a supply of fine material can be obtained, or unless fly ash can be processed, possibly by air separation, to remove the larger granules. No attempt was made to grout 0.01-in. cracks with grout containing ground slag, pumicite, or opaline shale. Difficulty would doubtless have been encountered with the slag and shale whose grain size exceeded 0.01 in.

The use of more finely ground cements, such as high-early strength cement, or ordinary cement processed through an air separator might be feasible.

Chemical Fluidifiers

The use of intrusion aid appeared to be a help in reducing the water ratio of the grout that could be pumped through cracks of 0.03-in. thickness with roughened surface, and 0.03- and 0.02-in. thickness with smooth surfaces. It is believed that the aid should also have promoted use of lower water-cement ratio grout for the roughened 0.02-in. crack but did not in these tests because of surface factors in the specimens. Intrusion aid was of no help in promoting penetration of 0.01-in. cracks at any water ratio tried because of the limits of penetration placed upon the grout containing fly ash by the coarseness of the fly ash. Penetration of 0.01-in. cracks with neat grout containing intrusion aid was not tried. The use of intrusion aid appeared to cause a small reduction in bleeding and a slight expansion in the grouts.

Intrusion aid and cls appeared to increase the fluidity of the neat grouts so that a seam of given thickness would pass a greater amount of such grout than of plain grout having the same water-cement ratio; conversely, grout with fluidifiers, at a lower water-cement ratio and at a given pressure, would penetrate a given crack better than grouts without fluidifiers.

Intrusion aid seemed to be more effective with neat grouts than with grouts containing fly ash. The cement fly ash grout with intrusion aid did not penetrate either the 0.02- or the 0.03-in. seams significantly better than the same grouts without aid.

Mineral Fines

Fly ash appeared to increase the fluidity of the grouts in which it was used. The ground slag also appeared to increase fluidity, however this was not

conclusive. The pumicite and opaline shale both greatly stiffened the grouts in which they were used; however, at comparable consistency with neat grout, the pumicite and opaline shale grouts pumped better than the neat grout. At equal consistency slag grout pumped about the same as neat grout, but fly ash grout did not pump as well.

Factors Affecting Quality of Grout Films

Water-Cement Ratio

The grout films having water-cement ratios of 0.5 or less appeared hard and filled the fissures completely with little evident bleeding. However, the bond of top to bottom half of the grouted specimen was not considered good except when water-cement ratios were lower than 0.4.

Bleeding occurs in grouts having water ratios in excess of 0.50, and becomes more severe the higher the unit water content. A narrow band of dense hard grout was always found next to the shim beneath which water had escaped. This band of dense grout was always narrow, never exceeding 3/4 in. in width, no matter what the original water content. It has been hypothesized that the original water content of a grout is not very important as the excess water is squeezed out into the pores of the rock and extremely fine seams (too fine to accept grout) leaving a dense hard material filling the cavity. It was not found possible to squeeze this water out with the 100-psi grouting pressure used, in the 10 to 15 minutes during which pressure was maintained, except in a narrow band around the edge of the specimen, even with the outer edges of the specimens open to the air at 0 (relative) pressure. However, it should be borne in mind that the results under discussion were obtained by grouting the space between the two concrete slabs and might not give a true picture of what occurs in grouting a foundation hole.

Setting time increased with water content. Neat grout with a water content as high as 2.06 required ten days to set in the setting-time tests. Thin grout containing intrusion aid (W/C 4.32) did not set in 14 days. These thin grouts can be shown to be incapable theoretically of developing any compressive strength when the water-cement ratio of the grout is so high that the space between cement grains, which in normal pastes and concretes is of capillary proportions and subsequently becomes filled with gel, is so great that it is not generally possible for the gel developed by the hydration of the individual particles or groups of particles to grow out through the space and make sufficient contact with that developing from other particles or groups of particles.[3] The higher water-solids ratio grouts were also much less resistant to leaching than those with lower ratios.

Chemical Fluidifiers

Bonding of the hardened grout films to the top slab was poor (25 per cent or less of film adhering to top) for all grouts except those containing fly ash with cls where the bond was considered good (40 per cent or more adhering to top). Bond strength as measured by shear tests on neat and neat-cement plus intrusion aid grouts was relatively low although the use of intrusion aid appeared somewhat to increase bonding between top and bottom halves of the specimen in neat grout. Cls did not appear to benefit the bond condition of specimens intruded with neat grout.

Both intrusion aid and cls prolonged setting time and reduced bleeding. The solids in the fly ash grouts tended to clump or agglomerate. This tendency appeared to be reduced but not eliminated by the fluidifier. Intrusion aid was not used in the tests for solubility of grout films, but cls had little effect on the leaching characteristics of the grouts tested.

Mineral Fines

Hardened grout films containing fly ash showed evidence of channeling action and apparent agglomeration. This tendency was not noted when slag, pumicite, and opaline shale were used. The use of ground slag, pumicite, and opaline shale greatly improved the apparent quality of the grout film, virtually eliminating evidence of bleeding, channeling, and agglomeration. Bond between top and bottom halves of the specimens was not improved by use of the several mineral fines.

The use of fly ash had little apparent effect on the solubility of the 0.4 water-ratio grouts, but appeared to increase the solubility of the 0.8 water-ratio grout. Slag reduced the leaching in all cases with the most pronounced effect in the higher water-ratio grouts. Pumicite increased the overall solubility of the 0.4 ratio grout but slightly decreased the overall solubility of the 0.8 ratio grout. The opaline shale greatly reduced the overall solubility of both the low- and high- water-solids ratio grouts in which they were used.

Curing

Grout films cured for 90 days appeared more resistant to leaching than those cured 7 days.

Measurement of Consistency

The measurement of consistency was readily accomplished in the laboratory with the torsion viscosimeter. Changes in consistency can also be detected and controlled readily by means of unit weight measurements. The flow cone was not too sensitive to small changes in viscosity, although a cone with an orifice restricted enough to require more time to discharge should prove suitable for field use. The torsion viscosimeter, because it is delicate and requires a quiet, level area for operation, would not be as suitable for field as for laboratory use.

CONCLUSIONS

1. The surface texture of a fissure has a distinct influence on the thickness of grout that can be used to fill it. The smoother the surface the lower the water-cement ratio of the grout that can penetrate the crack.
2. The maximum grain size of the solids in the grout determines the minimum crack width that can be grouted. The ratio of crack width to grain size should probably be three or more.
3. The use of certain chemical admixtures increases the fluidity of grouts, to some extent, thereby promoting penetration of a given crack width with grouts of a slightly lower water-cement ratio than could be used successfully without them. Bleeding can be reduced somewhat and setting time increased by use of these materials.

4. It was found impracticable to squeeze the excess water from a thin grout, thereby leaving a dense hard filler in the cavity, at the pressures and with the techniques used in this program.

5. Bleeding largely prevents bonding of the grouting material to the upper surface of the fissure.

6. The use of finely ground mineral admixtures such as granulated blast-furnace slag, pumicite, and opaline shale can reduce the bleeding of a grout and greatly improve the continuity and appearance of the hardened grout film.

7. The solubility of a grout film is influenced by the water-cement ratio and composition of the film and length of curing. Certain mineral admixtures can be used to reduce the amount of leaching that a grout film undergoes.

8. A straight-line pressure gradient occurs along a fissure being grouted only if the crack is of sufficient width.

REFERENCES

1. Machis, Alfred, "Experimental Observations on Grouting Sand and Gravels," ASCE, Transactions, vol 113 (Nov 1948), pp 181-205.

2. Taggart, A. F., Handbook of Mineral Dressing, Ores and Industrial Minerals, New York, J. Wiley and Sons (1945).

3. Powers, T. C. and Brownyard, L. T., "Studies of the Physical Properties of Hardened Portland Cement Paste," Proceedings American Concrete Institute, vol 43, pp 845-857.

Paper 1732 August, 1958 SM 3

Journal of the
SOIL MECHANICS AND FOUNDATIONS DIVISION
Proceedings of the American Society of Civil Engineers

GEOTECHNICAL PROPERTIES OF GLACIAL LAKE CLAYS

T. H. Wu,[1] A. M., ASCE
(Proc. Paper 1732)

SYNOPSIS

This article reports on a study of the properties of glacial lake clays. Data collected from a number of sites in the Great Lakes area of the United States are presented. Despite local variations in subsoil conditions and the large distances between the sites, the clay deposits investigated have much in common and it is possible to study them as a related family. An analysis was made of the principal factors that control the strength characteristics of the clays. The shearing resistance and sensitivity were found to be intimately related to the structure of the clay as well as the stress history.

INTRODUCTION

In North America the activities of continental glaciers led to the formation of many glacial lakes during Pleistocene times. Many of them have since disappeared or now exist in diminished sizes. A number of soft clay deposits extending to great depths are known to exist in areas that had been formerly occupied by glacial lakes. Among the most notable are the clays in the Great Lakes region such as the deposits at Chicago and Detroit. These deposits consist primarily of a heterogeneous and unstratified silty clay with some sand and gravel. The texture of these soils resembles closely that of glacial tills. Also present in these areas is the laminated clay and silt known as varved clay and generally considered as representative of lacutrine sediments.

As the majority of the glacial lake clays exhibit low strength accompanied by high compressibility, their properties have long been subjects of interest. A number of significant publications have described the engineering properties of lake clays as well as regional subsoil conditions. This article contains

Note: Discussion open until January 1, 1959. To extend the closing date one month, a written request must be filed with the Executive Secretary, ASCE. Paper 1732 is part of the copyrighted Journal of the Soil Mechanics Division, Proceedings of the American Society of Civil Engineers, Vol. 84, No. SM 3, August, 1958.

1. Associate Prof. of Civ. Eng., Michigan State Univ., East Lansing, Mich.

information on the physical properties and strength characteristics of several clay deposits in the Great Lakes region. Because of their uniformity and extensive depth, these deposits were selected for detailed study. The fundamental factors that govern the important characteristics as sensitivity and strength-consolidation relationship of these deposits were analyzed. Also included in this article are some supplementary data from a number of sites. These, although lacking in completeness, provide considerable information that support the main thesis.

Description of Clay Deposits

During the last great ice invasion, the Wisconsin, the continental glacier moved into the area from the north and east. At its climax, the glacier covered all of Michigan and extended deep into Indiana and Ohio. Subsequent recession of the glacier followed the same general directions. The numerous retreats and readvances of the glacier resulted in the formation, at various times, of large ice-front lakes. The shoreline of these lakes are traced on the map in Fig. 1.(1,2)

The four soil deposits investigated are all in the Great Lakes area. They are situated respectively, near the cities of Freemont, Detroit, Saginaw and Sault Ste. Marie as indicated in Fig. 1. Fig. 2 is a profile showing the subsoil conditions north of Freemont, Ohio. The major units in the subsoil consist of a layer of stratified clay and silt overlying a deposit of unstratified silty clay with sand and gravel. Both are soft to medium in consistency. Beneath these are found one or more old till sheets of very stiff clay with gravel and some boulders. Bedrock is encountered at elevations of about 540. Representative boring logs describing the physical properties of the soft clays at two sites are shown in Figs. 3 and 4.

Very similar subsoil conditions are found in the Detroit area. Fig. 5 contains a detailed log and summary of the test results obtained from a site near the Industrial Expressway and River Rouge. The data are representative of the subsoil conditions in this area. The uppermost unit is a layer of stratified clay and silt and it lies over a fairly thick deposit of unstratified clay with sand and gravel. In the transition a thin stratum of clay containing many irregular layers and lenses of sand is revealed in some borings. The thickness of this stratum where encountered, does not exceed two feet. At a depth of 75 ft., the unstratified clay with sand and gravel changes gradually into a layer of soft clay with occasional silt laminations. Remnants of old till sheets and heavily precompressed lacustrine clay are found between the soft clay and bedrock, which is located at about elev. 480.

At the site near Saginaw, the unstratified silty clay extends down to depth of about 51 feet. A layer of stratified clay and silt is found between depths of 51 and 65 feet and beneath this are layers of sand and still clay till. Data obtained from a representative boring are shown in Fig. 6.

Between Mackinac Straits and Sault Ste. Marie, in Northern Michigan is an extensive deposit of soft stratified clay and silt up to 60 ft. thick at some localities. The presence of hematite gives the clay a distinctive red color. Borings were made at two sites near Sault Ste. Marie and typical test results from each site are presented in Figs. 7 and 8.

Detailed study was made of the clay fraction of all the soils encountered by means of x-ray diffraction and differential thermal analyses. The results

FIGURE 1 LOCATION OF SOIL DEPOSITS

indicated that the principal constituent minerals are quartz, kaolinite, and illite, with small percentages of chlorite and vermiculite. The general uniformity in mineralogical contents is well expressed in Fig. 9, in which the plasticity indices of the clays are plotted against the clay fractions. All the clays belong to the class of inactive clays.[3] The index properties of the clays are summarized in Table 1.

Strength Characteristics

A comprehensive series of laboratory tests was performed to evaluate the strength and stress history of the clays. The tests included the consolidation, unconfined compression and triaxial tests. The subsequent paragraphs

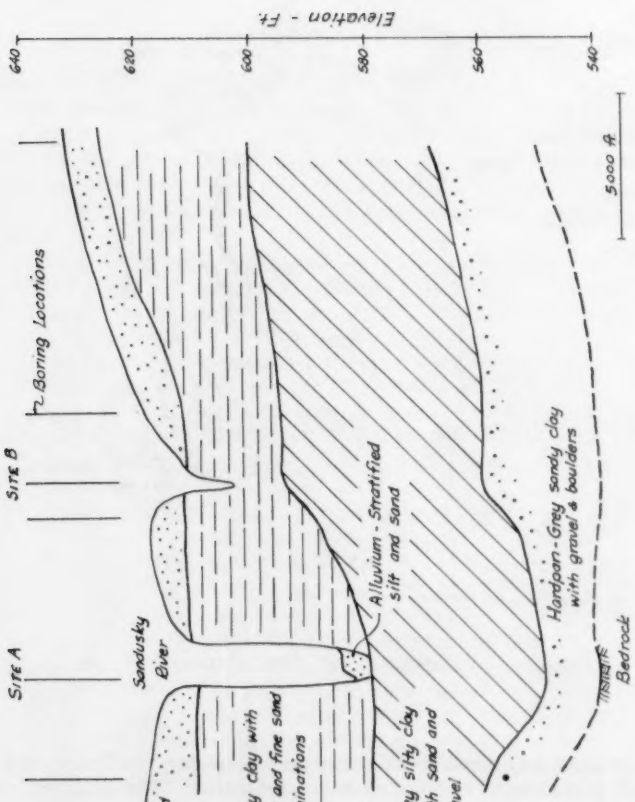

FIGURE 2 SUBSOIL PROFILE - FREMONT, OHIO

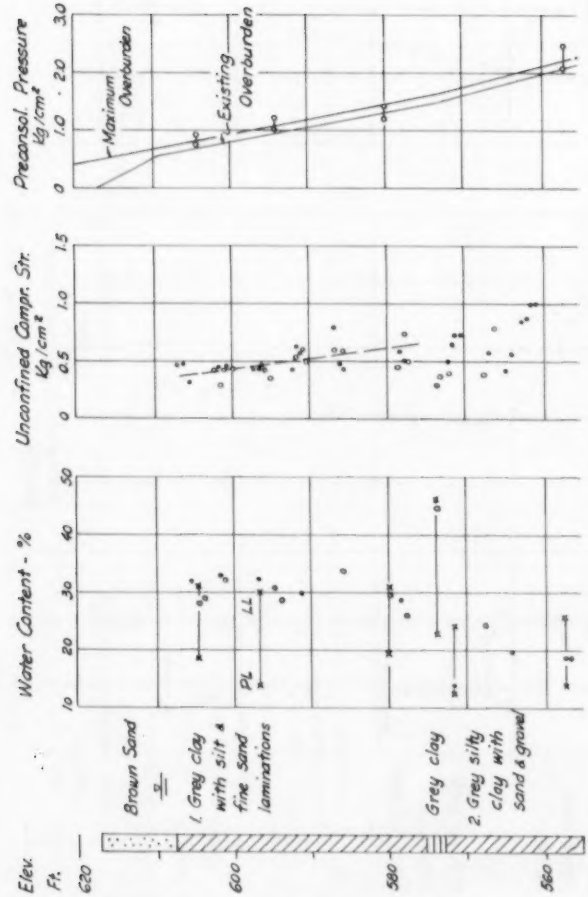

FIGURE 3 PHYSICAL PROPERTIES - FREMONT CLAY, SITE A

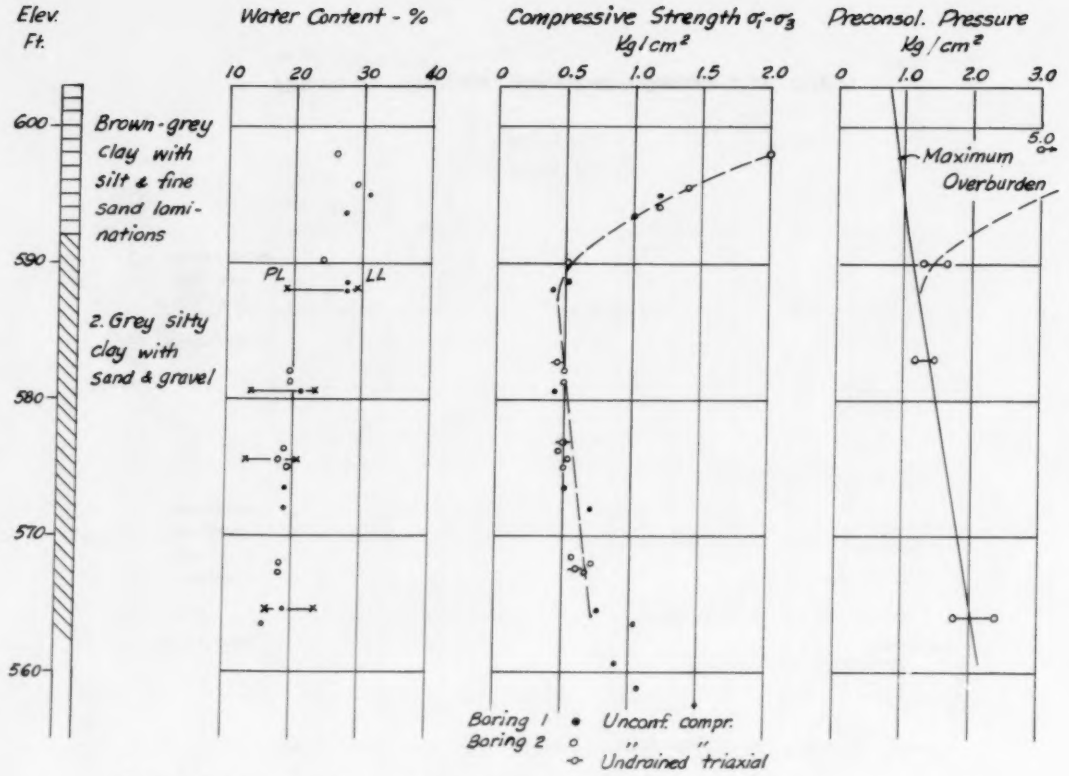

FIGURE 4 PHYSICAL PROPERTIES - FREEMONT CLAY, SITE B

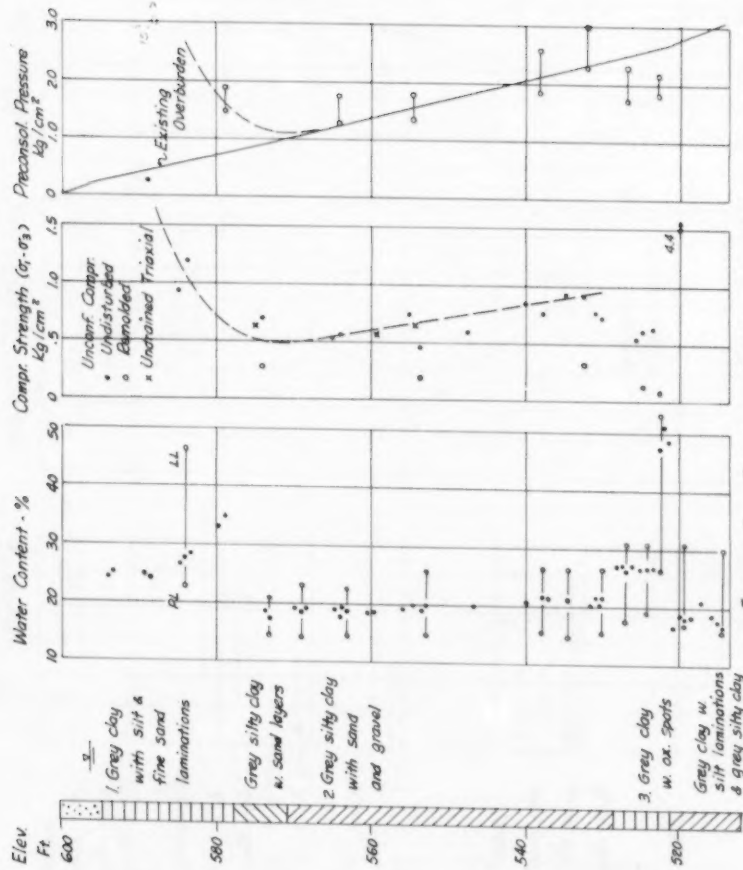

FIGURE 5 PHYSICAL PROPERTIES - DETROIT CLAY

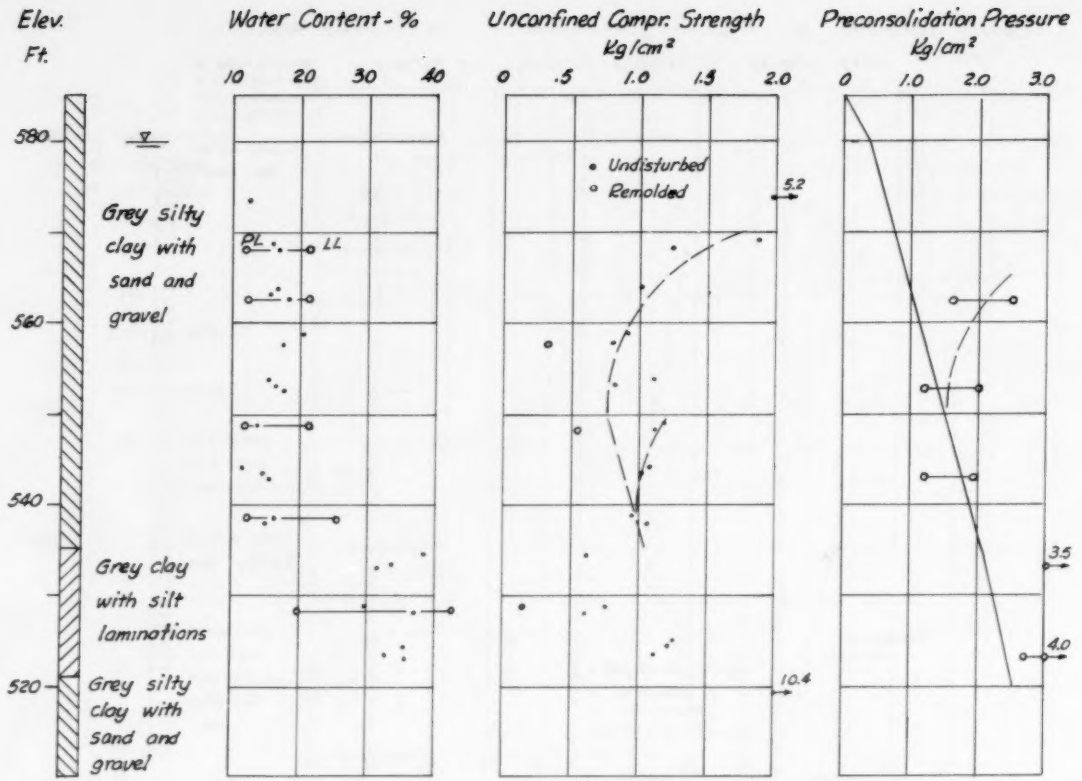

FIGURE 6 PHYSICAL PROPERTIES - SAGINAW CLAY

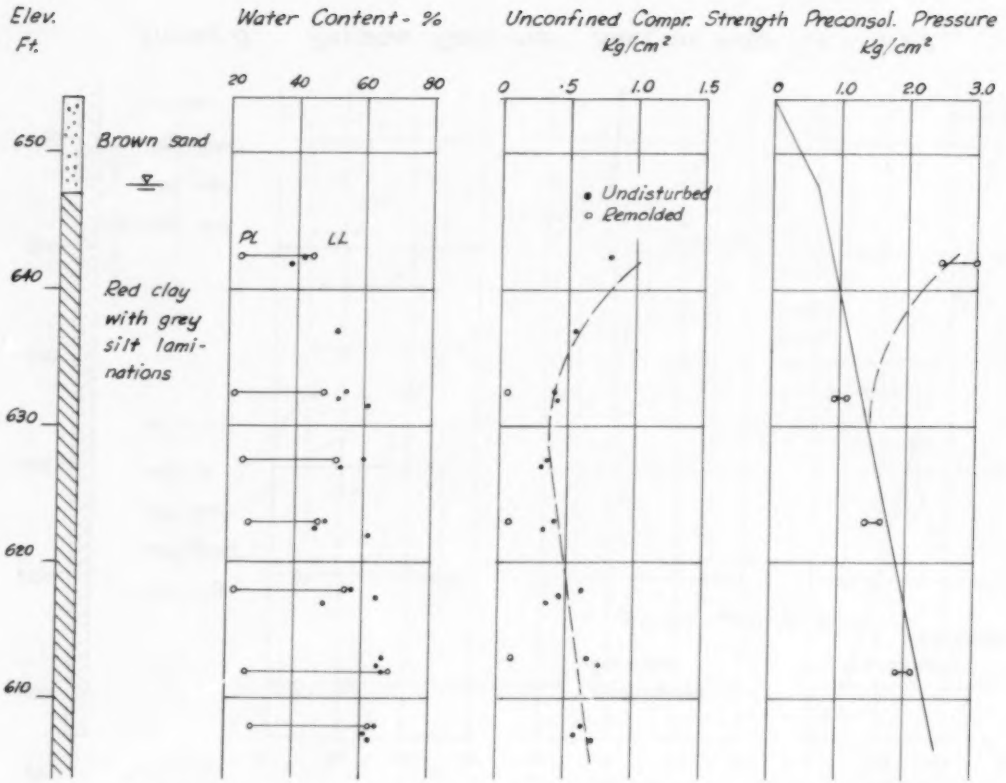

FIGURE 7 PHYSICAL PROPERTIES - SAULT STE. MARIE CLAY - SITE 1

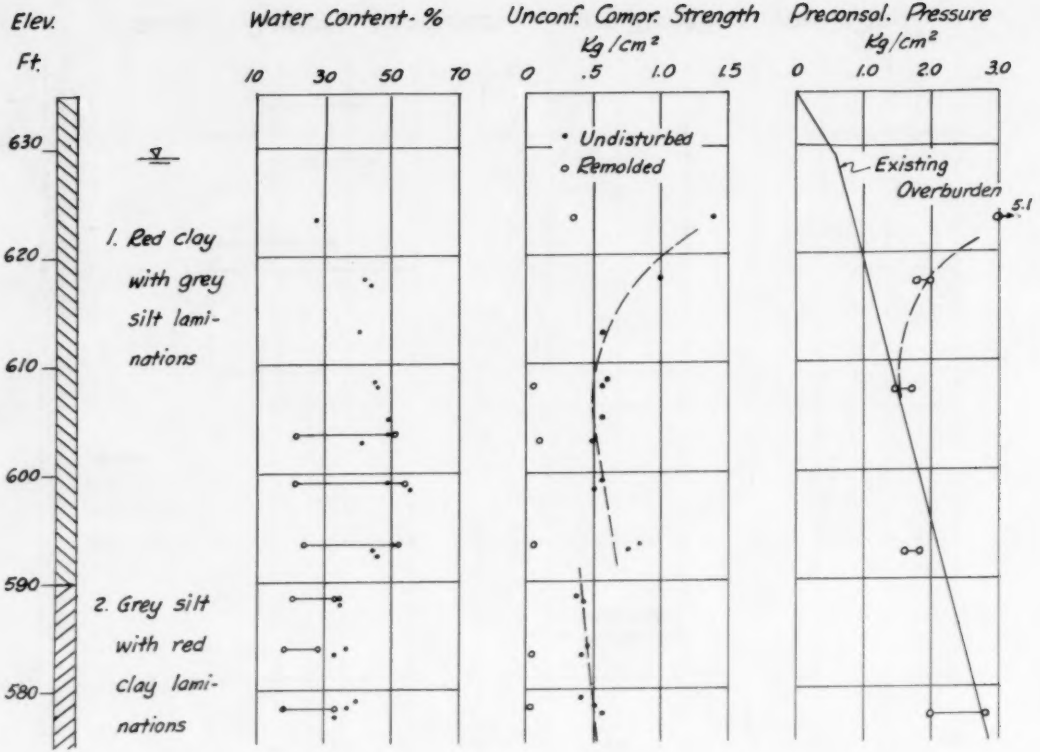

FIGURE 8 PHYSICAL PROPERTIES - SAULT STE. MARIE CLAY - SITE 2

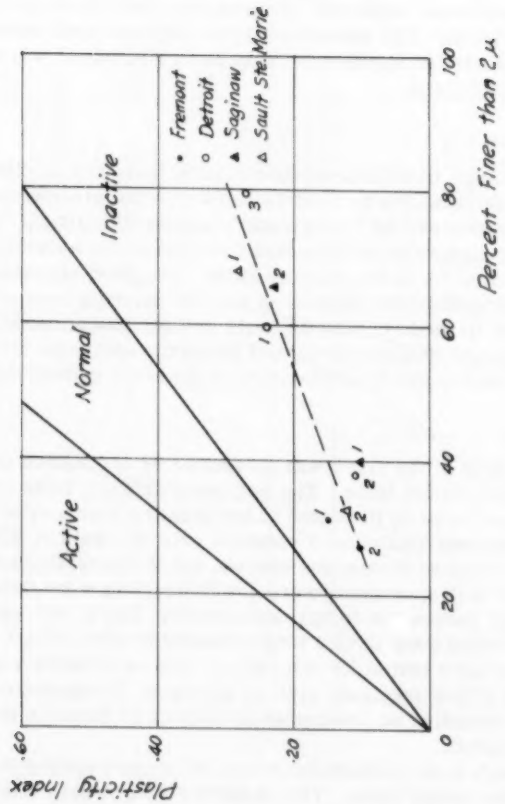

FIGURE 9 ACTIVITY OF CLAYS

describe the details of the laboratory investigation. A summary of the strength properties is given in Table 2.

Specimens

All specimens used in the laboratory investigation were obtained by seamless steel tube samplers with a wall thickness of 1/16 inch. From the Fremont site only two-inch diameter specimens were obtained. Both two-inch and three-inch diameter specimens were used in the investigation of the Detroit site. In this case, consolidation tests were performed only on the large diameter specimens, whereas, compression tests were performed on specimens of both sizes. The specimens from Saginaw were taken with three-inch tube samplers and the specimens from Sault Ste. Marie were taken with three-inch piston samplers.

Consolidation Tests

Some typical results of standard consolidation tests are plotted in Figs. 10 and 11. From these pressure vs void-ratio curves the preconsolidation pressures were determined by Casagrande's graphical method. Figs. 3 through 8 show the measured preconsolidation pressures as well as the existing overburden pressures at the various sites. The good agreement between the measured preconsolidation pressures and the existing overburden indicate the most of the soft to medium clay deposits are normally loaded. Only the top part of the deposits exhibit substantial precompression and these can be attributed to desiccation due to fluctuations in the local ground water table.

Shear Tests

The shear strength of the clays was measured by unconfined compression tests and undrained triaxial tests. The undrained triaxial tests utilized an all-around pressure equal to the value of the existing overburden pressure. The deviator stress was applied at a constant rate of strain of 2% strain per minute. The same rate of strain was adopted for the unconfined compression tests. When three-inch specimens were available, they were trimmed down to a diameter of 2.8 inches for compression tests. The 2 inch specimens were not trimmed. All specimens have a length-diameter ratio of 2.0. Since specimens of both sizes were tested for the Detroit site an attempt was made to evaluate the effect of the specimen size on strength. Comparison of results from five borings revealed no noticeable difference in strength between the two types of specimens.

In Figs. 3 through 8 are plotted the values of compressive strength as determined by the laboratory tests. The compressive strength was taken as equal to the maximum deviator stress. At all sites there is a general tendency for the strength to increase with depth within each individual stratum. Near the ground surface, the effect of preconsolidation is reflected in the relatively high strengths. However, some exceptions are noteworthy. At Detroit, a thin layer of soft clay is encountered at a depth of 75 ft. This is designated as clay no. 3 in Fig. 5. A similar clay exists at Saginaw between depths of 51 and 65 ft. Both units possess strengths far below those of the overlying soils. The sensitivity of the clays varied from 2 to almost 10. The sensitive clays include the clays at Sault Ste. Marie, clay no. 3 at Detroit and clay no. 2 at Saginaw. All the other clays are classified as having low sensitivity.

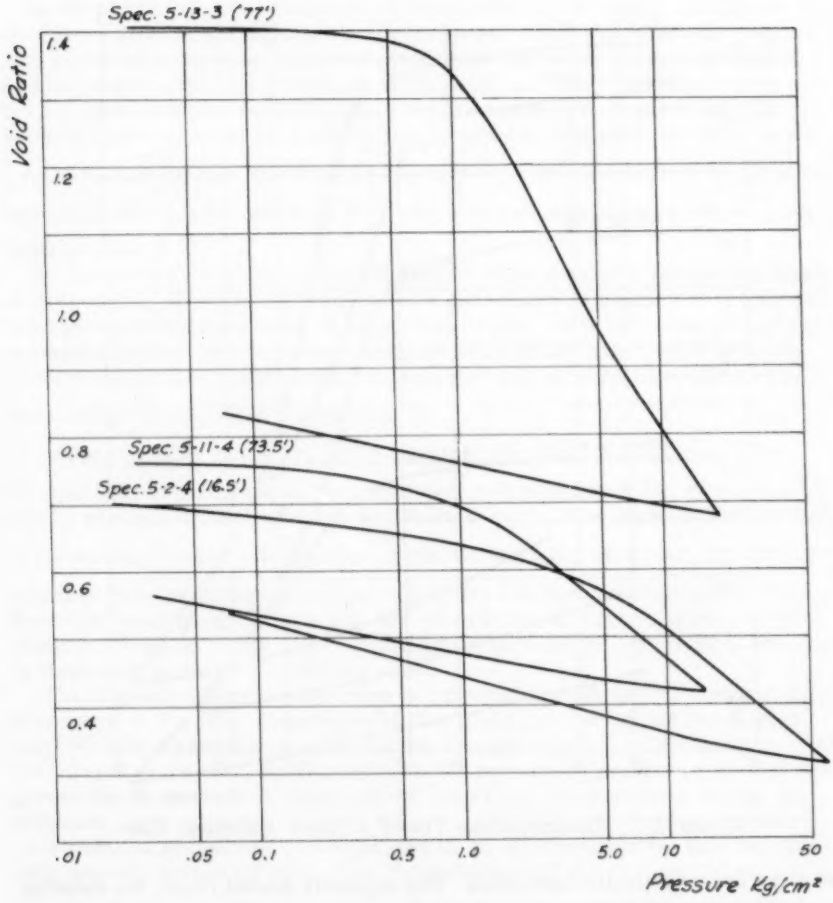

FIGURE 10 CONSOLIDATION CURVES - DETROIT CLAY

The Ratio $\frac{c}{p}$

Because of the high degree of uniformity of the soil deposits investigated, it is possible to analyze the relationship between strength and consolidation pressure in further detail.

From the consolidation and shear test data the ratio $\frac{c}{p}$ was computed. In this ratio c denotes the shear strength or one-half the compressive strength

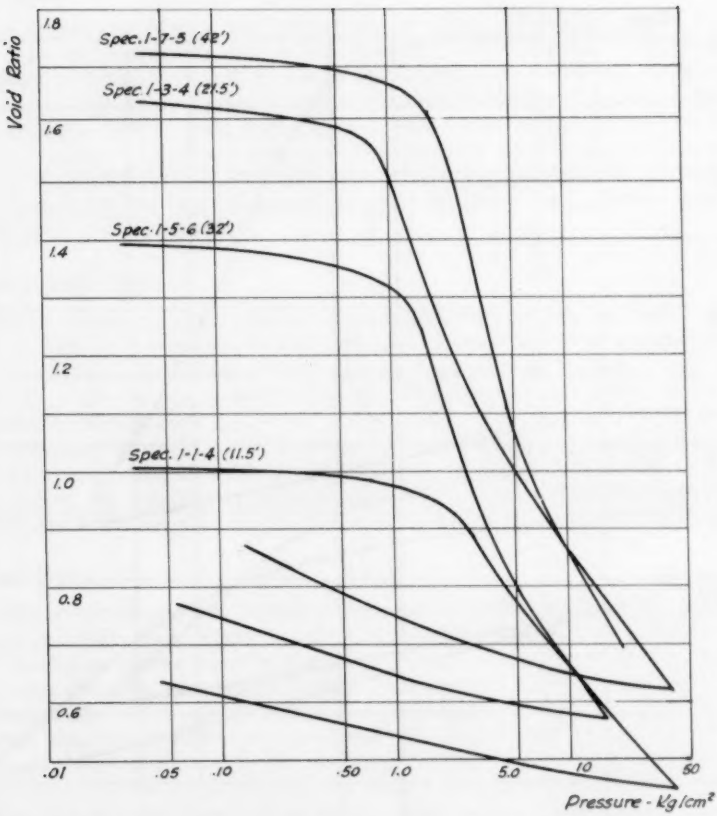

FIGURE 11 CONSOLIDATION CURVES - SAULT STE. MARIE CLAY

and p the preconsolidation pressure. For normally loaded clays, the existing overburden pressures were used in the computations. The computed values are listed in Table 2.

Besides the clay deposits reported in the preceding paragraphs considerable data are also available from other sites in this area, especially Chicago. The Chicago clay is an unstratified silty clay with variable percentages of sand and gravel and extends to a depth of about 60 ft.(4) G. H. Otto, after a thorough analysis of numerous boring data, concluded that the Chicago clay consists of a succession of till sheets deposited under water.(5) Consolidation test results presented by J. D. Parsons and R. B. Peck(6) indicate that the range of measured preconsolidation pressure agrees well with the existing overburden between elevations of -5 and -22, Chicago Datum. The most probable preconsolidation pressure as determined by the authors, however,

is slightly greater than the existing overburden. These results are in good agreement with those from another site in East Chicago reproduced in Fig. 12. When the most probable consolidation pressure is used, the computed $\frac{c}{p}$ ratio for the Chicago clay is about 0.20.

In the Cleveland area the repeated advances and retreats of the glacier ice alternated with the formation of ice front lakes. This has resulted in a complex series of lacustrine clays with or without silt laminations and unstratified clays with sand and gravel classified as tills. The Cleveland clay is heavily preloaded and no particularly soft materials are found in the area. From the data obtained by Peck[7] it is possible to estimate the value of the $\frac{c}{p}$ ratio as somewhere between 0.17 and 0.18 for units B and D. Fig. 13 contains laboratory test results on clay unit A at a site in the same area. The $\frac{c}{p}$ ratio is about 0.19.

At Green Bay, Wisconsin, a thick deposit of reddish clay exists to a depth of over 100 ft. The deposit consists of a succession of reddish silty clay till and some stratified material of lacustrine origin. Data from one boring are presented in Fig. 14. Between elevations 530 and 550, the clay is uniform. Preconsolidation pressures were determined only at elevations 539 and 540. From this, the computed $\frac{c}{p}$ ratio is 0.19.

In Fig. 15 the $\frac{c}{p}$ ratios are plotted against the plasticity indices. The straight line in the figure is the relationship obtained by A. W. Skempton[8] and L. Bjerrum[9] for estuarine and marine clays. The overall trend is one of increasing $\frac{c}{p}$ ratio with increasing plasticity index. However, the data obtained in this investigation appear to fall into two distant alignments. The first one, consisting of clays with low sensitivity, is slightly above but very close to Skempton's line. The second group falls far below the first one, and is composed entirely of sensitive clays.

The liquidity indices of the clays are plotted against their preconsolidation pressures in Fig. 16. Also shown in the figure are curves for the Horten clay[10] with a sensitivity of 17 and the Gosport clay[11] with a sensitivity of 2.4. For a given clay, consolidation under increasing pressures always progressively reduces the liquidity index. However, as is obvious in Fig. 16, different clays may possess very different liquidity indices at same preconsolidation pressures. As explained by A. W. Skempton[12] this relationship depends primarily upon the microstructure of the clay particles. Since the data in Fig. 13 show that low $\frac{c}{p}$ ratio and high sensitivity are limited to clays with a high liquidity index, it follows that these properties must be determined by the micro structure of the clay.

Stress-Strain Relationship

The larger number of unconfined compression tests also yielded considerable information on the stress-strain characteristics of the clays. This relationship may be classified into two distinctive types as illustrated in Fig. 17. The plot for specimen 5-13-4 Detroit exhibits a brittle material with a rather high value of initial modulus. The stress rapidly decreases after attaining a peak value at low strain. In contrast to this, the plot for specimen 5-5-4

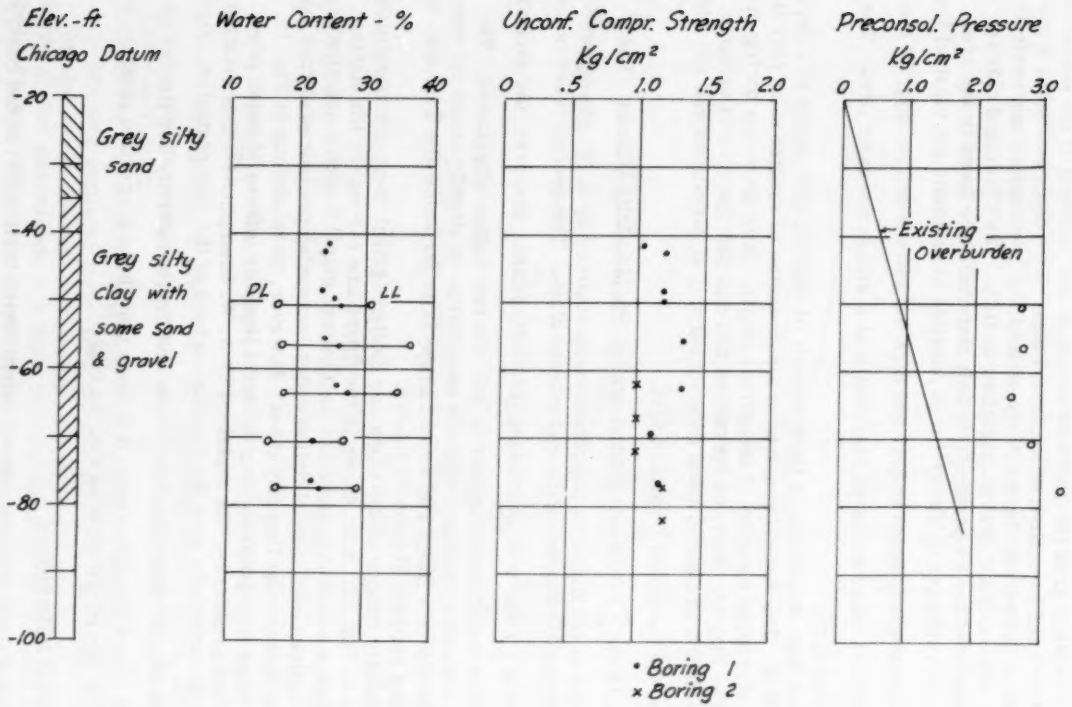

FIGURE 12 SUBSOIL PROPERTIES - E. CHICAGO

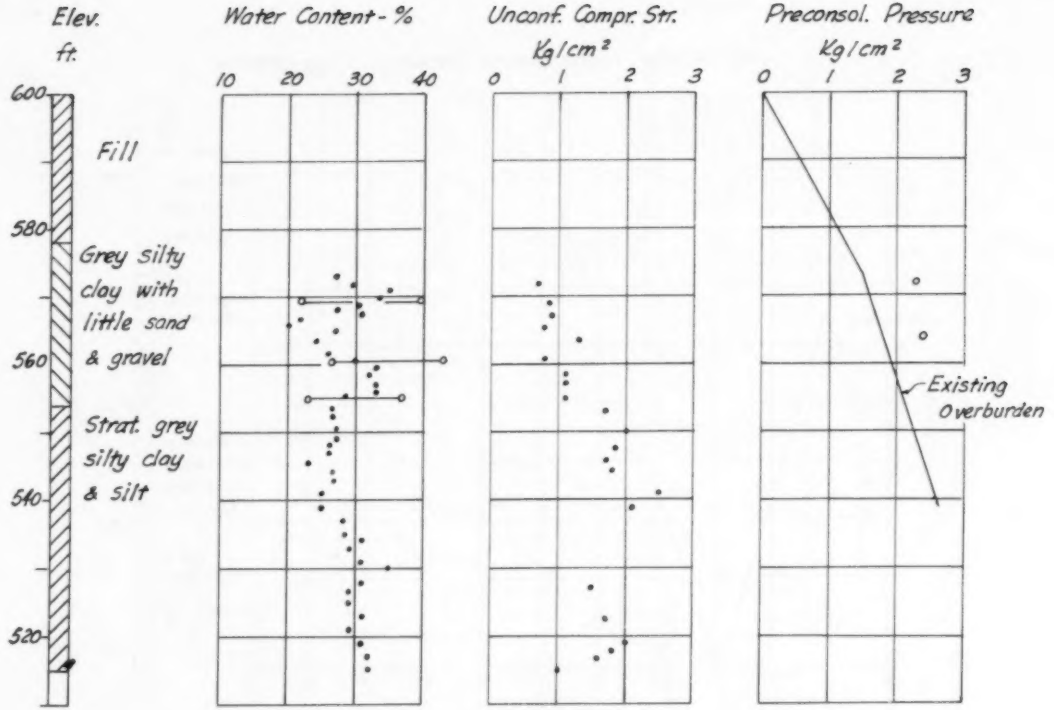

FIGURE 13 SUBSOIL PROPERTIES - CLEVELAND

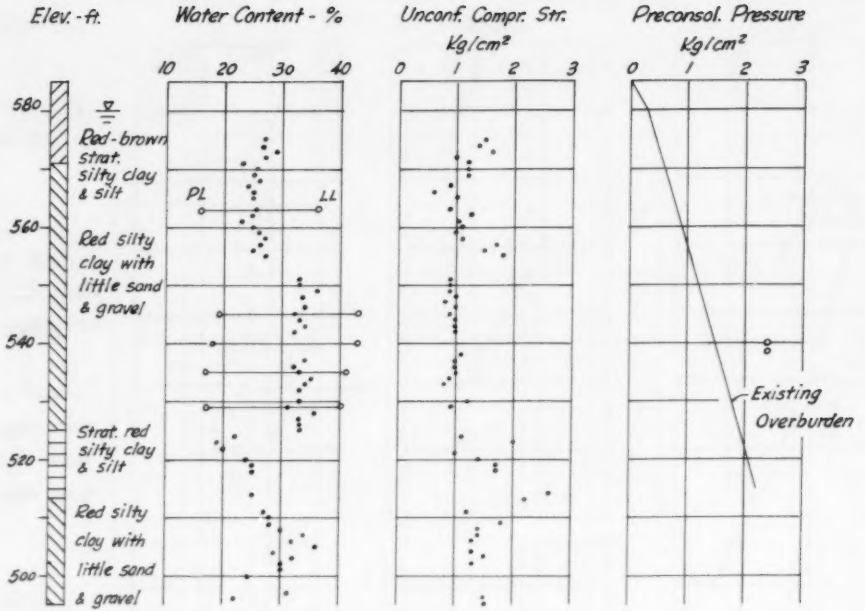

FIGURE 14 SUBSOIL PROPERTIES - GREEN BAY

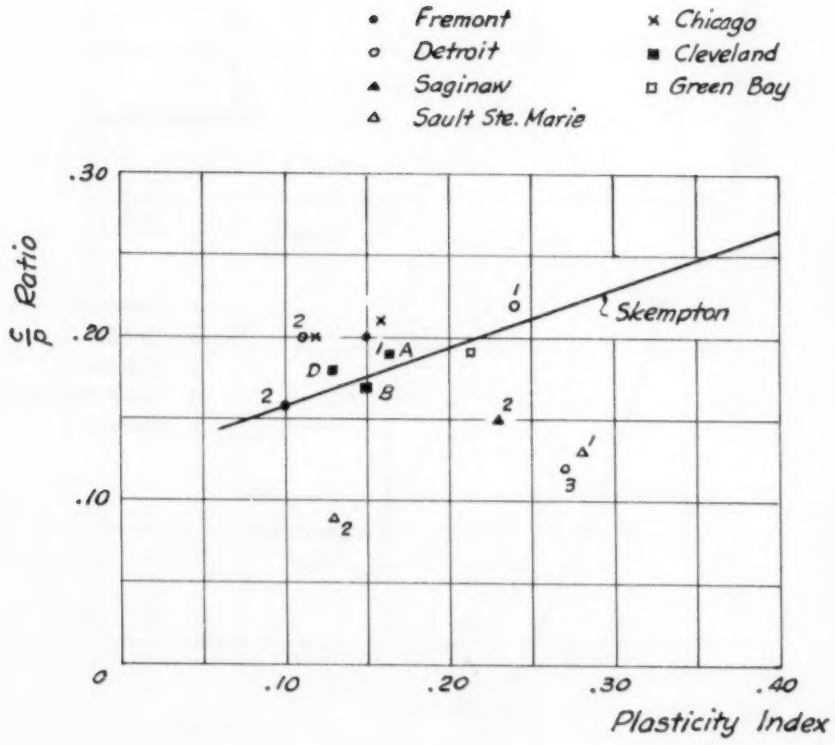

FIGURE 15 RELATIONSHIP BETWEEN $\frac{C}{p}$ & PI

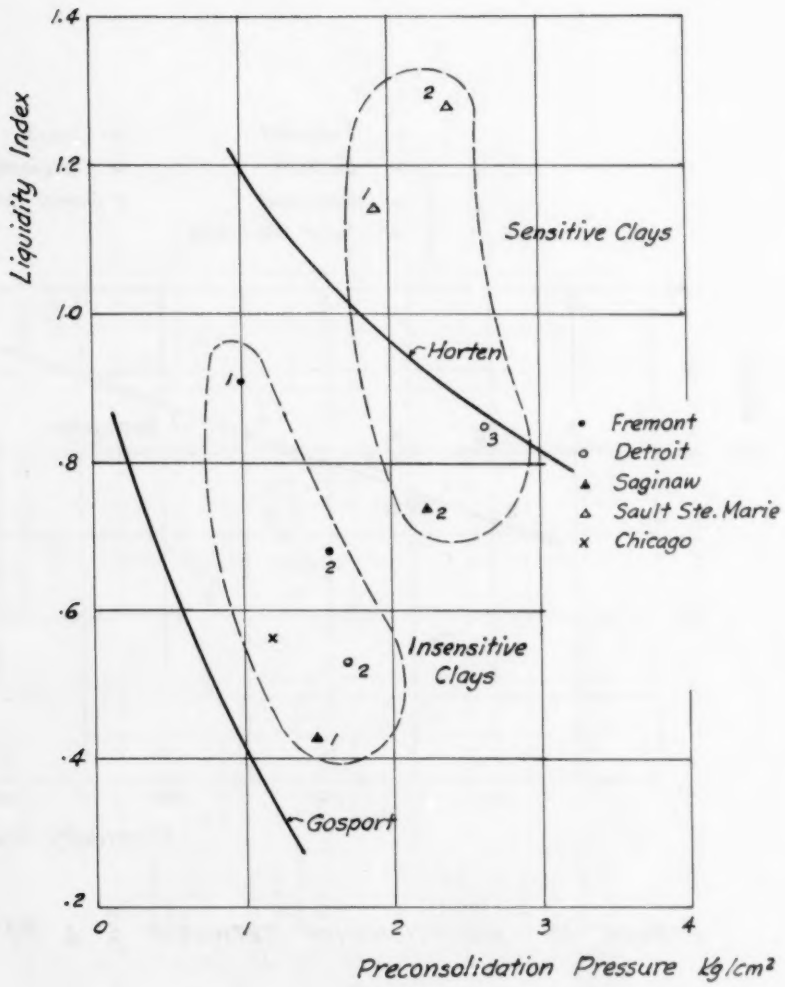

FIG. 16 RELATIONSHIP BETW. PRECONS. PRESSURE & L I

Detroit has the characteristic plastic nature. Its maximum stress is attained at a large strain of 35% and there is no significant reduction in stress with further strain. Photographs of the failed specimens are shown in Fig. 18. The strain at which maximum strength is attained with the various clays are listed in Table 2 as ϵ_p. The brittle soils are all sensitive clays and all

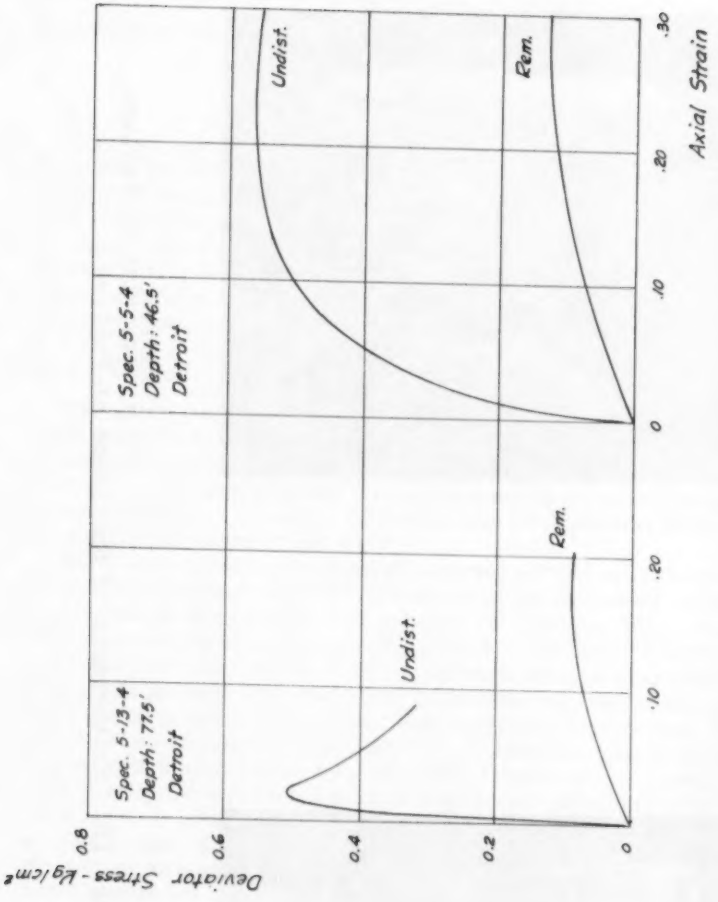

FIGURE 17 TYPICAL STRESS-STRAIN RELATIONSHIPS

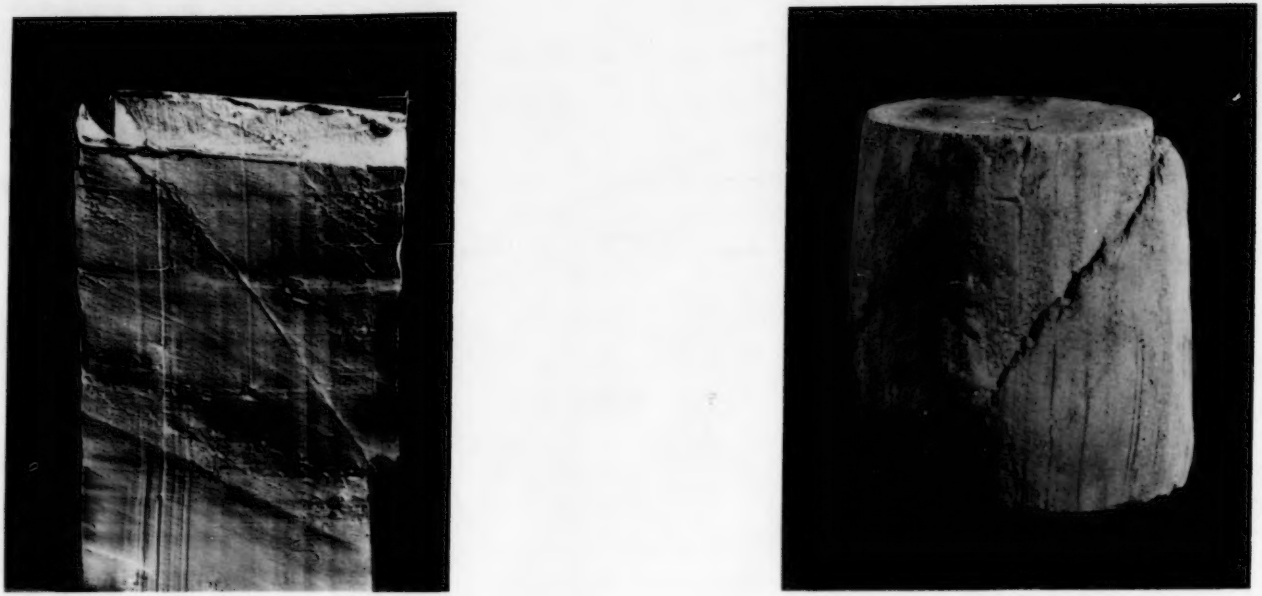

(a) Brittle Failure (b) Plastic Failure

Figure 18. Photographs of Specimens at Failure

evidence indicates that the stress-strain characteristics are governed by the same factors that govern the $\frac{c}{p}$ ratio and sensitivity.

Fabric of Clays

The investigation on strength has revealed that there are two groups of clays with very different strength characteristics in spite of their close similarity with respect to activity and mineralogical contents. It is further indicated that the major differences may be attributed to the micro-structure of the clays. The attention was, therefore, turned to the fabric of the clays. The fabric of a clay is usually defined as the arrangement of the clay flakes inside a given specimen or deposit. This arrangement may be either parallel or random depending upon the depositional environments.

Optical Studies

The optical properties of the clay minerals provide some means to evaluate the orientation of the clay flakes. Although most clay minerals are biaxial crystals, the difference in the indices of refraction are known to be small; and for the present study they are treated as uniaxial crystals with optical axes represented by a_1, a_2, and c, with the c axis perpendicular to the flat face of the particle as shown in Fig. 19a.

When flake-shaped clay-mineral particles settle from a deflocculated suspension, they come to rest with flakes one on top of another so that their basal plane surfaces are more or less parallel. Mitchel has found this to be true also for fresh water sediments.(13) In such a clay, the c axes of all the flakes are oriented in the vertical direction although the a_1 and a_2 axes of the flakes may not be parallel (Fig. 19b). The orientation can, therefore, be studied by examination of thin sections under a petrographic microscope. A vertical section of an oriented clay will exhibit four alternate stages of illumination and extinction when placed between crossed nicols of the microscope since light passing through such a section is polarized to vibrate in two perpendicular planes. A horizontal section will show no extinction or illumination as the a_1 and a_2 axes of the individual flakes lie in all directions (Fig. 19c). On the other hand, in a group of randomly oriented particles, none of the optical axes are alined in any given direction and illumination and extinction are non-existent in both vertical and horizontal sections. The predominance of the stages of illumination and extinction revealed in a vertical section, therefore, can be used as an index of the degree of orientation of the clay particles.

In this study the intensities of light transmitted through the microscope at the stages of illumination and extinction were measured by a phototube. The ratio of the light intensity at illumination to that at extinction was determined readily. This ratio is designated the orientation factor and reflects the arrangement of clay particles of the specimen. This ratio should be equal to infinity when a specimen exhibits complete extinction and is equal to one if the stages of extinction and illumination are non-existent. This sections 30 microns thick were used. The thin sections were prepared from clay specimens impregnated with a polyethylene glycol (Carbowax 6000) following the procedure described by J. K. Mitchell.(13) At least two thin sections were made from each clay and light readings were taken through the microscope with a 10x eyepiece and objectives of 1.0x, 10x and 45x. The values of the

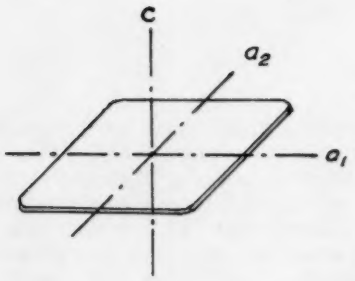

a. Optical axes of a clay mineral

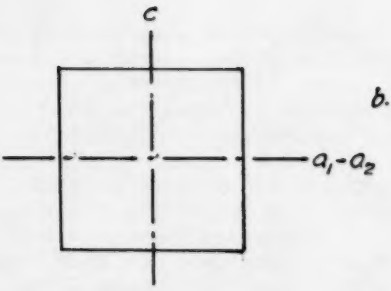

b. Optical axes of a vertical section thru a mass of oriented particles

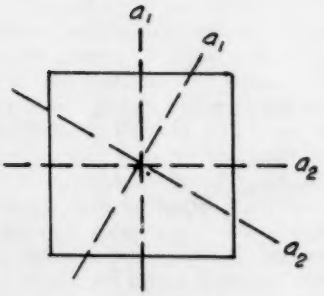

c Optical axes of a horiz. section thru. a mass of oriented particles

FIGURE 19 OPTICAL AXES OF CLAYS

readings are listed in Table 3. However, when the oriented areas were very small and when the directions of orientation were not the same in all areas, it was possible only to estimate the degree of orientation by visual examination.

Significance of Fabric

On the basis of the optical studies it is possible to further classify the clays according to their fabric. The first conclusion that may be drawn upon an examination of the data in Table 3 is that the till-like, unstratified silty clays all show random orientation over a large area. (Orientation factor = 1). This, of course, is understandable considering the large percentages of sand and silt in the soil. When magnified 450 times, it was found that the clay is actually well oriented around the silt and clay particles as shown in Fig. 20.

The fabric of the stratified lacustrine clays varied from well oriented (orientation factor from 2 to 3) to almost random. Fig. 21 shows micrographs of the illumination and extinction stages in a well oriented specimen and Fig. 22 micrograph of a specimen with little orientation. Both Detroit clay no. 1 and Fremont clay no. 1 exhibit a high degree of parallel arrangement whereas the Sault Ste. Marie clays 1 and 2 and Saginaw clay no. 2 show very little orientation. Since the percentages of silt and sand is very low in these clays, this lack of orientation can only result from a random structure. The findings regarding the particle orientation further substantiate the concept of micro-structure discussed previously. A flocculent or honeycomb structure is necessarily accompanied by random particle orientation. It is, therefore, this structure that gives the clays their high liquidity index, high sensitivity, and low $\frac{c}{p}$ ratio. The clays with pronounced parallel particle arrangement and the tills have low sensitivity and their $\frac{c}{p}$ ratios are close to values reported in the works of A. W. Skempton[8] and L. Bjerrum.[9]

Conditions of Deposition

To further check the micro-structure of the clays, the concentration of soluble salts in the porewater and the exchangeable cations were determined for the clays. It was reasoned that the flocculent structure of some clays may be the result of flocculation during deposition. This conceivably could have been brought about by deposition in waters of high salt concentration or by the very nature of the exchangeable cations.[14]

The results of soluble salt measurements and chemical analyses are given in Table 4. The salt concentration of lacustrine clays are very low and do not differ materially between clays with widely different structures. Furthermore, there is no significant difference in the exchangeable cations. The difference in micro-structure exhibited by the clays, therefore, cannot be explained by the results of chemical analyses.

CONCLUSIONS

In summary it may be said that the soft clays investigated are either lacustrine clays or tills deposited by glaciers under water. Consolidation of these soils is accomplished largely by the weight of the overburden and most of the clays can be considered as normally loaded. Despite the overall

(a) Illumination (b) Extinction

Figure 20. Micrographs showing orientation of clay around sand
Detroit Clay No. 2 (Mag. 500 X)

(a) Illumination (b) Extinction

Figure 21. Micrographs of a specimen with well oriented clay particles
Detroit Clay No. 1 (Mag. 100 X)

(a) Illumination

(b) Extinction

Figure 22. Micrographs of a specimen with poorly oriented clay particles
Sault Ste. Marie Clay No. 1 (Mag. 100 X)

similarity with respect to mode of deposition and mineralogical content and micro-structure of the clays was found to vary widely. In the case of lacustrine clays, the structure may be honeycombed and flocculent or the arrangement of the flake-shaped clay particles may be more or less parallel. The structure is accurately reflected by the relationship between the liquidity index and preconsolidation pressure. Important strength characteristics as sensitivity and the $\frac{c}{p}$ ratio were found to be dependent upon the micro-structure of the clays.

ACKNOWLEDGEMENT

This study is a part of the research program in soil mechanics at Michigan State University and was supported mainly by the Engineering Experiment Station. The writer is grateful to the many individuals that collaborated in this effort. He is indebted to Dr. M. M. Mortland who directed the x-ray diffraction and differential thermal analyses and to Dr. J. W. Trow for his assistance with the optical studies. The microscopic thin sections were skillfully prepared by Mr. G. S. Rev of Columbia University. Much information on the general subsoil conditions and foundation experiences in the various areas were made available to the writer through the generous cooperation of practicing engineers, especially Mr. A. E. Matthews of the Michigan Highway Department. The data from Green Bay and Cleveland were contributed by Professor R. B. Peck.

REFERENCES

1. Leverett, F., Glacial Formations and Drainage Features of the Erie and Ohio Basins, Monograph 41, U. S. Geological Survey, 1902.
2. Leverett, F. and Taylor, F. B., The Pleistocene of Indiana and Michigan, Monograph 53, U. S. Geological Survey, 1915.
3. Skempton, A. W., The Colloidal Activity of Clays, Proc. 3rd. Intern. Conf. on Soil Mech. and Found. Eng VI, p. 57, 1953.
4. Peck, R. B. and Reed, W. C., Engineering Properties of Chicago Subsoils, Bulletin 423, Engineering Exp. Sta., Univ. of Illinois, 1954.
5. Otto, G. H., An Interpretation of the Glacial Stratigraphy of the City of Chicago, Ph.D. thesis, Univ. of Chicago, 1942.
6. Parsons, J. D. and Peck, R. B., Discussion on "The Action of Soft Clay Along Friction Piles" by H. B. Seed and L. C. Reese, Proc. ASCE, No. 1028, V 82, 1956.
7. Peck, R. B., Foundation Conditions in the Cuyahoga River Valley, Proc. ASCE No. 513 V 80, 1954.
8. Skempton, A. W. and Henkel, D. J., The Post Glacial Clays of the Thames Estuary at Tilbury and Shellhaven, Proc. 3rd. Intern. Cong. on Soil Mech. and Found. Eng. V 1, p. 302, 1953.
9. Bjerrun, L., Geotechnical Properties of Norwegian Quick Clays, Geotechnique V 4, p. 49, 1954.

10. Hansen, J. B., Vane Tests in a Norwegian Quick Clay, Geotechnique V 2, p. 58, 1950.

11. Skempton, A. W., The Geotechnical Properties of a Deep Stratum of Post-Glacial Clay at Gosport, Proc. 2nd. Conf. on Soil Mech. and Found. Eng. V 1, p. 145, 1948.

12. Skempton, A. W. and Northey, R. D., The Sensitivity of Clays, Geotechnique V 3, p. 30, 1953.

13. Mitchell, J. K., The Fabric of Natural Clays and Its Relation to Engineering Properties, Proc. Hwy. Res. Board, V 35, p. 693, 1956.

14. Rosenquist, I. Th., Investigations in the Clay-Electrolyte-Water System. Publ. No. 9, Norwegian Geotechnical Institute, 1955.

Table 1. Index Properties of Clay Deposits

Location	Unit	Description	Particle Size Distr.			Atterberg Limits	
			Sand and Gravel	Silt	Clay	PI	LI
			.06	.06-2μ	< 2μ		
Fremont	1	Grey clay with silt and fine sand laminations	5	64	31	.15	.63
	2	Grey silty clay with sand and gravel	33	40	27	.10	.50
Detroit	1	Grey clay with silt and fine sand laminations	0	40	60	.24	.20
	2	Grey silty clay with sand and gravel	22	40	38	.11	.53
	3	Grey clay	0	20	80	.27	.85
Saginaw	1	Grey silty clay with sand and gravel	33	27	40	.10	.43
	2	Grey clay with silt laminations	4	30	66	.23	.74
Sault Ste. Marie	1	Red clay with silt laminations	2	30	68	.28	1.14
	2	Reddish grey silt with clay laminations	1	66	33	.13	1.28
Chicago		Grey silty clay with sand and gravel				.16	.56
Cleveland	A	Grey silty clay with sand and gravel				.15	.45
	B	Lake clay				.15	.27
	D	Lake clay				.13	.46
Green Bay		Red silty clay with sand and gravel				.22	.63

Table 2. Strength Characteristics of Clay Deposits

Location	Unit	P(Kg/cm^2)	c/P	St	ϵ_p
Fremont	1	1.00	0.20	3.0	.12
	2	1.60	0.16	2.5	.35
Detroit	1	9.00	0.22	3.0	.10
	2	1.70	0.20	2.9	.35
	3	2.65	0.12	8.6	.02
Saginaw	1	1.5		2.3	.30+
	2	2.25	0.15	5.8	.07
Sault Ste. Marie	1	1.90	0.13	8.0	.03
	2	2.40	0.09	10.0	.02
Chicago[5]		1.20	0.23	2.6	7.20
Cleveland[7]	A	2.40	0.19		
	B	12	0.17	3.0	7.20
	D	14	0.18	3.0	
Green Bay		2.40	0.19		

p - preconsolidation pressure

c - 1/2 compressive strength

S_t - sensitivity

ϵ_p - strain at max. stress

Table 3. Particle Orientation

Location	Unit	Orient. Factor over large area (5 mm)	Orient. Factor over small area (estimated)	Size of small orient. area	Remarks
Fremont	1	2.5			
	2	1.0	2.5	< 25 μ	Orient. around silt and sand particles.
Detroit	1	2.5 - 3.0			
	2	1.0	2.5	< 25 μ	Orient. around silt and sand particles.
	3	1.3			
Saginaw	1	1.0	2.5	< 25 μ	Orient. around silt and sand particles.
	2	1.1	1.2	< 10 μ	
Sault Ste. Marie	1	1.1	1.2	< 10 μ	
	2	1.0	1.1		
Chicago		Not Oriented	Well Oriented	10 - 20 μ	(13)

Table 4. Salt Concentration and Exchangeable Cations

Location	Unit	Salt Conc. in porewater gm/liter	Exchangeable Cation - m.e./100 gm. Soil			
			Na	K	Ca	Mg
Detroit	1	0.85	1.41	0.47	6.66	3.94
	2	2.98	1.04	0.27	11.98	3.94
	3	0.76	1.96	0.47	9.98	6.58
Saginaw	1	2.59				
	2	0.89				
Sault Ste. Marie	1	0.62	1.39	0.62	15.96	4.68
	2	0.93				

PROCEEDINGS PAPERS

The technical papers published in the past year are identified by number below. Technical-division sponsorship is indicated by an abbreviation at the end of each Paper Number, the symbols referring to: Air Transport (AT), City Planning (CP), Construction (CO), Engineering Mechanics (EM), Highway (HW), Hydraulics (HY), Irrigation and Drainage (IR), Pipeline (PL), Power (PO), Sanitary Engineering (SA), Soil Mechanics and Foundations (SM), Structural (ST), Surveying and Mapping (SU), and Waterways and Harbors (WW), divisions. Papers sponsored by the Board of Direction are identified by the symbols (BD). For titles and order coupons, refer to the appropriate issue of "Civil Engineering." Beginning with Volume 82 (January 1956) papers were published in Journals of the various Technical Divisions. To locate papers in the Journals, the symbols after the paper numbers are followed by a numeral designating the issue of a particular Journal in which the paper appeared. For example, Paper 1449 is identified as 1449 (HY 6) which indicates that the paper is contained in the sixth issue of the Journal of the Hydraulics Division during 1957.

VOLUME 83 (1957)

AUGUST: 1330(HY4), 1331(HY4), 1332(HY4), 1333(SA4), 1334(SA4), 1335(SA4), 1336(SA4), 1337(SA4), 1338 (SA4), 1339(CO1), 1340(CO1), 1341(CO1), 1342(CO1), 1343(CO1), 1344(PO4), 1345(HY4), 1346(PO4)[c], 1347 (BD1), 1348(HY4)[c], 1349(SA4)[c] 1350(PO4), 1351(PO4).

SEPTEMBER: 1352(IR2), 1353(ST5), 1354(ST5), 1355(ST5), 1356(ST5), 1357(ST5), 1358(ST5), 1359(IR2), 1360 (IR2), 1361(ST5), 1362(IR2), 1363(IR2), 1364(IR2), 1365(WW3), 1366(WW3), 1367(WW3), 1368(WW3), 1369 (WW3), 1370(WW3), 1371(HW4), 1372(HW4), 1373(HW4), 1374(HW4), 1375(PL3), 1376(PL3), 1377(IR2)[c],1378 (HW4)[c], 1379(IR2), 1380(HW4), 1381(WW3)[c], 1382(ST5)[c], 1383(PL3)[c], 1384(IR2), 1385(HW4), 1386(HW4).

OCTOBER: 1387(CP2), 1388(CP2), 1389(EM4), 1390(EM4),1391(HY5), 1392(HY5), 1393(HY5), 1394(HY5), 1395 (HY5), 1396(PO5), 1397(PO5), 1398(PO5), 1399(EM4), 1400(SA5), 1401(HY5), 1402(HY5), 1403(HY5), 1404 (HY5), 1405(HY5), 1406(HY5), 1407(SA5), 1408(SA5), 1409(SA5), 1410(SA5), 1411(SA5), 1412(EM4), 1413 (EM4), 1414(PO5), 1415(EM4)[c], 1416(PO5)[c], 1417(HY5)[c], 1418(EM4), 1419(PO5), 1420(PO5), 1421(PO5), 1422(SA5)[c], 1423(SA5), 1424(EM4), 1425(CP2).

NOVEMBER: 1426(SM4), 1427(SM4), 1428(SM4), 1429(SM4), 1430(SM4)[c], 1431(ST6), 1432(ST6), 1433(ST6), 1434(ST6), 1435(ST6), 1436(ST6), 1437(ST6), 1438(SM4), 1439(SM4), 1440(ST6), 1441(ST6), 1442(ST6)[c], 1443(SU2), 1444(SU2), 1445(SU2), 1446(SU2), 1447(SU2), 1448(SU2)[c].

DECEMBER: 1449(HY6), 1450(HY6), 1451(HY6), 1452(HY6), 1453(HY6), 1454(HY6), 1455(HY6), 1456(HY6)[c], 1457(PO6), 1458(PO6), 1459(PO6), 1460(PO6)[c], 1461(SA6), 1462(SA6), 1463(SA6), 1464(SA6), 1465(SA6), 1466(SA6)[c], 1467(AT2), 1468(AT2), 1469(AT2), 1470(AT2), 1471(AT2), 1472(AT2), 1473(AT2), 1474(AT2), 1475(AT2), 1476(AT2), 1477(AT2), 1478(AT2), 1479(AT2), 1480(AT2), 1481(AT2), 1482(AT2), 1483(AT2), 1484(AT2), 1485(AT2)[c], 1486(BD2), 1487(BD2), 1488(PO6), 1489(PO6), 1490(BD2), 1491(BD2), 1492(HY6), 1493(BD2).

VOLUME 84 (1958)

JANUARY: 1494(EM1), 1495(EM1), 1496(EM1), 1497(IR1), 1498(IR1), 1499(IR1), 1500(IR1), 1501(IR1), 1502 (IR1), 1503(IR1), 1504(IR1), 1505(IR1), 1506(IR1), 1507(IR1), 1508(ST1), 1509(ST1), 1510(ST1), 1511(ST1), 1512(ST1), 1513(WW1), 1514(WW1), 1515(WW1), 1516(WW1), 1517(WW1), 1518(WW1), 1519(ST1), 1520 (EM1)[c], 1521(IR1)[c], 1522(ST1)[c], 1523(WW1)[c], 1524(HW1), 1525(HW1), 1526(HW1)[c], 1527(HW1).

FEBRUARY: 1528(HY1), 1529(PO1), 1530(HY1), 1531(HY1), 1532(HY1), 1533(SA1), 1534(SA1), 1535(SM1), 1536(SM1), 1537(SM1), 1538(PO1)[c], 1539(SA1), 1540(SA1), 1541(SA1), 1542(SA1), 1543(SA1), 1544(SM1), 1545(SM1), 1546(SM1), 1547(SM1), 1548(SM1), 1549(SM1), 1550(SM1), 1551(SM1), 1552(SM1), 1553(PO1), 1554(PO1), 1555(PO1), 1556(PO1), 1557(SA1)[c], 1558(HY1)[c], 1559(SM1)[c].

MARCH: 1560(ST2), 1561(ST2), 1562(ST2), 1563(ST2), 1564(ST2), 1565(ST2), 1566(ST2), 1567(ST2), 1568 (WW2), 1569(WW2), 1570(WW2), 1571(WW2), 1572(WW2), 1573(WW2), 1574(PL1), 1575(PL1), 1576(ST2)[c], 1577(PL1), 1578(PL1)[c], 1579(WW2)[c].

APRIL: 1580(EM2), 1581(EM2), 1582(HY2), 1583(HY2), 1584(HY2), 1585(HY2), 1586(HY2), 1587(HY2), 1588 (HY2), 1589(IR2), 1590(IR2), 1591(IR2), 1592(SA2), 1593(SU1), 1594(SU1), 1595(SU1), 1596(EM2), 1597(PO2), 1598(PO2), 1599(PO2), 1600(PO2), 1601(PO2), 1602(PO2), 1603(HY2), 1604(EM2), 1605(SU1)[c],1606(SA2), 1607(SA2), 1608(SA2), 1609(SA2), 1610(SA2), 1611(SA2), 1612(SA2), 1613(SA2), 1614(SA2)[c], 1615(IR2)[c], 1616 (HY2)[c], 1617(SU1), 1618(PO2)[c], 1619(EM2)[c], 1620(CP1).

MAY: 1621(HW2), 1622(HW2), 1623(HW2), 1624(HW2), 1625(HW2), 1626(HW2), 1627(HW2), 1628(HW2), 1629 (ST3), 1630(ST3), 1631(ST3), 1632(ST3), 1633(ST3), 1634(ST3), 1635(ST3), 1636(ST3), 1637(ST3), 1638(ST3), 1639(WW3), 1640(WW3), 1641(WW3), 1642(WW3), 1643(WW3), 1644(WW3), 1645(SM2), 1646(SM2), 1647 (SM2), 1648(SM2), 1649(SM2), 1650(SM2), 1651(HW2), 1652(HW2)[c], 1653(WW3)[c], 1654(SM2), 1655(SM2), 1656(ST3)[c], 1657(SM2)[c].

JUNE: 1658(AT1), 1659(AT1), 1660(HY3), 1661(HY3), 1662(HY3), 1663(HY3), 1664(HY3), 1665(SA3), 1666 (PL2), 1667(PL2), 1668(PL2), 1669(AT1), 1670(PO3), 1671(PO3), 1672(PO3), 1673(PL2), 1674(PL2), 1675 (PO3), 1676(PO3), 1677(SA3), 1678(SA3), 1679(SA3), 1680(SA3), 1681(SA3), 1682(SA3), 1683(PO3), 1684 (HY3), 1685(SA3), 1686(SA3), 1687(PO3), 1688(SA3)[c], 1689(PO3)[c], 1690(HY3)[c], 1691(PL2)[c].

JULY: 1692(EM3), 1693(EM3), 1694(ST4), 1695(ST4), 1696(ST4), 1697(SU2), 1698(SU2), 1699(SU2), 1700(SU2), 1701(SA4), 1702(SA4), 1703(SA4), 1704(SA4), 1705(SA4), 1706(EM3), 1707(ST4), 1708(ST4), 1709(ST4), 1710 (ST4), 1711(ST4), 1712(ST4), 1713(SU2), 1714(SA4), 1715(SA4), 1716(SU2), 1717(SA4), 1718(EM3), 1719 (EM3), 1720(SU2), 1721(ST4)[c], 1722(ST4), 1723(ST4), 1724(EM3)[c].

AUGUST: 1725(HY4), 1726(HY4), 1727(SM3), 1728(SM3), 1729(SM3), 1730(SM3), 1731(SM3), 1732(SM3), 1733 (PO4), 1734(PO4), 1735(PO4), 1736(PO4), 1737(PO4), 1738(PO4), 1739(PO4), 1740(PO4), 1741(PO4), 1742 (PO4), 1743(PO4), 1744(PO4), 1745(PO4), 1746(PO4), 1747(PO4), 1748(PO4), 1749(PO4).

---

c. Discussion of several papers, grouped by divisions.

AMERICAN SOCIETY OF CIVIL ENGINEERS

OFFICERS FOR 1958

PRESIDENT

LOUIS R. HOWSON

VICE-PRESIDENTS

Term expires October, 1958:
FRANCIS S. FRIEL
NORMAN R. MOORE

Term expires October, 1959:
WALDO G. BOWMAN
SAMUEL B. MORRIS

DIRECTORS

Term expires October, 1958:
JOHN P. RILEY
CAREY H. BROWN
MASON C. PRICHARD
ROBERT H. SHERLOCK
R. ROBINSON ROWE
LOUIS E. RYDELL
CLARENCE L. ECKEL

Term expires October, 1959:
CLINTON D. HANOVER, Jr.
E. LELAND DURKEE
HOWARD F. PECKWORTH
FINLEY B. LAVERTY
WILLIAM J. HEDLEY
RANDLE B. ALEXANDER

Term expires October, 1960:
PHILIP C. RUTLEDGE
WESTON S. EVANS
TILTON E. SHELBURNE
CRAIG P. HAZELET
DONALD H. MATTERN
JOHN E. RINNE

PAST PRESIDENTS

Members of the Board

ENOCH R. NEEDLES

MASON G. LOCKWOOD

EXECUTIVE SECRETARY

WILLIAM H. WISELY

TREASURER

CHARLES E. TROUT

ASSISTANT SECRETARY

E. LAWRENCE CHANDLER

ASSISTANT TREASURER

CARLTON S. PROCTOR

PROCEEDINGS OF THE SOCIETY

HAROLD T. LARSEN
Manager of Technical Publications

PAUL A. PARISI
Editor of Technical Publications

COMMITTEE ON PUBLICATIONS

HOWARD F. PECKWORTH, *Chairman*

PHILIP C. RUTLEDGE, *Vice-Chairman*

E. LELAND DURKEE
TILTON E. SHELBURNE
R. ROBINSON ROWE
LOUIS E. RYDELL